



5-2005

Murine Herpetic Stromal Keratitis: Elucidating the Early Events Involved in its Pathogenesis

Partha S. Biswas
University of Tennessee - Knoxville

Follow this and additional works at: https://trace.tennessee.edu/utk_graddiss



Part of the [Medicine and Health Sciences Commons](#)

Recommended Citation

Biswas, Partha S., "Murine Herpetic Stromal Keratitis: Elucidating the Early Events Involved in its Pathogenesis. " PhD diss., University of Tennessee, 2005.
https://trace.tennessee.edu/utk_graddiss/666

This Dissertation is brought to you for free and open access by the Graduate School at TRACE: Tennessee Research and Creative Exchange. It has been accepted for inclusion in Doctoral Dissertations by an authorized administrator of TRACE: Tennessee Research and Creative Exchange. For more information, please contact trace@utk.edu.

To the Graduate Council:

I am submitting herewith a dissertation written by Partha S. Biswas entitled "Murine Herpetic Stromal Keratitis: Elucidating the Early Events Involved in its Pathogenesis." I have examined the final electronic copy of this dissertation for form and content and recommend that it be accepted in partial fulfillment of the requirements for the degree of Doctor of Philosophy, with a major in Comparative and Experimental Medicine.

Barry T. Rouse, Major Professor

We have read this dissertation and recommend its acceptance:

Robert N. Moore, Albert T. Ichiki, Mark Y. Sangster

Accepted for the Council:

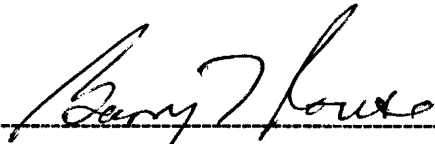
Carolyn R. Hodges

Vice Provost and Dean of the Graduate School

(Original signatures are on file with official student records.)

To the Graduate Council:

I am submitting herewith a dissertation written by Partha Sarathi Biswas entitled "Murine Herpetic Stromal Keratitis: Elucidating the Early Events Involved in its Pathogenesis". I have examined the final paper copy of this dissertation for form and content and recommend that it be accepted in partial fulfillment of the requirements for the degree of Doctor of Philosophy, with a major in Comparative and Experimental Medicine.



Barry T. Rouse, Major Professor

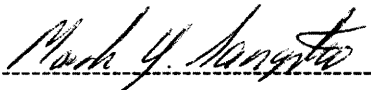
We have read this dissertation
and recommend its acceptance:



Robert N. Moore

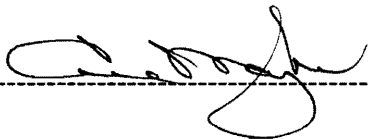


Albert T. Ichiki



Mark Y. Sangster

Accepted for the Council:



Vice Chancellor and
Dean of Graduate Studies

**MURINE HERPETIC STROMAL
KERATITIS: ELUCIDATING THE EARLY
EVENTS INVOLVED IN ITS PATHOGENESIS**

A

Dissertation Presented

For the Doctor of Philosophy Degree

The University of Tennessee, Knoxville

Partha Sarathi Biswas

May 2005

ACKNOWLEDGEMENTS

I express my deepest appreciation and gratitude towards my advisor Dr. Barry T. Rouse, working for whom for last three years has been a unique and memorable experience. The knowledge of Professor Rouse as well as his practical advice concerning the immunological research was highly valuable and helped me broaden my horizon and make me look at the research in a different perspective.

I sincerely appreciate and thank my advisory committee members, Dr Robert Moore, Dr. Albert Ichiki and Dr. Mark Sangster for their guidance and support.

I would also like to thank Dr. Paul R. Kinchington of the University Pittsburgh School of Medicine, Philadelphia, Dr David Johnson of the Oregon Health Center, for kindly providing the engineered viruses. I also thank Dr John Dunlap for his technical assistance in confocal microscopy.

I am very grateful to all the members of the laboratory, who have made my stay in the Rouse lab very productive and enjoyable. My special thanks go to Kaustuv, with him I have spent many inspiring moments. His friendly comments and constructive criticism on my work as well as some noteworthy and fascinating ideas for further research subjects were invaluable. Very special thanks to Pial, who gave me friendly support during my research work.

It would not have been possible for me to get through with this stage of my life had it not been for the immense support and faith my family (Ma, Dada, Boudi, Atai and all my well wishers and friends in India and Knoxville) have shown in me. Thanks to Urmi and Pritam for their constant support

during my stay in Knoxville. I am grateful to my wife, Sarmi, who has been especially supportive and a constant provider of encouragement and motivation.

ABSTRACT

Herpes simplex viruses (HSV) infection is a common cause of ocular disease and can result in a chronic inflammatory reaction that impairs vision. This latter manifestation is called herpetic stromal keratitis (HSK) and usually occurs as a consequence of virus reactivation from latency in the trigeminal ganglion. The pathogenesis process involves complex interactions of cellular and molecular events. HSK in humans, and certainly its murine experimental model, appears to be an immunopathologic disease process. The crucial cell type orchestrating the inflammation is a CD4⁺ T cell that has a Th1 cytokine-producing profile. However, prior to this immunoinflammatory phase, multiple events occur that set the stage for subsequent pathology. These include production of cytokines and chemokines, infiltration of innate immune cells and neovascularization of the avascular cornea.

Current understanding about human and murine HSK pathogenesis is reviewed in Part I. Part II progresses this knowledge using knockout and transgenic mice. Results in Part II clarify the essential role of IL-1, a proinflammatory cytokine, produced as a consequence of virus replication, in HSK pathogenesis. Part III, in addition to Part II, elucidate the mechanisms involved in IL-1 and IL-6 mediated polymorphonuclear leukocyte (PMN) influx and neovascularization of cornea following virus infection. These cytokines were shown to be produced quite early after infection and capable of inducing angiogenic factors, resulting in angiogenesis of the cornea. In addition, the role of IL-1 in inducing proinflammatory arachidonic acid metabolites has been discussed in PART IV. Cyclooxygenase 2 enzyme

produced from resident corneal cells in presence of IL-1 was shown to be crucial for creating an inflammatory milieu and facilitate early PMN influx in murine cornea. These results provide novel insights into the link between viral infections, pro-inflammatory mediators, PMN migration, angiogenesis and HSK development. Our understanding about the role of IL-1 in HSK pathogenesis was evaluated clinically in Part V using an IL-1 receptor antagonist (IL-1 ra) protein. Mice receiving IL-1 ra had diminished disease severity. The administration of IL-1 ra was shown to reduce the influx into the cornea of cells of both the innate and adaptive immune response. In addition, the treatment also diminished corneal VEGF levels resulting reduced angiogenic response. Our results show the importance of targeting early proinflammatory molecules such as IL-1 to counteract HSK and advocate IL-1 ra as an effective agent to achieve this. In Part VI, a novel flow cytometry based assay has been used to quantify corneal angiogenesis following ocular HSV infection. Our results indicate that, this assay was sensitive enough to be able to pick up the difference in angiogenic response between mice. Thus, estimation of angiogenesis on the basis of number of endothelial cells proved to be a useful approach to quantify corneal neovascularization.

This dissertation presents research aimed at elucidating both molecular and cellular events in HSK pathogenesis. These results will serve as guidelines for future development of more efficient prophylactic and therapeutic strategies.

TABLE OF CONTENTS

Part	Page
I. BACKGROUND AND OVERVIEW.....	1
Introduction.....	2
Virus entry in the cornea.....	3
Virus and early inflammatory events.....	5
Virus and Angiogenesis.....	15
Stromal Keratitis – the outcome of infection.....	20
Conclusion.....	25
Specific aims and rationale.....	25
List of references.....	27
Appendix.....	42
II. MICE TRANSGENIC FOR IL-1 RECEPTOR ANTAGONIST PROTEIN ARE RESISTANT TO HERPETIC STROMAL KERATITIS: POSSIBLE ROLE FOR IL-1 IN HERPETIC STROMAL KERATITIS PATHOGENESIS.....	51
Abstract.....	52
Introduction.....	53
Materials and Methods.....	54
Results.....	62
Discussion.....	65
List of references.....	70

Appendix.....	77
---------------	----

III. INVOLVEMENT OF IL-6 IN THE PARACRINE

PRODUCTION OF VEGF IN OCULAR HSV-1

INFECTION.....95

Abstract.....	96
---------------	----

Introduction.....	97
-------------------	----

Materials and Methods.....	98
----------------------------	----

Results.....	106
--------------	-----

Discussion.....	109
-----------------	-----

List of references.....	112
-------------------------	-----

Appendix.....	117
---------------	-----

IV. ROLE OF IL-1 INDUCED COX-2 IN

OCULAR IMMUNOPATHOLOGIC DISEASE;

HERPETIC STROMAL KERATITIS.....127

Abstract.....	128
---------------	-----

Introduction.....	129
-------------------	-----

Materials and Methods.....	131
----------------------------	-----

Results.....	140
--------------	-----

Discussion.....	145
-----------------	-----

List of references.....	150
-------------------------	-----

Appendix.....	159
---------------	-----

V.	COUNTERACTING CORNEAL IMMUNOINFLAMMATORY LESION WITH INTERLEUKIN-1 RECEPTOR ANTAGONIST PROTEIN	177
	Abstract.....	178
	Introduction.....	179
	Materials and Methods.....	180
	Results.....	185
	Discussion.....	190
	List of references.....	194
	Appendix.....	201
VI.	A NOVEL FLOW CYTOMETRY BASED ASSAY FOR QUANTIFICATION OF CORNEAL ANGIOGENESIS IN THE MOUSE MODEL OF HERPETIC STROMAL KERATITIS	215
	Abstract.....	216
	Introduction.....	217
	Materials and Methods.....	218
	Results.....	222
	Discussion.....	224
	List of references.....	227
	Appendix.....	230
	VITA.....	240

LIST OF FIGURES

Part	Figure	Page
I	Figure 1. Crucial events in HSK pathogenesis.....	43
	Figure 2. Schematic representation of some early events in HSK pathogenesis.....	44
	Figure 3. The molecular mimicry model of SK pathogenesis.....	46
	Figure 4. The Bystander activation model of SK pathogenesis.....	47
	Figure 5. The Hit and Run model of SK pathogenesis.....	49
II	Figure 1: Expression of corneal IL-1 Ra mRNA at various time points after HSV infection.....	78
	Figure 2: Reduced HSK severity in IL-1 Ra Tg mice.....	79
	Figure 3: IL-1 Ra Tg mice show reduced angiogenic response following HSV-1 infection at day 20 p. i.....	80
	Figure 4: Presence of abundant Gr-1+ve cells in the cornea of IL-1 Ra -/- and C57BL/6 mice but not in IL-1 Ra Tg mice at 48 hr p. i.....	82
	Figure 5: Reduced IL-6 and MIP-2 protein levels in HSV-1 infected corneas of IL-1 Ra Tg mice.....	83
	Figure 6: Increased Gr-1+ve cells and MIP-2 levels in recombinant murine IL-6 reconstituted IL-1 Ra Tg corneas at 48 hr p. i.....	84
	Figure 7: IL-1 α induced IL-6 production from corneal	

	epithelial cells.....	86
	Figure 8: Reduced VEGF protein levels and diminished expression of VEGFR-2 mRNA expression in HSV-1 RE infected corneas of IL- 1Ra Tg mice.....	88
	Figure 9: IL-1 α induces angiogenesis in a corneal intrastromal injection assay.....	90
	Figure 10: IL-1 α induces IL-6 and VEGF production in the cornea.....	92
	Figure 11: Neutralizing antibody against VEGF but not IL-6 can abrogate IL-1 α induced angiogenesis in the cornea.....	93
III	Figure 1. Uninfected and not infected corneal epithelial cells express VEGF following ocular infection with HSV-1 following 24 hr post infection.....	118
	Figure 2. Subconjunctival injection of recombinant murine IL-6 stimulates resident corneal cells to produce VEGF.....	120
	Figure 3. Unmanipulated corneal epithelial cells, MKT-1, DC2.4 and J774A.1 cell lines express transcripts for functional IL-6 receptor.....	122
	Figure 4. Interleukin 6 stimulation of corneal epithelial cells and stromal fibroblast result in the expression of VEGF transcript and protein respectively.....	123
	Figure 5. Macrophage cell line (J774A.1) produces VEGF following in vitro stimulation with various doses of recombinant murine IL-6.....	125

IV	Figure 1. Kinetics of COX-2 mRNA and PGE ₂ levels in HSV-1 infected corneas of Balb/c and C57BL6 mice.....	160
	Figure 2. Mice receiving COX-2 inhibitors show reduced HSK severity.....	161
	Figure 3. Mice receiving COX-2 inhibitor show diminished angiogenic response following HSV-1 infection at day 20 p. i.....	163
	Figure 4. Uninfected stromal fibroblasts are the major producers of COX-2 following ocular HSV-1 infection.....	165
	Figure 5. IL-1 β induced COX-2 expression in murine stromal fibroblast cell line.....	167
	Figure 6. Reduced PMN influx in COX-2 inhibitor treated mice at 48 hr. p. i.....	170
	Figure 7. Reduced levels of Cytokines and Prostanoids in the cornea of COX-2 inhibitor treated mice.....	172
	Figure 8. Compromised angiogenic responses in COX-2 inhibitor treated mice.....	174
V	Figure 1. Following Subconjunctival injection, presence of IL-1 ra was detectable in cornea for short period of time.....	202
	Figure 2. No difference in HSK score between locally administered IL-1 ra treated mice and vehicle control mice.....	203
	Figure 3. Mice treated with IL-1 ra protein locally demonstrated similar angiogenic response like vehicle control.....	205

Figure 4. Human recombinant Interleukin-1 receptor antagonist protein was detected in mice receiving a combination of systemic and local administration till day 7 post injection.....207

Figure 5. Mice receiving IL-1 ra systemically in conjunction with local administration demonstrated reduced HSK severity.....208

Figure 6. Mice receiving a combination of systemic and local administration of IL-1 ra protein showed diminished angiogenesis following ocular infection.....210

Figure 7. Presence of abundant Gr-1+ve cells in the cornea of vehicle control mice but not in IL-1 ra treated mice at 48 hr p. i.....212

Figure 8. Diminished CD4⁺ T cell influx in mice treated with IL-1 ra protein.....213

Figure 9. IL-1 ra treated mice demonstrated reduced protein levels of IL-6, MIP-2 and VEGF.....214

VI Figure 1. Endothelial cells constituting the new blood vessels in corneal stroma express CD31 at day 15 post infection.....231

Figure 2. Increase in the number of CD31⁺ cells is associated with heightened angiogenic response following corneal micropocket assay.....234

Figure 3. Increase in the number of CD31⁺ cells is associated with the increase in NV index at day 15 p. i.....235

Figure 4. Mice infected with higher dose of virus
demonstrated increased number of CD31⁺ cells/cornea
at day 15 p. i.....238

ABBREVIATIONS

COX-1.....	Cyclooxygenase 1
COX-2.....	Cyclooxygenase 2
CXCR2.....	CXC chemokines receptor 2
DC.....	Dendritic cell
HSV-1.....	Herpes simplex virus 1
ICAM-1.....	Intracellular cell adhesion molecule 1
IFN γ	Interferon gamma
IL-1, 6, 12, 18.....	Interleukin 1, 6, 12, 18
IL-1 ra.....	Interleukin 1 receptor antagonist
IP-10.....	Interferon gamma inducible protein 10
MHC.....	Major histocompatibility complex
MIP-1, 2.....	Macrophage inflammatory protein 1, 2
MMP-9.....	Matrix metalloproteinase 9
PAMP.....	Pathogen associated molecular patterns
PFU.....	Plaque forming unit
PMN.....	Polymorphonuclear leukocyte
RAG-/-.....	Recombinase activating gene knockout
SCID.....	Severe combined immunodeficiency
TCR.....	T cell receptor
TG.....	Trigeminal ganglion
Tg.....	Transgenic
TNF α	Tumor necrosis factor alpha
VEGF.....	Vascular endothelial growth factor

PART I

BACKGROUND AND OVERVIEW

Information provided in this chapter is a slightly modified version of a review article accepted for publication in the *Microbes and Infection* published by Partha Sarathi Biswas and Barry T. Rouse.

Biswas, P. S., and B. T. Rouse. Early events in SK pathogenesis- setting the stage for a blinding disease. *Microb. Infection*. In press.

My contributions in this review include (1) selection of the topic (2) compilation of information data analysis and interpretation (3) plan review outline (4) writing (5) preparation of figures and manuscript editing.

INTRODUCTION

On the basis of the fact that 80% or more of the adult human populations may be sero-positive for herpes simplex virus (HSV), this virus must be judged as a highly successful pathogen. Furthermore, the virus kills very few patients and most who suffer lesions recover without significant complications. However, when the eye becomes the site of infection, a chronic immuno-inflammatory syndrome may result that impairs vision (1). Such herpetic stromal keratitis (SK) lesions represent the commonest infectious cause of blindness in the western world. It is estimated that in USA, 400,000 persons are affected, with 20,000 new cases of SK occur annually; the incidences ranges from 4.1- 20.7 cases/100,000 patient years (2). In humans, SK is usually the sequel to recurrent infection following reactivation of virus from the trigeminal ganglion (1). The pathogenesis of human SK is considered to involve T cell

mediated inflammatory events, a notion strongly supported by experimental studies in a mouse model (1, 3, 4, 5). In this model, the lesions are mainly orchestrated by CD4⁺ T cells (4, 5) although the identities of target antigens that drive such cells remain ill-defined. In addition, several events occur in the infected eye prior to the onset of clinically evident SK. Since such events may be subject to manipulation and the control of lesion severity, understanding early events represents an important objective for SK research. This review describes recent work from our laboratory and others, which defines multiple pathogenic mechanisms ongoing during the early phase of SK in the mouse model. We also comment about what is understood about the clinical phase of SK.

VIRUS ENTRY IN THE CORNEA

Following primary infection, herpes viruses reaching the surface of the eye are initially suspended in the ocular tear film. The key feature of ocular surface innate resistance is the constant bathing of the ocular surface by tears produced from the lachrymal gland. Thus molecules, cells and infectious agents reaching the ocular surface may be washed away quickly and effectively. In addition, virus infections are vulnerable to a number of substances with antiviral activity present in tears. These include lysozyme, immunoglobulin A antibody, complement, lactate dehydrogenase, amylase and peroxidase. Interferons, particularly alpha and beta types also occur in tears during a viral infection of the ocular surface (6- 9). The intact corneal epithelial cell layer may act as an effective physical barrier to infection by

microorganisms, and its outer terminally differentiated cells may be refractory to infection, such as by HSV (10). However, whereas this broad spectrum of defenses limits the chance of infection, agents such as HSV do establish infection usually in the epithelial layer of the cornea (11).

Successful infection by HSV induces several key events that relate to the subsequent development of ocular pathology. One such event, which in fact does not require progeny virus production, is entrance into sensory nerve terminals in the corneal epithelium. Virus then travels by retrograde transport to the neuronal cell bodies in the trigeminal ganglia (TG) (12, 13). Using a LACz encoding virus, Hill and colleagues demonstrated that, virus can reach the TG within 24 hrs of ocular infection irrespective of the viral dose used (14). In the TG, virus either replicates usually killing cells, or enters into an alternative replication mode called latency which may persist in cells indefinitely (13, 15, 16). It is also conceivable that viruses may undergo a productive cycle but this is contained in some way by signals from immune cells, primarily CD8⁺ T cells (17, 18), [19]). While the latent state, which may involve 100 more copies of the viral genome, may be permanent in many cells, in others it is terminated in response to a variety of stimuli (15, 16). When this occurs virus reenters into the productive cycle, and progeny virus passes anterograde along nerve axons to produce a recurrent bout of virus replication at the initial site of infection (13, 15). Such recurrences may be subclinical or clinical and in the eye may either give rise to secondary lesions in the epithelium or cause a chronic inflammatory reaction in the underlying stroma.

The stromal inflammatory reaction occurs in around 20% of human cases and this is the lesion that is mainly responsible for vision impairment (2). The lesion is judged to largely represent a T cell mediated immuno-inflammatory event, but details of the pathogenesis are poorly understood (3, 4). Thus it is not clear if virus itself enters the stroma and if so whether this spreads from the infected epithelial site or arrives via axonal passage from the TG. Moreover, although T cells form a prominent part of the stromal response, the nature of target antigens that are being recognized remain to be identified. Most of our understanding of the pathogenesis of SK comes from experimental studies in the mouse where the lesions regularly occur as a sequel to primary infection. Similar lesions can occur by induced reactivation (20), but this perhaps more relevant model, is difficult to establish and occurs in only a minority of animals. Our description of events in the stroma that result in the chronic blinding immuno-inflammation applies to the primary disease model and when known the natural human disease.

VIRUS AND EARLY INFLAMMATORY EVENTS

Inflammatory cells

Following virus infection of the corneal epithelium, a prominent infiltrate of inflammatory cells, primarily consisting of neutrophils (PMN) (21), occur into stromal tissues subjacent to the infected epithelium (See Fig 1) (Note all figure in appendix). The cells escape from the limbal vessels presumably in response to signaling molecules generated from virus infected cells. This response starts around 18 hr post infection (p. i.), peaks at 48 hr p. i. and then declines such

that by 5 days after infection it is barely evident (21). This pattern of events correlates with the duration of virus detection and it seems that PMN may be responsible for viral clearance (21, 22). Thus depleting PMN with specific monoclonal antibodies resulted in delayed viral clearance from the cornea. It is not clear how virus, which is predominantly in the epithelium, is cleared by the mainly stromally located PMN. Ideas for the mediation of such defenses include TNF- α , nitric oxide and reactive oxygen metabolites production by PMN. Evidence for this comes from studies where corneal neutrophils were shown to produce these factors by in situ hybridization techniques (23).

The stromal PMN response may have other consequences. For example, factors released following PMN degranulation resulted in tissue destruction which may unmask corneal autoantigens. One of these factors is NO (24). Polymorphonuclear leukocytes as well other cells in the early response, also contribute to the ongoing inflammatory process by producing proinflammatory cytokines such as IL-1 β , TNF- α , IL-8 and IL-12 (23), thus setting the stage for the subsequent chronic immunoinflammatory phase. Crucial components of PMN include a source of preformed VEGF (25), as well as the tissue degrading enzyme matrix metalloproteinase-9 (MMP-9) required to breakdown the stromal matrix (26). Both molecules are involved in the neovascularization which results from HSV infection (discussed later) (26, 27) (See Fig 2).

Although PMN dominate the early inflammatory phase, other cell types can also be demonstrated in the stroma. These include macrophages (28), dendritic cells (DC) (29, 30), natural killer cells (NK cells) (31, 32) and

$\gamma\delta$ T cells (33). NK cells and macrophages likely also participate in corneal virus clearance and can also act as a source of cytokines, chemokines and angiogenic factors (28, 31, 32). In line with this notion, depletion of NK cells and macrophages following ocular HSV-1 infection resulted in more severe SK (28, 31, 32). Another prominent feature of the injured cornea, including that caused by HSV, is the invasion of Langerhans DC, likely from the conjunctiva, into the cornea (29, 30). However this event takes several days to occur. Presumably, such cells also act as a source of cytokines and chemokines but their major function in SK pathogenesis is probably to transport viral antigens to lymphoid tissues where the adaptive immune response is initiated (discussed later). However, recent findings by Carbone group question the role of Langerhans cells for antigen presentation. They contend that such cells pass on viral proteins to other subsets of DC which process Ag by cross priming and present antigen to CD8⁺ T cells (34). At present the respective roles of these numerous nonlymphoid inflammatory cells in the early response to HSV remains unresolved. Thus past observations have focused on a single cell type and usually ignored the role of others. One suspects that a large measure of cell to cell interaction could be occurring. This could include regulatory effects mediated by natural regulators such as NKT cells. Such effects have been noted to occur in the anterior chamber (35), but have yet to be investigated in the cornea.

Cytokines

HSV infection of the cornea causes the expression of multiple proteins associated with the inflammatory response. Among the numerous cytokines that are produced IL-1 and IL-6 are prominent and these may be pivotal in starting the cascade of events that results after several days in stromal lesions (36, 37). When HSV productively infects a cell, most host gene expression is turned off (38). Nevertheless infected cells are stimulated to produce IL-1 and IL-6 at least for a time and this may represent their major initial source (39-41). However, it is evident that uninfected cells ultimately become the major cell source of cytokines. It is not clear how the uninfected cells are induced to produce cytokines but one viable idea is that pathogen associated molecular patterns (PAMPS) expressed by virus infected cells, or perhaps extracellular virus itself, could bind to Toll-like receptors (TLR) on cells and cause them to synthesize and secrete cytokines and other inflammatory mediators. With respect to HSV, there is evidence that the viral DNA may have TLR-9 stimulating activity (42) although there may be insufficient extracellular viral DNA present in vivo to subserve that function. Furthermore, recently HSV was proposed to have TLR-2 binding activity although the viral components responsible for this await identification. At least in the central nervous system (CNS), it seems that HSV, via its TLR-2 activating property, may cause IL-6 production as well as other mediators (43). We are investigating this issue in the cornea where we anticipate that TLR-2 binding may be a critical stimulus for IL-1 production.

Whereas PAMPS may be important for initiating the inflammatory protein cascade, it also seems likely that the initial cytokines induced are also involved in driving the expression of other key molecules. Thus IL-1 can cause IL-6 production from uninfected epithelial cells (44), and IL-6 is known to induce macrophage inflammatory protein-2 (MIP-2) (CXCL8), likely a key molecule for PMN recruitment in the stroma (45, 46). This issue has been extensively studied by us and others using IL-6^{-/-} mice (46), CXCR2^{-/-} mice (47) and neutralization of MIP-2 using specific monoclonal antibody (45). In all these studies PMN ingress to the corneal stroma was shown to be severely compromised (45-47). In addition, IL-1 was also shown to influence PMN migration and via its stimulation of IL-6 expression (44). In line with this observation, mice transgenic for the IL-1 receptor antagonist protein showed a diminished early inflammatory response (48).

In addition to IL-6, another factor known to be upregulated in corneal stromal cells following IL-1 stimulation is Cyclooxygenase-2 (COX-2) (our unpublished data). COX-2 induced proinflammatory prostanoid synthesis such as prostaglandin E₂ (PGE₂) can cause PMN invasion in various inflammatory models (49). Corneal fibroblasts may act as a major cellular source of COX-2 (our unpublished data). Possible agonists that drive COX-2 production at an early time point include proinflammatory cytokines such as IL-1 β and TNF- α (our unpublished data). Thus blocking COX-2 activity at an early time point with a specific COX-2 inhibitor diminished PMN influx and resulted in less SK severity (our unpublished data). Another cytokine known to be upregulated following ocular HSV infection is TNF- α (50, 51). Recent studies

have demonstrated that TNF- α -/- mice were more susceptible to acute corneal HSV-1 infection than controls, as manifested by an increased ocular virus titers and mortality rate (51).

Another early cytokine event that may be pivotal in the pathogenesis of SK is IL-12. Our group was the first to demonstrate that a viral infection may cause IL-12 production (52). Using a sensitive radioimmunoassay, IL-12 transcripts were detected in HSV infected corneas as early as 1 day p. i., with peak levels around day 3 p. i. and sustained production until at least day 22 p. i. (52, 53). That IL-12 production is an important event was best shown by the observation that both p35-/- and p40-/- mice develop only mild lesions of HSK (54). However, it is still unclear how HSV infection induces IL-12 production. The best evidence is that the event is largely a paracrine one (53) but the identity of the stimulus for IL-12 production by uninfected cells remains to be identified. Possible mediators under consideration include cytokines, chemokines, stress proteins, and viral products released from infected cells. With regard to the latter, virions themselves would seem to be unlikely candidates, as UV-inactivated virus and fixed cells expressing viral proteins caused only minimal IL-12 induction (53). Another candidate could be viral DNA, a source of DNA rich in potentially bioactive CpG motifs known to be potent IL-12 inducers (55), but such issues await confirmation. The inflammatory cells such as PMN and macrophages, but not corneal resident cells, are the likely source of IL-12 following viral infection (23, 53).

The cytokine IL-12 has several downstream effects that have impact on SK pathogenesis. These include production of IFN- γ by cells with IL-12

receptors. Although not proven in eye, the most likely cells that respond and produce IFN- γ are NK cells, macrophages and neutrophils. Removal of each cell type may compromise the ability to clear virus from the cornea and CNS (22, 28, 31). Furthermore, IL-12 transgenic mice clear virus quickly by upregulating IFN- γ production in the cornea (56, 57). Previous observations suggest the role of STAT 4 dependent pathway in the production of IFN- γ following IL-12 stimulation (57). Supporting this scheme we were able to demonstrate that STAT4^{-/-} mice have lower levels of IFN- γ in the cornea following virus infection (our unpublished data). Whatever the source of IFN- γ is, this molecule appears to be pivotal in antigen processing as well as other events in HSK pathogenesis. These include aiding PMN influx in the corneal stroma by up-regulating PECAM-1 (Platelet endothelial cell adhesion molecule-1) expression on vascular endothelial cells (9). Conceivably, neutralization of PECAM-1 or IFN- γ resulted in diminished PMN ingress (9). In addition, in vitro stimulation of human corneal epithelial cells with IFN- γ caused upregulation of ICAM-1 expression, another cell adhesion molecule responsible for adhesion and extravasation of inflammatory cells (58). IFN- γ also upregulates MHC II expression on antigen presenting cells (APC) involved in the induction of antigen specific CD4⁺ T cells in the draining lymph nodes (59). Interestingly, murine stromal fibroblasts can express MHC II and present antigen following stimulation with IFN- γ (60). On the other hand, IFN- γ could help modulate lesion development since it also induces angiostatic chemokines such as IP-10 (CXCL10) (61). Thus, IL-12 and IFN- γ

response to HSV infection indirectly impacts on both inflammatory and regulatory effects during SK.

Another cytokine that deserves attention in SK pathogenesis is IL-17. Recent work by the Verjans group has demonstrated the presence of IL-17 and its role in PMN influx in human SK (62). In this report, IL-17 was shown to influence PMN infiltration through upregulation of IL-6 and IL-8 (62). In addition IL-17 might stimulate VEGF production and aid in the angiogenesis process (63) (discussed later). However, the cellular source as well as the stimulus of IL-17 in infected corneas remains ill-defined. One possibility is IL-23, which is well known to induce IL-17 from a variety of cell types in various inflammatory models (64). Usually IL-23 acts to induce IL-17 in lymphocytes, which in the HSV infected cornea, do not enter the cornea until 6-7 days p. i. (64). However since IL-23 and IL-17 producing CD4⁺ T cells were shown to be crucial events in some other chronic inflammatory conditions, their role in various stages of herpetic keratitis merits further investigation.

Much remains to be established with regard to cytokine expression and function during the early phase of ocular infection with HSV. One crucial step for the pathogenesis of SK that is initiated early after infection is neovascularization of the normally avascular cornea. As is discussed later, several cytokines may participate in the angiogenesis process by acting as stimulants for the induction of angiogenesis factors; some cytokines, however, may exert antiangiogenic activities (See Fig 2).

Chemokines

Following viral replication in the epithelial layer, several chemokine mRNAs are promptly upregulated in the cornea (65, 66). The fact that viral replication for an initial few days is essential has been established by showing feeble chemokine responses if virus was neutralized with antibodies (65) or corneas were infected with UV inactivated or replication incompetent mutant virus (67). The cellular source of chemokine and the nature of the induction stimuli remain ill-defined. Cells infected by the virus are the most logical candidate source, but once virus replication is well underway in a cell, host cell mRNA is curtailed (38). Some evidence does exist however, that the viral immediate early protein ICP0 is all that is necessary to induce chemokines expression (67). An alternate cellular source is the nearby corneal resident cells as well as inflammatory cells that are exposed to products from HSV infected cells. This issue of cellular source of various chemokines in HSV infected eye must await the refinement of approaches such as in situ hybridization and double color immunohistochemistry to study this topic.

Early after HSV infection CXC chemokines such as MIP-2 and KC (CXCL3) were shown to predominate (65, 67). In addition MCP-1 (CCL2), RANTES (CCL5), IP-10 (CXCL10) was also present (65). Recently one group demonstrated that corneal epithelial cells and stromal keratocytes express MIP-3 α (CCL20) mRNA and protein following ocular HSV-1 infection (68). Despite the representations of multiple chemokine during early HSV infection, some studies do indicate that single chemokines may be crucial for SK pathogenesis. Thus the Lausch group demonstrated that neutralization of the

CXC chemokine MIP-2 markedly suppressed the initial PMN influx (45). Even more significant suppression was obtained when both KC and MIP-2 were neutralized together (45). These observations were in fact supported by our own finding using CXCR2^{-/-} mice. These mice demonstrated significantly reduced PMN invasion at an early time point (47). However, the induction stimulus for these chemokines seemed to be proinflammatory cytokines produced as a consequence of virus replication in the corneal epithelium. We also know that IL-6 promotes MIP-2 production from resident cells in an autocrine- paracrine manner (44). In addition, corneal epithelial cells and stromal cells produce CCL20 following stimulation with IL-1 β and TNF- α (68). It will be important to determine what functions chemokines such as these are playing during the early phase. One possibility is that they serve to attract inflammatory cells that in turn also act as a source of chemokines.

An additional group of chemokines that lacks expression during the early inflammatory phase but are expressed during late preclinical phase are MIP-1 α (CCL3) and lymphotactin (XCL1) (67). What causes upregulation of these is not known, but they are likely responsible for CD4⁺ T cells influx during the clinical phase. Supporting this notion Lausch and his colleagues demonstrated that MIP-1 α ^{-/-} mice fail to show the secondary inflammatory cell influx and do not develop SK (69). In addition, neutralization of MIP-1 α , or the application of IL-10 which abrogates MIP-1 α production, resulted in diminished SK severity (70). However mechanistic explanations for these observations have not been provided. Another unresolved issue in SK pathogenesis includes an explanation for the markedly preferential invasion by

CD4⁺ T cells versus CD8⁺ T cells to the infected cornea. This issue is currently under investigation in our laboratory (discussed later).

VIRUS AND ANGIOGENESIS

One characteristic of HSV induced immunopathology is neovascularization of the cornea, an event shown necessary for SK pathogenesis (27). Whereas the normal cornea is avascular, in SK new blood vessels sprout from limbal vessels by day 1 p. i. reaching the central cornea by day 20 p. i. (71). Inflammatory cells readily escape from these highly permeable neovessels, giving rise to haze and vision impairment. Indeed neovascularization anywhere along the visual axis may impair vision, with vessel removal being highly problematic.

Although the cornea has been a favorite tissue to study angiogenesis, the identity of specific angiogenic factors involved in corneal neovascularization associated with HSV replication remains in its infancy. Curiously HSV replication in the epithelium results in angiogenesis in the underlying stroma. Furthermore unlike some other viruses, most notably human herpes virus 8 (72-75) and Orf virus (76), HSV appears not to encode proteins which are themselves directly angiogenic. In consequence, the means by which HSV infection results in angiogenesis likely involves a cascade of cytokine mediated or other paracrine events. These events in turn are assumed to cause expression of one or more proteins directly involved in angiogenesis. Our group has gathered support for these ideas. We have shown, for example, that HSV infection is followed by the expression of several known

angiogenesis factors in the cornea. These include Vascular endothelial growth factor (VEGF) (71), basic Fibroblast growth factor (bFGF) (our unpublished data), Matrix metalloproteinase 9 (MMP-9) (26) and E-L-R motif containing chemokines (47, 65, 67).

In SK, VEGF mediated angiogenesis is a prominent and early feature of the pathogenesis, with VEGF transcripts detectable by 12 hr p. i. and proteins by 24 hr p. i. (71). Such observations imply a role for VEGF in HSV induced angiogenesis; a notion supported by the fact that treatment of mice with a VEGF inhibitor resulted in reduced HSV induced angiogenesis (71). In addition, turning off VEGF and VEGF receptor 2 gene expressions using small interfering RNA (siRNA) resulted in diminished angiogenic responses following virus infection (77). In consequence, these mice demonstrated less severe SK (77). While looking for the cellular source of VEGF initially after infection, uninfected corneal epithelial cells and stromal cells were shown to be involved (71). However, with the infiltration of inflammatory cells, such as PMN and macrophages, these cells act as an additional and perhaps the major source of VEGF (71). Interestingly, the production of VEGF appeared to be a paracrine effect of molecules released from virus infected cells, since uninfected corneal cells and not infected cells stained positive for VEGF. As seen in corneal tissue sections, the VEGF producing cells were close to infected cells but were seldom infected themselves (71).

The above observations raise the question as to the mechanisms by which HSV infection of a cell triggers another cell to turn on VEGF gene expression. Although productive HSV infection, by virtue of its virion host

shut-off protein, eliminates most host cell protein synthesis (38), evidence suggests that some proinflammatory cytokine genes such as IL-1 and IL-6 are upregulated for a time in infected cells ((39-41). These cytokines are known to be potent stimulators of VEGF production (78-81). In addition, intrastromal injection of IL-1 and IL-6 results in corneal neovascularization in a VEGF dependent manner, since neutralizing VEGF with a monoclonal antibody resulted in a significant reduction in the angiogenesis process (44, 47). Supporting this scheme, we could demonstrate that blocking IL-1 with an IL-1 receptor antagonist protein resulted in compromised angiogenesis following ocular HSV infection (48).

An additional paracrine stimulus for VEGF production may be HSV DNA, rich in bio-active CpG motifs. Our group was the first to demonstrate that bioactive CpG motifs can induce corneal angiogenesis by upregulating VEGF, indicating an essential role for TLR-9 mediated signaling events (82). However, the exact mechanism of VEGF upregulation is not fully understood. One possibility is HSV CpG TLR 9 interaction induces a signal transduction mechanism that proceeds through a MyD88 dependent or independent pathway to activate various transcription factors such as NF κ B. An alternative idea to explain this issue is that bioactive CpG ODN induces the production of cytokines such as IL-1 and IL-6, which in turn upregulate VEGF production. Such notions await confirmation.

Since certain chemokines with E-L-R motifs are well known to have angiogenic activity (83), these also represent likely candidates for induction of ocular angiogenesis. One such chemokine known to be upregulated following

ocular HSV infection is MIP-2 (47, 65, 70). Curiously, other chemokines such as some CXC chemokines lacking the E-L-R motif, may inhibit angiogenesis (84). Some of the angiostatic chemokines exert their function by binding to heparan sulphate on target cells (85). Interestingly, heparan sulphate is also a molecule involved in HSV entry into target cells (86). Thus, it is conceivable that HSV may bind heparan sulphate and block the angiostatic activity thus driving the process towards angiogenesis. These issues are currently under investigation in our lab.

Another molecular species involved in HSV induced angiogenesis was the collagenase MMP-9, an enzyme that degrades the stromal matrix material. MMP-9 has been associated with tumor angiogenesis (87, 88), but the first evidence that MMP-9 contributes to corneal angiogenesis came from our laboratory (26). The cellular source of MMP-9 was shown to be PMN, since depletion of cells resulted in diminished MMP-9 levels in corneal extracts (26). It appears that targeting MMP-9 production with for example siRNA can result in diminished corneal angiogenesis (89). In addition to PMN, corneal epithelial cells may produce MMP-9 in response to inflammatory cytokines such as IL-1 and TNF α (90).

While the majority of the proinflammatory cytokines are indirectly involved in the corneal angiogenesis process, evidence accumulates to indicate that some cytokines such as IL-12 (61) and IL-18 (our unpublished data) inhibit corneal angiogenesis by downregulating VEGF expression. Thus overexpression of these cytokines in the cornea following virus infection resulted in diminished angiogenesis and less severe HSK (Lee *et al*, 2002a)

(61). It seemed that IL-12 and IL-18 through their inhibitory effect act as negative regulators and keep the neovascularization process under a tight control following virus infection.

As is well known in both the fields of ocular pathology and cancer biology, it is easier to prevent angiogenesis than removing already established blood vessels. Thus early targeting of the angiogenesis process is essential because inhibition of neovascularization has no benefit in terms of HSK lesions if the vascular bed has already developed (71). To achieve a satisfactory level of angiogenesis inhibition, currently the best bet might be to use a combination of approaches and a variety of angiogenic molecules need to be targeted. These include direct inhibition of VEGF and MMP-9 using a combination of the VEGF antagonist (mFlt-immunoglobulinG) (71) and the Tissue inhibitor of metallo proteinase 1 (TIMP-1) (26) or indirectly control angiogenesis by limiting inflammation using anti-inflammatory drugs such as the IL-1 receptor antagonist protein (48) and COX-2 inhibitors (our unpublished data). A promising new candidate for therapeutic applications is the recently used siRNA targeted against various angiogenic factors in the cornea (77). However a major constraint in all these approaches includes the lack of effective corneal delivery systems. So far, practical methods to achieve efficient corneal delivery of antiangiogenic molecules are not on hand, but given the extensive level of investigation in this area of research, success is to be anticipated.

STROMAL KERATITIS – THE OUTCOME OF INFECTION

Following the early events described previously which usually include the cessation of viral replication and the removal of readily demonstrable viral antigens from the eye, lymphocytes and other inflammatory cells invade the stroma producing clinically evident SK. This process usually begins 6-9 days p. i. and the cellular responses are at their peak around 2-3 week p. i (91). Few studies have followed lesions for long periods to note subsequent changes in the inflammatory response. However observations on human lesions indicate that they usually fail to resolve spontaneously, and require prolonged treatment with anti-inflammatory drugs (11, 92). The pathogenesis of SK provides us with several unresolved questions. Among the most difficult to explain is what drives the inflammatory reaction after the virus infection itself appears to have been contained. Moreover, it is difficult, if not impossible, to generate SK either with inactivated viral preparations or indeed with nonvirulent mutant viruses (93). In our hands, replication by wild type viruses is necessary for at least 2 days to induce SK (94). Furthermore, so far we have been unable to cause SK by introducing antigen into the corneal stroma of animals with adoptively transferred antigen reactive T cells.

It seems that replicating virus is necessary to drive the array of early events described previously which are essential for SK development. However, neither replicating virus, nor as far as we can measure, persistent viral antigen in the cornea, is involved in driving the chronic immunoinflammatory phase (93). Presumably, early events leave the corneal stroma in a condition that attracts inflammatory cells with these recruits perhaps further

activated to participate in tissue damage. We know that one step necessary for this event to occur is neovascularization, driven by VEGF and other angiogenesis factors (26, 27, 71). Moreover, new blood vessels induced by VEGF are quite permeable and readily leak vascular contents. In the stroma, this leakiness cannot be random, since the majority of inflammatory cells in the site express homing molecules such as the integrin VLA-4 (95). In addition, in mouse SK lesions, inflammatory CD4⁺ T lymphocytes outnumber CD8⁺ T cells (96). This observation cannot be explained by a failure of the HSV infection to activate a CD8⁺ T cell population. In fact, at least in the C57BL6 mouse, HSV infection activates a higher frequency of CD8⁺ than CD4⁺ T cells, yet even in such mice demonstrating CD8⁺ T cells in SK lesions are problematic (96). Furthermore, even adoptive transfers of transgenic CD8⁺ T cells that recognize viral antigen are difficult to demonstrate in the corneal lesions (96). Curiously, viral specific CD8⁺ T cells are readily demonstrable in other inflammatory reactions caused by HSV such as in the TG (97). Reasons why CD8⁺ T cells sparsely infiltrate stromal lesions need to be found.

With regard to the CD4⁺ population that forms part of the SK lesions, the spectrum of antigens such cells recognize remains unknown. We anticipate that viral antigens are the targets for some CD4⁺ T cells especially early during the reaction, although this point has not been confirmed. What is known is that CD4⁺ T cells are needed to generate lesions (98, 99). Furthermore, the inflammatory function of CD4⁺ T cells can be modulated by other subsets of CD4⁺ T cells that exert regulatory function (95). This seemingly IL-10

producing function is assumed to be viral antigen specific, but this issue has also not been firmly established.

Clearly the role of viral antigen in driving specific CD4⁺ T cells in stromal lesions requires further study. In fact using TCR transgenic mice on a SCID or RAG background that were unable to recognize viral antigens, SK could be induced in these mice although as in immunocompetent animals, this only occurred following infection with replication competent virus (100, 101). In these TCR transgenic models, even administering the cognate antigen into the cornea failed to induce SK. Hence in this model too, we are left with the dilemma of explaining why it is necessary to administer infectious virus in order to generate SK lesions. Conceivably, the T cells involved may recognize a wide range of antigens which could include autoantigens unmasked in the cornea by the inflammatory response.

One favored explanation to explain the pathogenesis of SK is that the lesions may be initiated by viral damage but subsequently they become autoinflammatory (102) (See Fig 3). This concept explains that the virus replication somehow unmasks autoantigens in the eye and additionally stimulates an antiviral T cell response that is cross-reactive with the corneal autoantigens. The best evidence for this notion comes from the Cantor laboratory, which maintains that the UL6 protein of HSV acts as a molecular mimic for a corneal auto-peptide (103). This provocative hypothesis has not been independently confirmed and our laboratory and others have raised questions about the interpretation (104). Indeed molecular mimicry as an

explanation for an association between virus and any autoimmune disease has been difficult to prove.

If molecular mimicry is not an explanation for SK pathogenesis, conceivably some form of sustained bystander activation of T cells could be involved. However currently this intriguing notion lacks a mechanistic explanation of where and how such bystander activation takes place. One possibility is that inflammatory molecules produced as a consequence of ocular HSV infection activate the T cells in a non TCR mediated manner (See Fig 4A). This idea is supported by the observation that it is possible to develop lesions identical to HSK in animals whose T cells are genetically incapable of recognizing viral antigens (94, 105). In these models, the chronic source of activating cytokines was cells dying of HSV infection. In this instance, virus persisted and spread to the stromal tissue location in some way (94, 101). We have hypothesized that, this continually replicating virus in the corneal stroma acts, possibly by TLR ligand activity, as the chronic stimulus for cytokine /chemokine production that in turn activates the incoming T cells. Such cells then produce inflammatory mediators which participate in tissue damage.

The conclusion is that the stromal viral persistence is necessary, but the mechanistic explanation for the source of virus is controversial. The possibilities include direct cell-to-cell spread from corneal epithelium to stroma or virus reactivation from the TG. Previous work from our group using a thymidine kinase knock out (tk^{-/-}) virus (virus unable to reactivate in TG) demonstrated that viral antigens were undetectable in the corneal stroma and lesions were minimal (94). This observation indicates that the source of virus

in the corneal stroma is from the TG, an interpretation further supported using an Us9^{-/-} mutant virus that retains normal peripheral virulence but fails to transport anterograde after any reactivation (personal communication with Dr, David Johnson, Oregon Health Centre). We observed that irrespective of the dose used, Us9^{-/-} virus failed to arrive in the corneal stroma and the mice had diminished, although not absent SK lesions (our unpublished data). These results support a mechanistic role for stromal virus in the bystander model but do not reveal how such virus contributes to the inflammatory effect. We are currently evaluating the role of a number of candidate mechanisms. These include the PAMP effect, superantigen expression and inflammatory reactions driven by stress proteins

In immunocompetent animals, it could be that HSV induces SK indirectly in a “hit and run” fashion. Thus virus replication might only serve to set off an inflammatory and angiogenic response that becomes sustained without the further participation of virus. Should this be the case, then HSV induced immunopathological lesion differs from most viral immunopathologies since viral persistence is the normal circumstance. Our view is that HSV replication is required to marshal a complex of events, which we term the “alarm complex”. This collage of molecules serves directly or indirectly to signal the ingress and subsequent activation of neutrophils and DCs in the stroma and angiogenic sprouting from the limbal blood vessels. The PMN are activated to release more proangiogenic and angiogenic factors that expand the vascular bed. Once sufficient in extent, these leaky vessels act as conduits for T cells which now include the HSV specific T cells from

lymph nodes. Meanwhile, viral antigens are taken up and processed by DCs which present them to viral antigen specific CD4⁺ T cells. These respond by releasing more inflammatory mediators which serve to recruit and activate additional T cells, most of which are now not HSV specific and some of which may be autoreactive. These recruits release more inflammatory molecules (bystander activation) in a positive feedback loop that gradually ceases as levels of activators fall and terminators increase (Fig 4B, 5). The stroma is left with a damaged matrix and unwanted vascular bed that is slow to resolve. Current studies are ongoing to verify this pathogenesis scheme of events.

CONCLUSION

In conclusion, the pathogenesis of SK, as revealed by animal studies, is complex. Virus replication is necessary for the lesions but may not be directly involved in driving the chronic immunopathology. Many early events caused by virus have been identified and shown to form part of the process. The mystery remains as to mechanistic events which account for the chronic progressive lesion that impairs vision. One hopes that understanding this process could reveal clues that may help control this unfortunate disease.

SPECIFIC AIMS AND RATIONALE

Studies with the mouse model for HSK have revealed the involvement of complex cellular and molecular mechanisms in its pathogenesis. Several areas, both in the clinical and pre-clinical phase, require further elucidation. These include viral replication, the early proinflammatory events, innate and

adaptive immune cell influx and neovascularization of the avascular cornea. Understanding these early events is critical, since many of these early events are subject to modulation providing an approach to controlling this important cause of human blindness. Studies described here have been aimed at understanding the above mechanisms further.

LIST OF REFERENCES

LIST OF REFERENCES

1. Streilein, J. W., M. R. Dana, and B. R. Ksander. 1997. Immunity causing blindness: five different paths to herpes stromal keratitis. *Immunol. Today* 18: 443.
2. Pepose, J. D., in: J. S. Pepose, G. N. Holland, K. R. Wilhelmus (Eds.), Herpes simplex virus diseases: Anterior segment of the eye. *In Ocular Infection and Immunity, Mosby, St Louis, 1996, pp. 905-932.*
3. Metcalf, J. F., D. S. Hamilton, and R. W. Reichert. 1979. Herpetic keratitis in athymic (nude) mice. *Infect. Immun.* 26:1164.
4. Russell, R. G., M. P. Nasisse, H. S. Larsen, and B. T. Rouse. 1984. Role of T-lymphocytes in the pathogenesis of herpetic stromal keratitis. *Invest. Ophthalmol. Vis. Sci.* 25:938.
5. Mercadal, C. M., D. M. Bouley, D. DeStephano, and B. T. Rouse. 1993. Herpetic stromal keratitis in the reconstituted *scid* mouse model. *J Virol.* 67:3404.
6. Kaufman, H. E., R. F. Meyer, P. R. Laibson, S. R. Waltman, A. B. Nesburn, and J. J. Shuster. 1976. Human leukocyte interferon for the prevention of recurrences of herpetic keratitis. *J Infect. Dis.* 133 Suppl A:165.
7. Hendricks, R. L., P. C. Weber, J. L. Taylor, A. Koumbis, T. M. Tumpey, and J. C. Glorioso. 1991. Endogenously produced interferon alpha protects mice from herpes simplex virus type 1 corneal disease. *J Gen. Virol.* 72 (Pt 7):1601.

8. Babu, J. S., S. Kanangat, and B. T. Rouse. 1995. T cell cytokine mRNA expression during the course of the immunopathologic ocular disease herpetic stromal keratitis. *J Immunol.* 154:4822.
9. Tang, Q., and R. L. Hendricks. 1996. Interferon gamma regulates platelet endothelial cell adhesion molecule 1 expression and neutrophil infiltration into herpes simplex virus-infected mouse corneas, *J Exp. Med.* 184: 1435.
10. Klyce, S. D., and R. W. Beuerman, in: H. E. Kaufman, B. A. Barron, M. B. McDonald, (Eds.), Structure and function of the cornea, *The Cornea. Boston, Butterworth-Heinemann, 1998, pp.3–50.*
11. Deshpande, S., K. Banerjee, P. S. Biswas, and B. T. Rouse. 2004. Herpetic eye disease: immunopathogenesis and therapeutic measures. *Expert Rev. Mol. Med.:1.*
12. Knotts, F. B., M. L. Cook, and J. G. Stevens. 1974. Pathogenesis of herpetic encephalitis in mice after ophthalmic inoculation. *J Infect. Dis.* 130:16.
13. Enquist, L. W., P. J. Husak, B. W. Banfield, and G. A. Smith. 1998. Infection and spread of alphaherpesviruses in the nervous system. *Adv. Virus Res.* 51:237.
14. Shimeld, C., S. Efstathiou, and T. Hill. 2001. Tracking the spread of a lacZ-tagged herpes simplex virus type 1 between the eye and the nervous system of the mouse: comparison of primary and recurrent infection. *J Virol.* 75:5252.

15. Fraser, N. W., and T. Valyi-Nagy. 1993. Viral, neuronal and immune factors which may influence herpes simplex virus (HSV) latency and reactivation. *Microb. Pathog.* 15 :83.
16. Wagner, E. K., and D. C. Bloom. 1997. Experimental investigation of herpes simplex virus latency. *Clin. Microbiol. Rev.* 10:419.
17. Liu, T., K. M. Khanna, X. Chen, D. J. Fink, and R. L. Hendricks. 2000. CD8(+) T cells can block herpes simplex virus type 1 (HSV-1) reactivation from latency in sensory neurons. *J Exp. Med.* 191:1459.
18. Liu, T., K. M. Khanna, B. N. Carriere, and R. L. Hendricks. 2001. Gamma interferon can prevent herpes simplex virus type 1 reactivation from latency in sensory neurons. *J Virol.* 75:11178.
19. Khanna, K. M., A. J. Lepisto, V. Decman, and R. L. Hendricks. 2004. Immune control of herpes simplex virus during latency. *Curr. Opin. Immunol.* 16:463.
20. Shimeld, C., T. Hill, B. Blyth, and D. Easty. 1989. An improved model of recurrent herpetic eye disease in mice. *Curr Eye. Res.* 8:1193.
21. Thomas, J., S. Gangappa, S. Kanangat, and B. T. Rouse. 1997. On the essential involvement of neutrophils in the immunopathologic disease: herpetic stromal keratitis. *J Immunol.* 158:1383.
22. Tumpey, T. M., S. H. Chen, J. E. Oakes, and R. N. Lausch. 1996. Neutrophil-mediated suppression of virus replication after herpes simplex virus type 1 infection of the murine cornea. *J Virol.* 70:898.

23. Daheshia, M., S. Kanangat, and B. T. Rouse. 1998. Production of key molecules by ocular neutrophils early after herpetic infection of the cornea. *Exp. Eye Res.* 67:619.
24. Mistry, S. K., M. Zheng, B. T. Rouse, and S. M. Jr. Morris. 2001. Induction of arginases I and II in cornea during herpes simplex virus infection. *Virus Res.* 73:177.
25. Scapini, P., F. Calzetti, and M. A. Cassatella. 1999. On the detection of neutrophil-derived vascular endothelial growth factor (VEGF). *J Immunol. Methods* 232:121.
26. Lee, S., M. Zheng, B. Kim, and B. T. Rouse. 2002b. Role of matrix metalloproteinase-9 in angiogenesis caused by ocular infection with herpes simplex virus. *J Clin. Invest.* 110:1105.
27. Zheng, M., M. A. Schwarz, S. Lee, U. Kumaraguru, and B. T. Rouse. 2001b. Control of stromal keratitis by inhibition of neovascularization. *Am. J Pathol.* 159:1021.
28. Bauer, D., S. Mrzyk, N. van Rooijen, K. P. Steuhl, and A. Heiligenhaus. 2000. Macrophage-depletion influences the course of murine HSV-1 keratitis. *Curr. Eye Res.* 20:45.
29. Jager, M. J., S. Atherton, D. Bradley, and J. W. Streilein. 1991. Herpetic stromal keratitis in mice: less reversibility in the presence of Langerhans cells in the central cornea. *Curr. Eye Res.* 10:69.
30. Jager, M. J., D. Bradley, S. Atherton, and J. W. Streilein. 1992. Presence of Langerhans cells in the central cornea linked to the development of ocular herpes in mice. *Exp. Eye Res.* 54:835.

31. Tamesis, R. R., E. M. Messmer, B. A. Rice, J. E. Dutt, and C. S. Foster. 1994. The role of natural killer cells in the development of herpes simplex virus type 1 induced stromal keratitis in mice. *Eye* 8:98.
32. Bouley, D. M., S. Kanangat, and B. T. Rouse. 1996. The role of the innate immune system in the reconstituted SCID mouse model of herpetic stromal keratitis. *Clin. Immunol. Immunopathol.* 80:23.
33. Inoue, T., Y. Inoue, R. Kosaki, K. Nishida, Y. Shimomura, Y. Tano, and K. Hayashi. 2001. Immunohistological study of infiltrated cells and cytokines in murine herpetic keratitis. *Acta. Ophthalmol. Scand.* 79:484.
34. Allan, R. S., C. M. Smith, G. T. Belz, A. L. van Lint, L. M. Wakim, W. R. Heath, and F. R. Carbone. 2003. Epidermal viral immunity induced by CD8alpha+ dendritic cells but not by Langerhans cells. *Science* 301:1925.
35. Faunce, D. E., K. H. Sonoda, J. Stein-Streilein. 2001. MIP-2 recruits NKT cells to the spleen during tolerance induction. *J Immunol.* 166:313.
36. Staats, H. F., and R. N. Lausch. 1993. Cytokine expression in vivo during murine herpetic stromal keratitis. Effect of protective antibody therapy. *J Immunol.* 151:277.
37. Lausch, R. N., S. H. Chen, T. M. Tumpey, Y. H. Su, and J. E. Oakes. 1996. Early cytokine synthesis in the excised mouse cornea. *J Interferon Cytokine Res.* 16:35-40.
38. Kwong, A. D., and N. Frenkel. 1989. The herpes simplex virus virion host shutoff function. *J Virol.* 63:4834.

39. Kanangat, S., J. S. Babu, D. M. Knipe, and B. T. Rouse. 1996a. HSV-1-mediated modulation of cytokine gene expression in a permissive cell line: selective upregulation of IL-6 gene expression. *Virology* 219:295.
40. Tran, M. T., D. A. Dean, R. N. Lausch, and J. E. Oakes. 1998. Membranes of herpes simplex virus type-1-infected human corneal epithelial cells are not permeabilized to macromolecules and therefore do not release IL-1alpha. *Virology* 244:74.
41. Paludan, S. R. 2001. Requirements for the induction of interleukin-6 by herpes simplex virus-infected leukocytes. *J Virol.* 75: 8008.
42. Lund, J., A. Sato, S. Akira, R. Medzhitov, and A. Iwasaki. 2003. Toll-like receptor 9-mediated recognition of Herpes simplex virus-2 by plasmacytoid dendritic cells. *J Exp. Med.* 198:513.
43. Kurt-Jones, E. A., M. Chan, S. Zhou, J. Wang, G. Reed, R. Bronson, M. M. Arnold, D. M. Knipe, and R. W. Finberg. 2004. Herpes simplex virus 1 interaction with Toll-like receptor 2 contributes to lethal encephalitis. *Proc. Natl. Acad. Sci. U S A* 101:1315.
44. Biswas, P. S., K. Banerjee, B. Kim, and B. T. Rouse. 2004a. Mice transgenic for IL-1 receptor antagonist protein are resistant to herpetic stromal keratitis: possible role for IL-1 in herpetic stromal keratitis pathogenesis. *J Immunol.* 172:3736.
45. Yan, X. T., T. M. Tumpey, S. L. Kunkel, J. E. Oakes, and R. N. Lausch. 1998. Role of MIP-2 in neutrophil migration and tissue injury in the herpes simplex virus-1-infected cornea. *Invest. Ophthalmol. Vis. Sci.* 39:1854.

46. Fenton, R. R., S. Molesworth-Kenyon, J. E. Oakes, and R. N. Lausch. 2002. Linkage of IL-6 with neutrophil chemoattractant expression in virus-induced ocular inflammation. *Invest. Ophthalmol. Vis. Sci.* 43:737.
47. Banerjee, K., P. S. Biswas, B. Kim, S. Lee, and B. T. Rouse. 2004a. CXCR2^{-/-} mice show enhanced susceptibility to herpetic stromal keratitis: a role for IL-6-induced neovascularization. *J Immunol* 172:1237.
48. Biswas, P. S., K. Banerjee, M. Zheng, and B. T. Rouse. 2004b. Counteracting corneal immunoinflammatory lesion with interleukin-1 receptor antagonist protein. *J Leukoc. Biol.* 76:868.
49. Linton, M. F., and S. Fazio. 2004. Cyclooxygenase-2 and inflammation in atherosclerosis. *Curr. Opin. Pharmacol.* 4:116.
50. Keadle, T. L., N. Usui, K. A. Laycock, J. K. Miller, J. S. Pepose, and P. M. Stuart. 2000. IL-1 and TNF-alpha are important factors in the pathogenesis of murine recurrent herpetic stromal keratitis. *Invest. Ophthalmol. Vis. Sci.* 41:96.
51. Minagawa, H., K. Hashimoto, and Y. Yanagi. 2004. Absence of tumour necrosis factor facilitates primary and recurrent herpes simplex virus-1 infections. *J Gen. Virol.* 85 :343.
52. Kanangat, S., J. Thomas, S. Gangappa, J. S. Babu, and B. T. Rouse. 1996b. Herpes simplex virus type 1-mediated up-regulation of IL-12 (p40) mRNA expression. Implications in immunopathogenesis and protection. *J Immunol.* 156:1110.

53. Kumaraguru, U., and B. T. Rouse. 2002. The IL-12 response to herpes simplex virus is mainly a paracrine response of reactive inflammatory cells. *J Leukoc. Biol.* 72:564.
54. Osorio, Y., S. L. Wechsler, A. B. Nesburn, and H. Ghiasi. 2002. Reduced severity of HSV-1-induced corneal scarring in IL-12-deficient mice. *Virus Res.* 90:317.I
55. Bradford, M., A. J. Schroeder, H. C. Morse 3rd, S. N. Vogel, and J. S. Cowdery. 2002. CpG DNA induced IL-12 p40 gene activation is independent of STAT1 activation or production of interferon consensus sequence binding protein. *J Biomed. Sci.* 9:688..
56. Al-Khatib, K., I. L. Campbell, and D. J. Carr. 2002. Resistance to ocular herpes simplex virus type 1 infection in IL-12 transgenic mice. *J Neuroimmunol.* 132:41.
57. Lund, R. J., Z. Chen, J. Scheinin, and R. Lahesmaa. 2004. Early target genes of IL-12 and STAT4 signaling in th cells. *J Immunol.* 172:6775.
58. Yannariello-brown, J., C. K. Hallberg, H. Haberle, M. M. Brysk, Z. Jiang, J. A. Patel, P. B. Ernst, and S. D. Trocme. 1998. Cytokine modulation of human corneal epithelial cell ICAM-1 (CD54) expression. *Exp. Eye Res.* 67:383.
59. Mester, J. C., and B. T. Rouse. 1991. The mouse model and understanding immunity to herpes simplex virus. *Rev. Infect. Dis.* 13:S935.
60. Seo, S. K., B. M. Gebhardt, H. Y. Lim, S. W. Kang, S. Higaki, E. D. Varnell, J. M. Hill, H. E. Kaufman, and B. S. Kwon. 2001. Murine keratocytes function as antigen-presenting cells. *Eur. J Immunol.* 31:3318.

61. Lee, S., M. Zheng, S. Deshpande, S. K. Eo, T. A. Hamilton, and B. T. Rouse. 2002a. IL-12 suppresses the expression of ocular immunoinflammatory lesions by effects on angiogenesis. *J Leukoc. Biol.* 71:469.
62. Maertzdorf, J., A. D. Osterhaus, and G. M. Verjans. 2002. IL-17 expression in human herpetic stromal keratitis: modulatory effects on chemokine production by corneal fibroblasts. *J Immunol.* 169:5897.
63. Numasaki, M., J. Fukushi, M. Ono, S. K. Narula, P. J. Zavodny, T. Kudo, P. D. Robbins, H. Tahara, and M. T. Lotze. 2003. Interleukin-17 promotes angiogenesis and tumor growth. *Blood* 101:2620.
64. Aggarwal, S., N. Ghilardi, M. H. Xie, F. J. de Sauvage, and A. L. Gurney. 2003. Interleukin-23 promotes a distinct CD4 T cell activation state characterized by the production of interleukin-17. *J Biol. Chem.* 278:1910.
65. Su, Y. H., X. T. Yan, J. E. Oakes, and R. N. Lausch. 1996. Protective antibody therapy is associated with reduced chemokine transcripts in herpes simplex virus type 1 corneal infection. *J Virol.* 70:1277.
66. Kumaraguru, U., I. Davis, and B. T. Rouse. 1999. Chemokines and ocular pathology caused by corneal infection with herpes simplex virus. *J Neurovirol.* 5:42.
67. Thomas, J., S. Kanangat, and B. T. Rouse. 1998. Herpes simplex virus replication-induced expression of chemokines and proinflammatory cytokines in the eye: implications in herpetic stromal keratitis. *J Interferon Cytokine Res.* 18:681.
68. Shirane, J., T. Nakayama, D. Nagakubo, D. Izawa, K. Hieshima, Y. Shimomura, and O. Yoshie. 2004. Corneal epithelial cells and stromal

keratocytes efficiently produce CC chemokine-ligand 20 (CCL20) and attract cells expressing its receptor CCR6 in mouse herpetic stromal keratitis. *Curr. Eye Res.* 28:297.

69. Tumpey, T. M., H. Cheng, D. N. Cook, O. Smithies, J. E. Oakes, and R. N. Lausch. 1998a. Absence of macrophage inflammatory protein-1alpha prevents the development of blinding herpes stromal keratitis. *J Virol.* 72:3705.

70. Tumpey, T. M., H. Cheng, X. T. Yan, J. E. Oakes, and R. N. Lausch. 1998b. Chemokine synthesis in the HSV-1-infected cornea and its suppression by interleukin-10, *J Leukoc. Biol.* 63:486.

71. Zheng, M., S. Deshpande, S. Lee, N. Ferrara, and B. T. Rouse. 2001a. Contribution of vascular endothelial growth factor in the neovascularization process during the pathogenesis of herpetic stromal keratitis. *J Virol.* 75:9828.

72. Boshoff, C. 1998. Kaposi's sarcoma. Coupling herpesvirus to angiogenesis. *Nature* 391:24.

73. Bais, C., B. Santomasso, O. Coso, L. Arvanitakis, E. G. Raaka, J. S. Gutkind, A. S. Asch, E. Cesarman, M. C. Gershengorn, and E. A. Mesri. 1998. G-protein-coupled receptor of Kaposi's sarcoma-associated herpesvirus is a viral oncogene and angiogenesis activator. *Nature* 391:86.

74. Haque, N. S., J. T. Fallon, M. B. Taubman, and P. C. Harpel. 2001. The chemokine receptor CCR8 mediates human endothelial cell chemotaxis induced by I-309 and Kaposi sarcoma herpesvirus-encoded vMIP-I and by lipoprotein(a)-stimulated endothelial cell conditioned medium. *Blood* 97:39.

76. Meyer, M., M. Clauss, A. Lepple-Wienhues, J. Waltenberger, H. G. Augustin, M. Ziche, C. Lanz, M. Buttner, H. J. Rziha, and C. Dehio. 1999. A

novel vascular endothelial growth factor encoded by Orf virus, VEGF-E, mediates angiogenesis via signalling through VEGFR-2 (KDR) but not VEGFR-1 (Flt-1) receptor tyrosine kinases. *Embo. J* 18:363.

77. Kim, B., Q. Tang, P. S. Biswas, J. Xu, R. M. Schiffelers, F. Y. Xie, A. M. Ansari, P. V. Scaria, M. C. Woodle, P. Lu, and B. T. Rouse. 2004. Inhibition of ocular angiogenesis by siRNA targeting vascular endothelial growth factor pathway genes: therapeutic strategy for herpetic stromal keratitis. *Am. J Pathol.* 165:2177.

78. Salven, P., K. Hattori, B. Heissig, and S. Rafii. 2002. Interleukin-1alpha promotes angiogenesis in vivo via VEGFR-2 pathway by inducing inflammatory cell VEGF synthesis and secretion. *Faseb J* 16:1471.

79. Saijo, Y., M. Tanaka, M. Miki, K. Usui, T. Suzuki, M. Maemondo, X. Hong, R. Tazawa, T. Kikuchi, K. Matsushima, and T. Nukiwa. 2002. Proinflammatory cytokine IL-1 beta promotes tumor growth of Lewis lung carcinoma by induction of angiogenic factors: in vivo analysis of tumor-stromal interaction. *J Immunol.* 169:469.

80. Nakahara, H., J. Song, M. Sugimoto, K. Hagihara, T. Kishimoto, K. Yoshizaki, N. Nishimoto. 2003. Anti-interleukin-6 receptor antibody therapy reduces vascular endothelial growth factor production in rheumatoid arthritis. *Arthritis Rheum.* 48:1521..

81. Wei, L. H., M. L. Kuo, C. A. Chen, C. H. Chou, K. B. Lai, C. N. Lee, and C. Y. Hsieh. 2003. Interleukin-6 promotes cervical tumor growth by VEGF-dependent angiogenesis via a STAT3 pathway. *Oncogene* 22:1517.

82. Zheng, M., D. M. Klinman, M. Gierynska, and B. T. Rouse. 2002. DNA containing CpG motifs induces angiogenesis. *Proc. Natl. Acad. Sci. U S A* 99:8944.
83. Arenberg, D. A., P. J. Polverini, S. L. Kunkel, A. Shanafelt, J. Hesselgesser, R. Horuk, and R. M. Strieter. 1997. The role of CXC chemokines in the regulation of angiogenesis in non-small cell lung cancer. *J Leukoc. Biol.* 62:554.
84. Cao, Y., C. Chen, J. A. Weatherbee, M. Tsang, and J. Folkman. 1995. gro-beta, a -C-X-C- chemokine, is an angiogenesis inhibitor that suppresses the growth of Lewis lung carcinoma in mice. *J Exp. Med.* 182:2069.
85. Luster, A. D., S. M. Greenberg, and P. Leder. 1995. The IP-10 chemokine binds to a specific cell surface heparan sulfate site shared with platelet factor 4 and inhibits endothelial cell proliferation. *J Exp. Med.* 182:219.
- (86) WuDunn, D. and P. G. Spear. 1989. Initial interaction of herpes simplex virus with cells is binding to heparan sulfate. *J Virol.* 63:52.
87. Sang, Q. X. 1998. Complex role of matrix metalloproteinases in angiogenesis. *Cell Res.* 8:171.
88. Bergers, G., R. Brekken, G. McMahon, T. H. Vu, T. Itoh, K. Tamaki, K. Tanzawa, P. Thorpe, S. Itohara, Z. Werb, and D. Hanahan. 2000. Matrix metalloproteinase-9 triggers the angiogenic switch during carcinogenesis. *Nat. Cell Biol.* 2:737.
89. Kursat, A. A., B. Kim, S. Suvas, Y. Lee, U. Kumaraguru, and B. T. Rouse. Blocking mouse MMP-9 production in tumor cells and mouse cornea by short hairpin (sh)RNA encoding plasmids. *Oligoneucleotide, In press.*

90. Li, D. Q., B. L. Lokeshwar, A. Solomon, D. Monroy, Z. Ji, and S. C. Pflugfelder. 2001. Regulation of MMP-9 production by human corneal epithelial cells. *Exp. Eye Res.* 73:449.
91. Deshpande, S. P., M. Zheng, S. Lee, and B. T. Rouse. 2002. Mechanisms of pathogenesis in herpetic immunoinflammatory ocular lesions. *Vet. Microbiol.* 86:17.
92. Tullo, A. 2003. Pathogenesis and management of herpes simplex virus keratitis. *Eye* 17:919.
93. Babu, J. S., J. Thomas, S. Kanangat, L. A. Morrison, D. M. Knipe, and B. T. Rouse. 1996. Viral replication is required for induction of ocular immunopathology by herpes simplex virus. *J Virol.* 70:101..
94. Deshpande, S., M. Zheng, S. Lee, K. Banerjee, S. Gangappa, U. Kumaraguru, and B. T. Rouse. 2001a. Bystander activation involving T lymphocytes in herpetic stromal keratitis. *J Immunol.* 167: 2902.
95. Suvas, S., A. K. Azkur, B. S. Kim, U. Kumaraguru, and B. T. Rouse. 2004. CD4+CD25+ regulatory T cells control the severity of viral immunoinflammatory lesions. *J Immunol.* 172:4123.
96. Banerjee, K., P. S. Biswas, and B. T. Rouse. 2004c. Elucidating the protective and pathologic T cell species in the virus-induced corneal immunoinflammatory condition herpetic stromal keratitis. *J Leukoc. Biol.* 77:24.
97. Banerjee, K., P. S. Biswas, U. Kumaraguru, S. P. Schoenberger, and B. T. Rouse. 2004b. Protective and pathological roles of virus-specific and bystander CD8+ T cells in herpetic stromal keratitis. *J Immunol.* 173:7575.

98. Niemialtowski, M. G., and B. T. Rouse. 1992a. Phenotypic and functional studies on ocular T cells during herpetic infections of the eye. *J Immunol.* 148:1864.
99. Niemialtowski, M. G., and B. T. Rouse. 1992b. Predominance of Th1 cells in ocular tissues during herpetic stromal keratitis. *J Immunol.* 149:3035.
100. Gangappa, S., S. P. Deshpande, and B. T. Rouse. 1999. Bystander activation of CD4(+) T cells can represent an exclusive means of immunopathology in a virus infection. *Eur. J Immunol.* 29:3674.
101. Gangappa, S., S. P. Deshpande, and B. T. Rouse. 2000. Bystander activation of CD4+ T cells accounts for herpetic ocular lesions. *Invest. Ophthalmol. Vis. Sci.* 41:453.
102. Panoutsakopoulou, V., M. E. Sanchirico, K. M. Huster, M. Jansson, F. Granucci, D. J. Shim, K. W. Wucherpfennig, and H. Cantor. 2001. Analysis of the relationship between viral infection and autoimmune disease. *Immunity* 15:137.
103. Zhao, Z. S., F. Granucci, L. Yeh, P. A. Schaffer, and H. Cantor. 1998. Molecular mimicry by herpes simplex virus-type 1: autoimmune disease after viral infection. *Science* 279:1344.
104. Deshpande, S. P., S. Lee, M. Zheng, B. Song, D. Knipe, J. A. Kapp, and B. T. Rouse. 2001b. Herpes simplex virus-induced keratitis: evaluation of the role of molecular mimicry in lesion pathogenesis. *J Virol.* 75:3077.
105. Banerjee, K., S. Deshpande, M. Zheng, U. Kumaraguru, S. P. Schoenberger, and B. T. Rouse. 2002. Herpetic stromal keratitis in the absence of viral antigen recognition. *Cell. Immunol.* 219:108.

APPENDIX

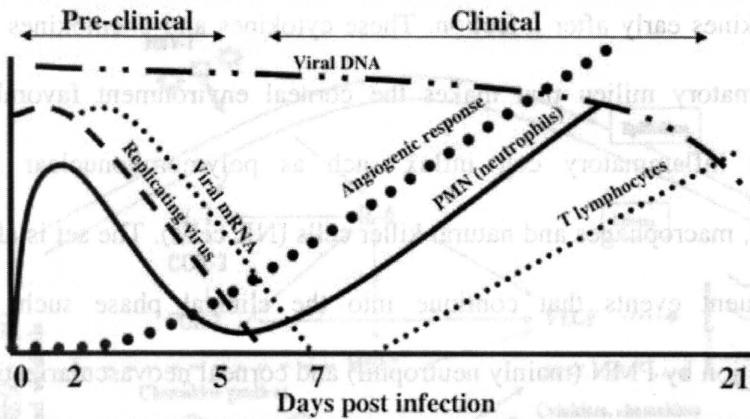


Fig 1. Crucial events in HSK pathogenesis.

Following Herpes simplex virus type 1 (HSV-1) infection replicating virus is detectable in the cornea till 5- 6 days p. i. Viral mRNA is detectable till 7- 8 days p. i. However viral DNA persists in the cornea till day 20 p. i. Angiogenesis or new blood vessel development from existing limbal vessels starts at 24 hr p.i. and gradually peaks around day 15 p. i. The early cell influx in the corneal stroma is dominated by polymorphonuclear leukocytes (PMN). PMN influx is characterized by a typical biphasic response. This response starts around 18 hr p. i., peaks at 48 hr p. i., declines around 5 days p.i. and then comes back during the clinical phase. Whereas the T cells enter the cornea during the clinical phase around 8-9 days p. i.

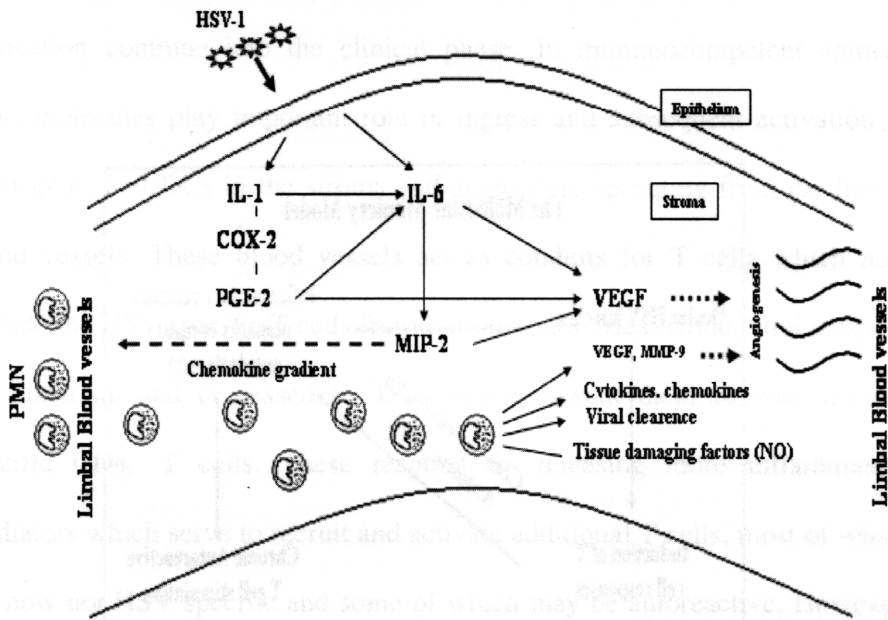
Fig 2. Schematic representation of some early events in HSK pathogenesis.

Herpes simplex virus type 1 (HSV-1) infection of the corneal epithelial cell layer resulted in the production of plethora of proinflammatory cytokines and chemokines early after infection. These cytokines and chemokines create an inflammatory milieu that makes the corneal environment favorable for a prompt inflammatory cell influx such as polymorphonuclear leukocyte (PMN), macrophages and natural killer cells (NK cells). The set is also set for subsequent events that continue into the clinical phase such as tissue destruction by PMN (mainly neutrophil) and corneal neovascularization which is mainly regulated by an interplay between angiogenic factors (VEGF, MMP-9) and antiangiogenic factors (IP-10). Newly developed blood vessels in corneal stroma in turn act as a conduit for inflammatory cell influx during the clinical phase. Question mark (?) indicates identity of factors responsible for paracrine IL-12 production is not known.

Abbreviations: IL, Interleukin; IFN- γ , Interferon gamma; VEGF, vascular endothelial growth factor; COX-2, Cyclooxygenase 2; PGE₂, Prostaglandin E₂; MIP-2, Macrophage Inflammatory protein 2; IP-10, Interferon inducible protein 10; MiG, Monokine induced by IFN- γ ; PECAM 1, Platelet endothelial cell adhesion molecule 1; MHC II, Major Histocompatibility complex II; MMP-9, Matrix metallo proteinase 9; PMN, Ploymorphonuclear leukocyte, NK cells, Natural killer cells.

Fig 1A and B. The Bystander activation model of SK pathogenesis.

A summary of events initiated at the postclinical phase and ensuing in the clinical phase of herpetic stromal keratitis is shown in both immunocompetent and immunocompromised lesion. The inflammatory events set off by viral



in immunocompetent and immunocompromised lesion. The inflammatory events set off by viral

consequences of ocular HSV infection activate the T cells in a non T.H.1 mediated manner. In this instance, virus particles are detected and spread to the stroma located in some way. This is usually replication of virus in the epithelium. The right summarizes the relative roles of molecular factors and non-specific inflammation in SK pathogenesis. This concept explains that the virus replication and non-specific immune responses cause how disease ensues. Additionally, stimulus an antiviral T cell response that is cross-reactive with the corneal autoantigen.

Fig 2. Schematic representation of some early events in HSK pathogenesis.

Herpes simplex virus type 1 (HSV-1) infection of the corneal epithelial cell layer resulted in the production of plethora of pro-inflammatory cytokines and chemokines early after infection. These cytokines and chemokines create an inflammatory milieu that makes the corneal environment favorable for a prompt inflammatory cell influx such as polymorphonuclear leukocyte

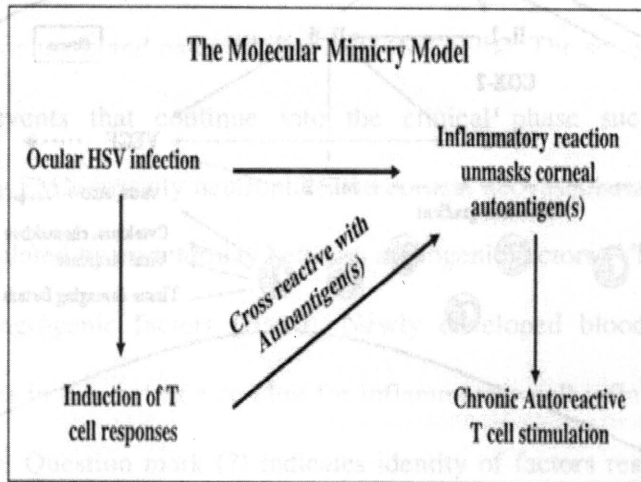


Fig 3. The molecular mimicry model of SK pathogenesis

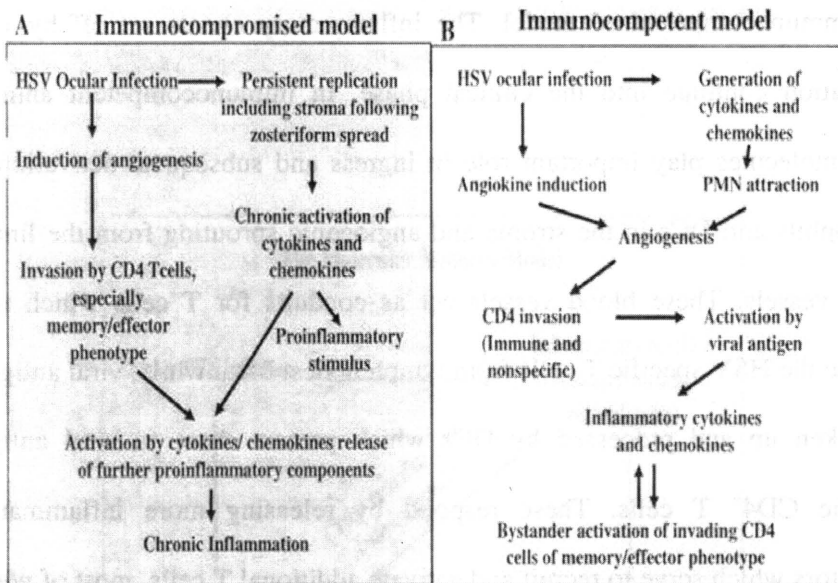
The figure summarizes the relative roles of molecular mimicry and nonspecific inflammation in SK pathogenesis. This concept explains that the virus replication and non specific immune responses somehow unmask autoantigens in the eye and additionally stimulates an antiviral T cell responses that is cross-reactive with the corneal autoantigens.

Fig 4A and B. The Bystander activation model of SK pathogenesis.

A summary of events initiated at the preclinical phase and ending in the clinical phase of herpetic stromal keratitis is shown in both immunocompetent and immunocompromised model. The inflammatory events set off by viral replication continue into the clinical phase. In immunocompetent animals these molecules play important role in ingress and subsequent activation of neutrophils and DCs in the stroma and angiogenic sprouting from the limbal blood vessels. These blood vessels act as conduits for T cells which now include the HSV specific T cells from lymph nodes. Meanwhile, viral antigens are taken up and processed by DCs which present them to viral antigen specific CD4⁺ T cells. These respond by releasing more inflammatory mediators which serve to recruit and activate additional T cells, most of which are now not HSV specific and some of which may be autoreactive. However, in immunocompromised animals inflammatory molecules produced as a consequence of ocular HSV infection activate the T cells in a non TCR mediated manner. In this instance, virus persisted and spread to the stromal tissue location in some way. This continually replicating virus in the corneal stroma acts, possibly by TLR ligand activity, as the chronic stimulus for cytokine /chemokine production that in turn activates the incoming T cells. Such cells then produce inflammatory mediators which participate in tissue damage.

A summary of events initiated at the preclinical phase and ending in the clinical phase of herpetic stromal keratitis both immunocompetent

Bystander activation



are now not HSV-specific and some of which may be autoreactive. However,

in immunocompromised animals inflammatory molecules produced as a

consequence of ocular HSV infection activate the T cells in a non-TFH

regulated manner. In this instance, viral particles and spread to the stroma

these location in some way. The constitutively replicating virus in the stroma

stroma acts possibly by ILR ligand release in the chronic stimulus for

cytokine/chemokine production that in turn activates the memory T cells.

Such cells then produce inflammatory mediators which participate in tissue

damage.

the T cells in the stroma then either die or migrate

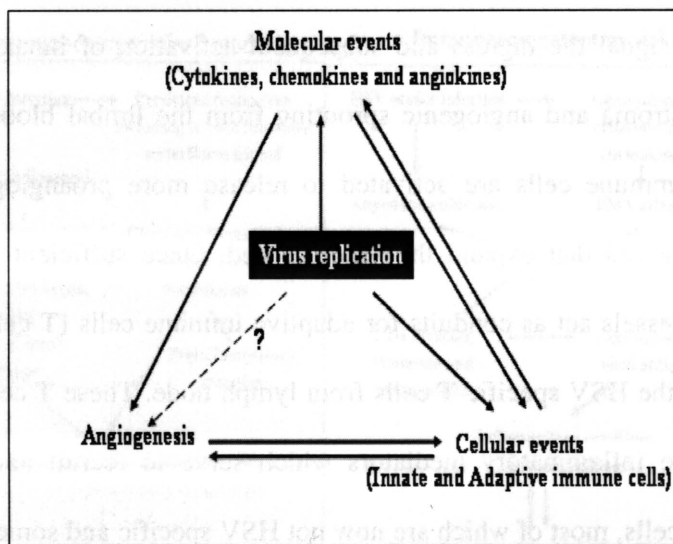
to peripheral tissues and the virus may be reactivated.

Fig 5. The Hit and Run model of SK pathogenesis.

HSV-1 replication is required to marshal a complex of molecular events, which we term the “alarm complex”. These molecules serve directly or indirectly to signal the ingress and subsequent activation of innate immune cells in the stroma and angiogenic sprouting from the limbal blood vessels. The innate immune cells are activated to release more proangiogenic and angiogenic factors that expand the vascular bed. Once sufficient in extent, these leaky vessels act as conduits for adaptive immune cells (T cells) which now include the HSV specific T cells from lymph node. These T cells in turn produce more inflammatory mediators which serve to recruit and activate additional T cells, most of which are now not HSV specific and some of which may be autoreactive. These recruits release more inflammatory molecules (bystander activation) in a positive feedback loop. The stroma is left with a damaged matrix and unwanted vascular bed that is slow to resolve. The dotted arrow and the question mark indicate that still no evidence is available about the direct involvement of virus or viral components in the angiogenesis process.

Fig. 2. The HIV and KSHV model of KIP pathogenesis.

HIV-1 replication is required to establish a complex of molecular events, which we term the "stromal complex". This complex serves directly or



may be autoreactive. These events release more inflammatory molecules (cytokines, chemokines, angiokines) in a positive feedback loop. The stroma is left with a damaged matrix and unwanted vascular bed that is slow to resolve. The dotted arrow and the question mark indicate that still no evidence is available about the direct involvement of virus or viral component in the angiogenesis

process.

PART II

**MICE TRANSGENIC FOR IL-1 RECEPTOR
ANTAGONIST PROTEIN ARE RESISTANT
TO HERPETIC STROMAL KERATITIS:
POSSIBLE ROLE FOR IL-1 IN HERPETIC
STROMAL KERATITIS PATHOGENESIS**

Research described in this chapter is a slightly modified version of an article published in 2004 in *The Journal of Immunology* by Partha Sarathi Biswas, Kaustuv Banerjee, Bumseok Kim and Barry T. Rouse.

Biswas, P. S., K. Banerjee, B. Kim, and B. T. Rouse. 2004. Mice transgenic for IL-1 receptor antagonist protein are resistant to herpetic stromal keratitis: possible role for IL-1 in herpetic stromal keratitis pathogenesis. *J. Immunol.* 172: 3736. Copyright 2004. *The American Association of Immunologists, Inc.*

In this chapter “we” and “our” refers to co-authors and me. My contributions in the paper include (1) selection of the topic (2) data analysis and interpretation (3) planning experiments (4) compiling and interpretation of the literature (5) understanding how results fit with the literature (7) compilation of contributions into one paper (8) providing structure to the paper (9) making graphs, figures and tables (10) writing and editing.

ABSTRACT

Ocular infection with herpes simplex virus (HSV) may result in the blinding immunoinflammatory lesion Stromal Keratitis (SK). Early events in the pathogenesis that set the stage for SK are poorly understood. The present report evaluates the role of IL-1 using a transgenic mouse that overexpresses the IL-1 receptor antagonist protein. Such transgenic mice were markedly resistant to SK compared to IL-1 Ra *-/-* and C57BL/6 control animals. Targeting IL-1 could prove to be a worthwhile therapeutic approach to control SK, an important cause of human blindness.

INTRODUCTION

Herpes simplex virus (HSV) infection is a major cause of vision loss (1). This results mainly from a chronic inflammatory reaction in the normally transparent and avascular cornea. A complex of humoral and cellular events are involved in the pathogenesis of SK, but the critical event responsible for clinically evident lesions is CD4⁺ T cell mediated immunopathology (2, 3). Prior to the T cell mediated immunoinflammatory phase, multiple events occur after virus infection that set the stage for the subsequent pathology. These events include the production of proinflammatory cytokines and chemokines and a prominent invasion of the cornea by PMN (4, 5). The later response appears protective and helps clear virus (4, 5). However, PMN invasion also contributes to pathology since the cells are a major source of angiogenesis factors (6) and perhaps also damaging factors such as NO (7). Neovascularization, represents a major step in SK pathogenesis and multiple molecules are involved in this process (8). It is not clear how HSV infection, which in the mouse model is usually confined to the corneal epithelium, results in neovascularization into the underlying stroma. Thus once a cell is productively infected by HSV most cellular proteins cease production (9). Exceptions include IL-6 (10, 11) and probably IL-1 (12) which are briefly induced by HSV infection by mechanisms that remain undefined. These cytokines could represent key molecules that set off a cascade of events that culminate in the clinically evident immunoinflammatory lesions. After HSV infection, both IL-1 and IL-6 have been shown to be eminent by day 2 post

infection and reached peak levels at day 10, and then diminished over the next few days (13, 14). In consequence, counteracting IL-1 and IL-6 could be a valuable control measure at least if performed early after infection. The aim of this study was to determine if inhibition of IL-1, as could be achieved by using a transgenic mouse that overexpressed the IL-1 receptor antagonist, had an effect on SK pathogenesis. Such transgenic mice have been used in other inflammatory models and were shown to block IL-1 and diminish disease expression (15-18). Our results with ocular infection with HSV demonstrate that IL-1 Ra Tg mice developed significantly milder disease and reduced corneal angiogenesis compared to IL-1 Ra $-/-$ and C57BL/6 mice. This difference in disease phenotype was an indirect event and was shown to be the consequence of changed expression of molecules such as IL-6, MIP-2 and the angiogenesis factor VEGF normally unregulated by IL-1 during an inflammatory process (19-21). Our results demonstrate that IL-1 production is a critical event in SK pathogenesis and that inhibiting this cytokine represents a valuable approach for disease control.

MATERIALS AND METHODS

Mice

IL-1 receptor antagonist transgenic (T14 hemizygous line) and knockout mice were kindly provided by Dr. David Hirsh (Department of Biochemistry and Molecular Biophysics, College of Physician and Surgeons, Columbia University). Wild type female 4 to 5 weeks old C57BL/6 mice were purchased from Harlan Sprague-Dawley (Indianapolis, Indiana). Animals were sex and

age matched for all experiments. All manipulations involving the immunocompromized mice were performed in a laminar flow hood. To prevent bacterial superinfections, all mice received prophylactic treatment with Sulphatrim pediatric suspension (Barre-National Baltimore, MD). All experimental procedures were in complete agreement with the Association for Research in Vision and Ophthalmology (ARVO) resolution on the use of animals in research.

Virus

HSV-1 RE (obtained from Dr. Robert Hendricks Laboratory, University of Pittsburgh School of Medicine) was used in the present study. The virus was propagated and titrated on monolayers of Vero cells (ATCC, Cat No. CCL81) using standard protocols (22). Infected Vero cells were harvested, titrated and stored in aliquots at -80° C until used.

Corneal HSV-1 infection

Corneal infections of all mice groups were conducted under deep anesthesia induced by intraperitoneal injection of Avertin (Sigma). Mice were scarified on their corneas with a 27-gauge needle and a 4 μ l drop containing the required dose of virus was applied to the eye and gently massaged with the eyelids.

Clinical observations and Angiogenesis Scoring

The eyes were examined on different days post infection by a slit-lamp biomicroscope (Kowa Co. Nagoya, Japan), and the clinical severity of keratitis of individually scored mice was recorded as described before (8). Angiogenesis severity was measured as described previously (23). Briefly, a grade of 4 for a given quadrant of the circle represents a centripetal growth of 1.5mm toward the corneal center. The score of the 4 quadrants of the eye were then summed to derive the NV index (range 0-16) for each eye at a given point.

***In vitro* stimulation of corneal epithelial cell culture**

Isolation of corneal epithelium cells were performed as described before (24). Briefly corneal buttons were incubated at 37° C in phosphate buffered saline containing 10mM tetra sodium diaminetetracetate dehydrate (Sigma) for 45 minutes. After incubation, the epithelial cell layer was separated from the adjacent corneal tissue by gentle teasing with a fine forceps. The intact epithelial layer was washed several times in PBS followed by treatment with collagenase D (Roche) at 37° C for 30 minutes. The disrupted epithelial cells were then passed through a 40µm filter to make a single cell suspension. Cells were counted and suspended in F-12K medium (ATCC) with 10% FCS and plated in 48 well tissue culture plates at 37° C in 5% CO₂. Purity of cultured corneal epithelial cells was determined by flow cytometry using anti K12 antibody (kindly provided by Dr. Winston Kao, University of Cincinnati). The corneal epithelial cell culture yielded 75-80% purity.

Adherent monolayer of epithelial cells was stimulated with different doses of recombinant murine IL-1 α and IL-1 β (R & D systems) in serum free F-12 K medium for 24hr and 48hr. After incubation, the supernatant was collected and stored at -80° C till further use. For blocking studies, different doses of anti-murine IL-1 α antibody (Pharmingen) was mixed with 800pg (dose selected on the basis of dose response curve) of IL-1 α . Rat IgG was used as isotype control.

Corneal intrastromal injection assay

Corneal intrastromal injection was performed as described before (¹). Under direct stereomicroscopic observation, a nick in the epithelium and anterior stroma of mouse cornea was made with a ½- inch 30-gauge needle with a 30° bevel in the mid periphery. Eight eyes were injected per group. The needle was introduced into the corneal stroma and advanced 1.5 mm to the corneal center. Two microlitres of solution containing the required concentration of recombinant murine IL-1 α (100ng, 200ng and 400ng) (Pharmingen) and anti murine VEGF antibody [5 μ g (25)](R & D system) was forcibly injected into the stroma to separate the corneal lamellae and disperse the solution. PBS was used as control.

Subconjunctival inoculations

Subconjunctival inoculation of recombinant murine IL-6 [50ng (26)] (Pharmingen) and anti murine IL-6 antibody [5 μ g/ μ l (26)] was performed as described previously (26). Briefly, subconjunctival inoculations were done

using a 2 cm 32 gauge needle and syringe (Hamilton) to penetrate the perivascular region of conjunctiva and deliver 4 μ l into the subconjunctival space. Control mice received PBS. Mice received recombinant murine IL-6 a day before corneal infection with HSV-1 RE.

Viral titration

Eye swabs were taken from the infected corneas (3 mice/group) using sterile cotton swabs soaked in DMEM containing 10 IU/ml penicillin and 100 μ g/ml streptomycin. All manipulations are done under sterile conditions. Swabs were stored in tubes containing serum free DMEM at -80 $^{\circ}$ C. For detection of virus, samples were thawed and vortexed. Duplicate samples (200 μ l) were plated on Vero cells grown to confluence in 24 well plates at 37 $^{\circ}$ C in 5% CO₂ for 90 minutes. Medium was aspirated and 500 μ l of DMEM containing 1% LMP agarose was added to each well. Titers were calculated as log₁₀ pfu/ml as per standard protocol (22).

Histopathology

For histopathological analysis, eyes were extirpated and fixed in 10% buffered neutral formalin. Staining was performed with Hematoxylin and Eosin (Richard Allen Scientific, MI).

RT-PCR

Total RNA from 4 corneas per time point was extracted by using Tri-reagent (Molecular Biology Inc., Cincinnati, Ohio). Total RNA (1 μ g) was reverse

transcribed using murine leukemia virus reverse transcriptase (Gibco BRL Life Technologies, Bethesda MD) with oligodT as primer (Invitrogen, CA). All cDNA samples were aliquoted and stored at -20°C until further use. Polymerase chain reaction was performed in PTC-100 Programmable Thermal Controller (MJ Research Inc.) using Hot Start PCR Master Mix (Promega, WI). The primers used were murine GAPDH Forward CATCCTGCACCACCAACTGCTTAG Reverse GCCTGCTTCACCACCTTCTTGATG and murine IL-1 Ra Tg Forward TAGACATGGTGCCTATTGAC Reverse GAGGCTCACAGGACGGTCAG.

Flow Cytometry

Single-cell suspensions were prepared from 4 corneas at 24 and 48 hr post infection as described elsewhere (27), with some modifications. Briefly, corneal buttons were incubated with collagenase D (Roche) for 60 min at 37°C in a humidified atmosphere at 5% CO₂. After incubation, eyes were disrupted by grinding with a syringe plunger and passing through a cell strainer. Cells were washed and suspended in RPMI 1640 with 10% FBS. The F_c receptors on the cells were blocked with unconjugated anti-CD16/32 (Pharmingen) for 30 min. Samples were incubated with FITC labeled anti Gr-1 antibody (Clone RB6-8C5, Pharmingen) and isotype controls for 30 minutes. All samples were collected on a FACScan (BD Biosciences), and data were analyzed using CellQuest 3.1 software (BD Biosciences).

Cytokine ELISA of corneal lysate

For preparation of corneal lysates, 6 corneas per time point were pooled and minced. All procedures were done on an ice bath. Minced pieces were collected in 1ml DMEM without FCS and homogenized using a tissue homogenizer (PRO Scientific Inc., Mourse) four times, 15 seconds each, with a gap of 1 minute between homogenization to allow the sample to cool. The lysate was then clarified by centrifugation at 14,000 rpm for 5 minute at 4°C. The supernatant was collected and used immediately or stored at -80°C until further use. Lysates were analyzed using a standard sandwich ELISA protocol. Anti IL-6 capture and biotinylated detection antibodies were from Pharmingen (Clone MP5-20F3) and standard recombinant murine IL-6 was from R&D Systems Inc, Minneapolis. Anti MIP-2 and anti VEGF₁₆₄ capture and biotinylated detection antibodies and recombinant standards for murine MIP-2 and murine VEGF₁₆₄ were from R & D Systems. The color reaction was developed using ABTS (Sigma) and measured with an ELISA reader (Spectramax 340, Molecular Devices) at 405nm. The detection limit was 2pg/ml. Quantification was performed with Spectramax ELISA reader software version 1.2.

Quantitative real time PCR

Total RNA from 4 corneas per time point was extracted by using RNeasy RNA extraction Kit (Qiagen, CA). Briefly, tissues were lysed in RLT buffer and RNA was purified following manufacturer's instructions (Qiagen, CA). DNase treatment (Qiagen, CA) was done to remove any contaminating

genomic DNA. To generate cDNA, 1µg total RNA was reverse transcribed using murine leukemia virus reverse transcriptase (Gibco BRL Life Technologies, Bethesda MD) with oligodT as primer (Invitrogen, CA), according to manufacturer's instructions. All cDNA samples were aliquoted and stored at -20°C until further use.

Real time PCR was performed using a DNA Engine Opticon (MJ Research Inc.). PCR was performed using SYBR Green I reagent (Qiagen, CA) according to manufacturer's protocol. PCR amplification of house keeping gene, murine glyceraldehyde 3-phosphate dehydrogenase was done for each sample as a control for sample loading and to allow normalization between samples. A standard curve was constructed with PCR-II topo cloning vector (Invitrogen, CA) containing the inserted same fragment amplified by the SYBR I system. PCR reactions for each sample was analyzed in three dilutions in duplicate for both GAPDH and target gene. The target gene was then normalized to 10^6 copies of GAPDH control and data represented as copy numbers/ 10^6 GAPDH. The primers used were murine GAPDH Forward
CATCCTGCACCACCAACTGCTTAG Reverse
GCCTGCTTCACCACCTTCTTGATG and murine VEGFR-2 Forward
TGTC AAGTGGCGGTAAAGG Reverse
CACAAAGCTAAAATACTGAGGACTTG.

Statistical analysis

A standard student's t test was employed for statistical analysis.

RESULTS

IL-1 Ra Tg mice show reduced Stromal Keratitis and corneal angiogenesis

Three groups of genetically different mice, IL-1 Ra Tg, IL-1 Ra *-/-* and wild type C57BL/6, were evaluated clinically for the development of SK following HSV-1 (5×10^6 pfu) corneal infection over a 20 day test period. Naïve and infected corneas of IL-1 Ra Tg mice demonstrated higher level of IL-1 Ra mRNA in comparison to wild type control (Fig. 1). As shown in Fig. 2A, whereas the pattern and severity of SK in both IL-1 Ra *-/-* and wild type C57BL/6 mice was similar (mean scores 3.5 and 2.7 respectively), SK in IL-1 Ra Tg mice was strikingly reduced (mean score of 1.4) (Fig. 2A). In addition whilst 75% of eyes of IL-1 Ra *-/-* mice developed clinically evident lesions (score 3 or greater), only 25% of IL-1 Ra Tg mice developed such lesions (data not shown). Attempts to infect IL-1 Ra Tg mice with a higher virus dose (10^7 pfu) resulted in lethality, but still few developed SK of ≥ 3 (data not shown). Histopathological analysis of representative eyes of IL-1 Ra Tg mice revealed mild inflammatory changes and cellular infiltrations in the corneal stroma and epithelium at day 20 p. i. (Fig. 2B). However both IL-1 Ra *-/-* and C57BL/6 mice developed more severe inflammatory changes (Fig. 2B).

One characteristic of corneal HSV-1 infection is neovascularization into the normally avascular corneal stroma, an event deemed necessary for the full expression of SK (28). In comparison to the extent of angiogenesis following HSV infection in IL-1 Ra *-/-* and C57BL/6, the eyes of IL-1 Ra Tg mice revealed marked reduction of this process (Fig 3A, 3C). By day 20 p. i,

the angiogenesis score was greater than 10 in 13 of 16 IL-1 Ra $-/-$ eyes and 8 of 16 C57BL/6 mice (Fig 3B) but only 4 out of 16 eyes of IL-1 Ra Tg mice had such a score (Fig 3B). Taken together these results indicate that overexpression of IL-1 Ra protein led to diminished angiogenesis as well as stromal keratitis.

PMN inflammatory response in IL-1 Ra Tg mice:

A major event following ocular infection with HSV is a prompt PMN influx into the corneal stroma (4, 5). This reaction at 24 and 48 hr p. i. was significantly less in IL-1 Ra Tg mice compared to either IL-1 Ra $-/-$ and wild type mice (Fig. 4, Table 1). PMN are considered as involved in antiviral defense (4, 5). In line with this notion viral clearance was impaired in IL-1 Ra Tg mice compared to IL-1 Ra $-/-$ and wild type mice (Table 2). Accordingly virus was present in ocular swabs for around 2 extra days in IL-1 Ra Tg mice (Table 2).

One reason considered for the scant PMN response in IL-1 Ra Tg mice was that IL-1, must, in normal situations serves to induce molecules that are directly or indirectly chemotactic for PMN. Based on the results of others (26, 29) prime candidates considered were IL-6 and MIP-2. Levels of these proteins were compared in the 3 mouse strains at various time points after HSV infection. Both IL-6 and MIP-2 protein levels in corneal extracts were significantly less in IL-1 Ra Tg mice compared to IL-1 Ra $-/-$ and wild type animals at all time points analyzed (Fig. 5A & 5B). In addition, if recombinant murine IL-6 protein was injected subconjunctivally into IL-1 Ra Tg animals 1

day prior to corneal infection, there was an approximately 4 fold increase in PMN influx in HSV infected IL-1 Ra Tg mice compared to controls given PBS (Fig. 6A, Table 3). Such eyes demonstrated a higher IL-6 level in comparison to PBS control at day 2 post injection (data not shown). Furthermore, IL-6 reconstitution also resulted in significantly higher levels ($p<0.05$) of the chemokine MIP-2 in corneal extracts (Fig. 6B).

To evaluate which corneal cells might act as a source of IL-6 upon IL-1 stimulation, corneal epithelial cell cultures were stimulated in vitro with different doses of recombinant IL-1 α and IL-1 β . Interleukin-1 α , but not IL-1 β , could induce IL-6 production from corneal epithelial cells in a dose dependent manner at 24 hr and 48 hr (Fig. 7A). The presence of neutralizing antibody against murine IL-1 α , but not control IgG, blocked the IL-6 production from these cells in a dose dependent manner (Fig. 7B).

Environment favorable for corneal angiogenesis is severely compromised in IL-1 Ra Tg mice

As noted above, IL-1 Ra Tg mice developed markedly diminished angiogenic responses compared to either IL-1 Ra $-/-$ and wild type controls. Protein levels of VEGF was significantly lower ($p<0.05$) in IL-1 Ra Tg mice compared to IL-1 Ra $-/-$ and C57BL/6 animals at all time points analyzed (Fig. 8A). In addition, real time PCR demonstrated a significantly higher level of VEGFR-2 mRNA transcript in IL-1 Ra $-/-$ and C57BL/6 mice than in IL-1 Ra Tg animals (Fig. 8B).

Previous studies demonstrated that IL-1 α could upregulate the angiogenesis factor VEGF in human PBMC in vitro (20). To demonstrate the angiogenic activity of IL-1 α in murine cornea, different doses of recombinant murine IL-1 α was injected intrastromally and the extent of angiogenesis was measured at day 2 and 4 days postinjection. Corneal ELISA revealed a significant increase in IL-1 α level at day 2 post injection in comparison to PBS control (data not shown). Interestingly, IL-1 α induced a dose dependent angiogenic response (Fig. 9A, 9B). In such eyes, both IL-6 and VEGF protein levels were elevated (Fig. 10A, 10B). Administration of neutralizing antibody against murine VEGF could abrogate IL-1 α induced angiogenesis demonstrating the key involvement of VEGF in this process (Fig. 11A). Such eyes demonstrated diminished VEGF level in comparison to IgG control (data not shown). In order to rule out the possible involvement of IL-6 in the IL-1 α mediated corneal angiogenesis, anti IL-6 antibody was administered with IL-1 α protein. Interestingly the presence of neutralizing antibody against IL-6 reduced, but did not abrogate IL-1 α induced corneal angiogenesis (Fig. 11B).

DISCUSSION

This report deals with early events in the pathogenesis of the blinding immunoinflammatory lesion Stromal Keratitis caused by ocular infection with HSV. Our results demonstrate that transgenic mice that overexpress the IL-1 receptor antagonist protein are markedly resistant to SK compared to control C57BL/6 mice. The resistance appeared to be the consequence of a reduced

expression of molecules usually induced by IL-1, which in turn participate in inflammatory cell recruitment and angiogenesis. In the present report, we evaluate the critical role of IL-1 using a transgenic mouse that overexpress IL-1 receptor antagonist protein. Thus IL-1 Ra Tg mice had reduced levels IL-6, the chemokine MIP-2; as well the angiogenesis factor VEGF and its receptor VEGFR-2. In consequence, the IL-1 Ra Tg mice showed less PMN influx and neovascularization than did control C57BL/6 animals. Our results imply that blocking IL-1 activity could represent a valuable therapeutic approach to control SK.

One striking difference noted between C57BL/6 control and IL-1 Ra Tg mice was a marked difference in PMN invasion 2 days post HSV infection. This early PMN response was shown previously to be in part responsible for viral clearance (4, 5). This viewpoint was also supported by the present studies. Thus, IL-1 Ra Tg mice, which expressed a diminished PMN response, also showed a delay in viral clearance. How IL-1 in normal infected mice causes PMN influx remains unclear. However, since IL-1 itself is not chemotactic for PMN (30), the effect must be indirect, with IL-1 inducing one or more chemokines. A likely candidate is MIP-2, since MIP-2 neutralized mice develop minimal PMN responses to ocular HSV infection (29). The results of the present study indicate that IL-1 did induce MIP-2 but this was an indirect consequence of IL-6 induction. In support, IL-1 α was shown to induce IL-6 in vitro in corneal epithelial cells. In addition, MIP-2, as well as other chemokines, such as MIP-1 α and MCP-1, were shown by others to be induced by IL-6 (26, 31). Our studies also demonstrated that IL-1 was

upregulated in virus infected corneal epithelial cells (data not shown). This observation as well as others (10-12) indicates that HSV infection results in the autocrine production of IL-1 as well as IL-6. This process may be brief since as HSV infection proceeds, host mRNA synthesis and protein translation is inhibited in productively infected cells (9). However, IL-1 also drives IL-6 production by uninfected cells, which together with that produced by infected cells themselves, sets off a cascade of events that result in PMN influx. Supporting the scheme we could show that the provision of exogenous IL-6 intrastromally to the transgenic mice, reconstituted the PMN invasion.

Although PMN play a protective function in HSV ocular infection, they also participate in lesion expression and act as a source of angiogenesis factors (6) as well as molecules such as nitric oxide (7) that damage corneal tissues. Thus, in line with the minimal early PMN response noted in IL-1 Ra Tg mice, such animals showed a marked reduction in angiogenesis compared to controls. One factor derived from PMN, as well as from other cell types involved in neovascularization, is VEGF (32, 33). We demonstrated that VEGF was significantly downregulated in IL-1 Ra Tg mice in comparison to control animals. Similar observations were reported previously in a nonspecific model of ocular inflammation (34). The diminished VEGF response of transgenic mice may be explained by the fact that the presence of the IL-1 receptor antagonist suppressed IL-1 induced VEGF production from uninfected corneal cells such as PMN. Previously, HSV infection was shown to cause VEGF production but not from the cells actually infected with virus (8). Conceivably, cytokines such as IL-1 released from infected cells explain

the paracrine induction of VEGF. Supporting this scheme, the presence of IL-1 Ra suppressed the VEGF response. In addition, the angiogenic response induced in mice by intrastromal injection of IL-1 could be largely inhibited by anti VEGF antibody. Furthermore, intrastromal injection of IL-1 α was shown to induce VEGF in the cornea. These observations as well as others in tumor systems (20, 35) indicate that IL-1 can cause cells to produce VEGF.

Even though IL-1 produced from HSV infected cells may act as an inducer for VEGF production, an additional VEGF stimulant appeared to be mediated by the cytokine IL-6. Thus we demonstrated that corneal cells exposed to IL-1 in vitro produce IL-6, and IL-6 was shown previously to be a strong agonist for VEGF production ((36, 37). Further support that IL-1 induced angiogenesis depended in part on IL-6 production was the observation that it was partially blocked by anti IL-6 antibody. The relative importance of the direct and indirect effect of IL-1 on VEGF production and angiogenesis remains to be evaluated.

Finally, our results demonstrated that corneal RNA samples from transgenic mice showed diminished VEGFR-2 levels measured by Real Time PCR. In tumor systems, IL-1 was shown to upregulate VEGFR-2 expression on endothelial cells (38), the latter known to be critical for pathological angiogenesis (39). Evidently, the absence of IL-1 activity, as occurred in IL-1 Ra Tg mice, results in reduced expression of VEGFR-2. The consequence is lack of stimulation for the endothelial cells to proliferate, resulting in reduced angiogenesis. However it is not clear why transgenic mice demonstrated reduced VEGFR-2 expression. We believe there may be two possibilities.

Firstly, IL-1 may directly upregulate VEGFR-2 expression on corneal endothelial cells and blocking its activity by specific antagonist protein results reduced receptor expression. Secondly, reduced proliferation of endothelial cells as a consequence of diminished VEGF and inflammatory response in these mice. We are currently attempting to ascertain which of these two mechanisms accounts for the major effect of IL-1 on angiogenesis.

Taken together, our results support the hypothesis that the inflammatory milieu and angiogenic stimuli created early after infection play an important role in HSV induced ocular lesions. An important participant of this environment is IL-1. Antagonizing the effect of IL-1 by a specific receptor antagonist protein abrogates the cascade of events that culminate in HSK. This regulation is indirectly mediated by downregulating various signaling molecules previously known to be important in HSK pathogenesis and corneal angiogenesis. It would seem that targeting IL-1 could prove to be a worthwhile therapeutic approach to control SK, an important cause of human blindness.

LIST OF REFERENCES

LIST OF REFERENCES

1. Streilein, J. W., M. R. Dana, and B. R. Ksander. 1997. Immunity causing blindness: five different paths to herpes stromal keratitis. *Immunol Today* 18:443.
2. Russell, R. G., M. P. Nasisse, H. S. Larsen, and B. T. Rouse. 1984. Role of T-lymphocytes in the pathogenesis of herpetic stromal keratitis. *Invest Ophthalmol Vis Sci* 25:938.
3. Niemialtowski, M. G., and B. T. Rouse. 1992. Phenotypic and functional studies on ocular T cells during herpetic infections of the eye. *J Immunol* 148:1864.
4. Tumpey, T. M., S. H. Chen, J. E. Oakes, and R. N. Lausch. 1996. Neutrophil-mediated suppression of virus replication after herpes simplex virus type 1 infection of the murine cornea. *J Virol* 70:898.
5. Thomas, J., S. Gangappa, S. Kanangat, and B. T. Rouse. 1997. On the essential involvement of neutrophils in the immunopathologic disease: herpetic stromal keratitis. *J Immunol* 158:1383.
6. Lee, S., M. Zheng, B. Kim, and B. T. Rouse. 2002. Role of matrix metalloproteinase-9 in angiogenesis caused by ocular infection with herpes simplex virus. *J Clin Invest* 110:1105.
7. Daheshia, M., S. Kanangat, and B. T. Rouse. 1998. Production of key molecules by ocular neutrophils early after herpetic infection of the cornea. *Exp Eye Res* 67:619.
8. Zheng, M., S. Deshpande, S. Lee, N. Ferrara, and B. T. Rouse. 2001. Contribution of vascular endothelial growth factor in the

- neovascularization process during the pathogenesis of herpetic stromal keratitis. *J Virol* 75:9828.
9. Kwong, A. D., J. A. Kruper, and N. Frenkel. 1988. Herpes simplex virus virion host shutoff function. *J Virol* 62:912.
 10. Kanangat, S., J. S. Babu, D. M. Knipe, and B. T. Rouse. 1996. HSV-1-mediated modulation of cytokine gene expression in a permissive cell line: selective upregulation of IL-6 gene expression. *Virology* 219:295.
 11. Paludan, S. R. 2001. Requirements for the induction of interleukin-6 by herpes simplex virus-infected leukocytes. *J Virol* 75:8008.
 12. Tran, M. T., D. A. Dean, R. N. Lausch, and J. E. Oakes. 1998. Membranes of herpes simplex virus type-1-infected human corneal epithelial cells are not permeabilized to macromolecules and therefore do not release IL-1alpha. *Virology* 244:74.
 13. Thomas, J., S. Kanangat, and B. T. Rouse. 1998. Herpes simplex virus replication-induced expression of chemokines and proinflammatory cytokines in the eye: implications in herpetic stromal keratitis. *J Interferon Cytokine Res* 18:681.
 14. Staats, H. F., and R. N. Lausch. 1993. Cytokine expression in vivo during murine herpetic stromal keratitis. Effect of protective antibody therapy. *J Immunol* 151:277.
 15. Thompson, R. C., D. J. Dripps, and S. P. Eisenberg. 1992. Interleukin-1 receptor antagonist (IL-1ra) as a probe and as a treatment for IL-1 mediated disease. *Int J Immunopharmacol* 14:475.

16. Kary, S., and G. R. Burmester. 2003. Anakinra: the first interleukin-1 inhibitor in the treatment of rheumatoid arthritis. *Int J Clin Pract* 57:231.
17. Cominelli, F., C. C. Nast, B. D. Clark, R. Schindler, R. Lierena, V. E. Eysselein, R. C. Thompson, and C. A. Dinarello. 1990. Interleukin 1 (IL-1) gene expression, synthesis, and effect of specific IL-1 receptor blockade in rabbit immune complex colitis. *J Clin Invest* 86:972.
18. Mikuniya, T., S. Nagai, M. Takeuchi, T. Mio, Y. Hoshino, H. Miki, M. Shigematsu, K. Hamada, and T. Izumi. 2000. Significance of the interleukin-1 receptor antagonist/interleukin-1 beta ratio as a prognostic factor in patients with pulmonary sarcoidosis. *Respiration* 67:389.
19. Yano, S., H. Nokihara, A. Yamamoto, H. Goto, H. Ogawa, T. Kanematsu, T. Miki, H. Uehara, Y. Saijo, T. Nukiwa, and S. Sone. 2003. Multifunctional interleukin-1beta promotes metastasis of human lung cancer cells in SCID mice via enhanced expression of adhesion-, invasion- and angiogenesis-related molecules. *Cancer Sci* 94:244.
20. Salven, P., K. Hattori, B. Heissig, and S. Rafii. 2002. Interleukin-1alpha promotes angiogenesis in vivo via VEGFR-2 pathway by inducing inflammatory cell VEGF synthesis and secretion. *Faseb J* 16:1471.
21. Garat, C., and W. P. Arend. 2003. Intracellular IL-1Ra type 1 inhibits IL-1-induced IL-6 and IL-8 production in Caco-2 intestinal epithelial

- cells through inhibition of p38 mitogen-activated protein kinase and NF-kappaB pathways. *Cytokine* 23:31.
22. Spear, P. G., and B. Roizman. 1972. Proteins specified by herpes simplex virus. V. Purification and structural proteins of the herpesvirion. *J Virol* 9:143.
 23. Dana, M. R., S. N. Zhu, and J. Yamada. 1998. Topical modulation of interleukin-1 activity in corneal neovascularization. *Cornea* 17:403.
 24. Lausch, R. N., S. H. Chen, T. M. Tumpey, Y. H. Su, and J. E. Oakes. 1996. Early cytokine synthesis in the excised mouse cornea. *J Interferon Cytokine Res* 16:35.
 25. Zheng, M., D. M. Klinman, M. Gierynska, and B. T. Rouse. 2002. DNA containing CpG motifs induces angiogenesis. *Proc Natl Acad Sci U S A* 99:8944.
 26. Fenton, R. R., S. Molesworth-Kenyon, J. E. Oakes, and R. N. Lausch. 2002. Linkage of IL-6 with neutrophil chemoattractant expression in virus-induced ocular inflammation. *Invest Ophthalmol Vis Sci* 43:737.
 27. Deshpande, S., M. Zheng, S. Lee, K. Banerjee, S. Gangappa, U. Kumaraguru, and B. T. Rouse. 2001. Bystander activation involving T lymphocytes in herpetic stromal keratitis. *J Immunol* 167:2902.
 28. Zheng, M., M. A. Schwarz, S. Lee, U. Kumaraguru, and B. T. Rouse. 2001. Control of stromal keratitis by inhibition of neovascularization. *Am J Pathol* 159:1021.
 29. Yan, X. T., T. M. Tumpey, S. L. Kunkel, J. E. Oakes, and R. N. Lausch. 1998. Role of MIP-2 in neutrophil migration and tissue injury

- in the herpes simplex virus-1-infected cornea. *Invest Ophthalmol Vis Sci* 39:1854.
30. Calkins, C. M., D. D. Bensard, B. D. Shames, E. J. Pulido, E. Abraham, N. Fernandez, X. Meng, C. A. Dinarello, and R. C. McIntyre, Jr. 2002. IL-1 regulates in vivo C-X-C chemokine induction and neutrophil sequestration following endotoxemia. *J Endotoxin Res* 8:59.
 31. Yoshida, K., I. Ichimiya, M. Suzuki, and G. Mogi. 1999. Effect of proinflammatory cytokines on cultured spiral ligament fibrocytes. *Hear Res* 137:155.
 32. Kasama, T., K. Kobayashi, N. Yajima, F. Shiozawa, Y. Yoda, H. T. Takeuchi, Y. Mori, M. Negishi, H. Ide, and M. Adachi. 2000. Expression of vascular endothelial growth factor by synovial fluid neutrophils in rheumatoid arthritis (RA). *Clin Exp Immunol* 121:533.
 33. Scapini, P., F. Calzetti, and M. A. Cassatella. 1999. On the detection of neutrophil-derived vascular endothelial growth factor (VEGF). *J Immunol Methods* 232:121.
 34. Moore, J. E., T. C. McMullen, I. L. Campbell, R. Rohan, Y. Kaji, N. A. Afshari, T. Usui, D. B. Archer, and A. P. Adamis. 2002. The inflammatory milieu associated with conjunctivalized cornea and its alteration with IL-1 RA gene therapy. *Invest Ophthalmol Vis Sci* 43:2905.
 35. Saijo, Y., M. Tanaka, M. Miki, K. Usui, T. Suzuki, M. Maemondo, X. Hong, R. Tazawa, T. Kikuchi, K. Matsushima, and T. Nukiwa. 2002.

- Proinflammatory cytokine IL-1 beta promotes tumor growth of Lewis lung carcinoma by induction of angiogenic factors: in vivo analysis of tumor-stromal interaction. *J Immunol* 169:469.
36. Nakahara, H., J. Song, M. Sugimoto, K. Hagihara, T. Kishimoto, K. Yoshizaki, and N. Nishimoto. 2003. Anti-interleukin-6 receptor antibody therapy reduces vascular endothelial growth factor production in rheumatoid arthritis. *Arthritis Rheum* 48:1521.
37. Wei, L. H., M. L. Kuo, C. A. Chen, C. H. Chou, K. B. Lai, C. N. Lee, and C. Y. Hsieh. 2003. Interleukin-6 promotes cervical tumor growth by VEGF-dependent angiogenesis via a STAT3 pathway. *Oncogene* 22:1517.
38. Ristimaki, A., K. Narko, B. Enholm, V. Joukov, and K. Alitalo. 1998. Proinflammatory cytokines regulate expression of the lymphatic endothelial mitogen vascular endothelial growth factor-C. *J Biol Chem* 273:8413.
39. Ferrara, N., H. P. Gerber, and J. LeCouter. 2003. The biology of VEGF and its receptors. *Nat Med* 9:669.

APPENDIX

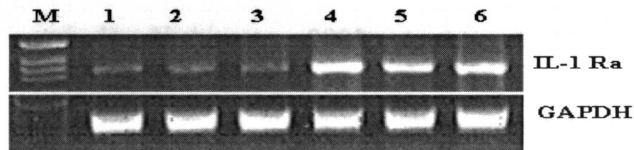


Fig 1. Expression of corneal IL-1 Ra mRNA at various time points after HSV infection

At different time points p. i., corneas ($n = 4$) were isolated and total RNA was extracted using Tri-Reagent. Total RNA ($1\mu\text{g}$) was converted into cDNA as described in the materials and methods. Polymerase chain reaction was performed in PTC-100 Programmable Thermal Controller, M J Research Incorporation. Murine GAPDH served as internal control. Lane M- Molecular weight marker; Lane 1- C57BL/6 naïve; Lane 2- C57BL/6 day 2 p. i.; Lane 3- C57BL/6 day 5 p. i.; Lane 4- IL-1 Ra Tg naïve; Lane 5- IL-1 Ra Tg day 2 p. i.; Lane 6- IL-1 Ra Tg day 5 p. i.

Fig 2. IL-1 Ra Tg mice show reduced antigenic response following HSV-1 infection at day 20 p. i.

A. Kinetics of corneal neovascularization process in mice infected with 5×10^6

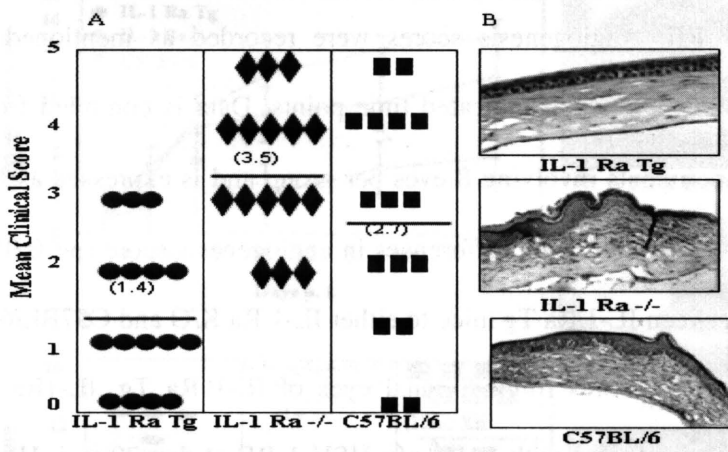


Fig 2. Reduced HSK severity in IL-1 Ra Tg mice

A. Mean lesion HSK score at day 20 p. i. of mice infected with 5×10^6 pfu HSV-1 RE. Each dot represents the HSK score from one eye. Horizontal bars and figures in the parenthesis indicate the mean for each group. Data is compiled from two separate experiments consisting of 8 eyes in each group.

B. Mice were infected with 5×10^6 pfu HSV-1 RE. Mice were terminated at day 20 p. i. and eyes were processed for paraffin embedding. Hematoxylin and Eosin staining was carried out on 6μ sections. Magnification x 200.

Fig 3. IL-1 Ra Tg mice show reduced angiogenic response following HSV-1 infection at day 20 p. i.

A. Kinetics of corneal neovascularization process in mice infected with 5×10^6 pfu HSV-1 RE. Angiogenesis scores were recorded as mentioned in the Materials and Methods at indicated time points. Data is compiled from two separate experiments involving 8 eyes per group and is expressed as Mean \pm SD. *Statistically significant differences in angiogenesis score ($p < 0.05$) were observed between IL-1 Ra Tg mice to either IL-1 Ra K/O and C57BL/6 mice.

B. Angiogenesis scores for individual eyes of IL-1 Ra Tg, IL-1Ra -/- and C57BL/6 mice infected with 5×10^6 pfu HSV-1 RE at day 20 p. i. Horizontal bars and figures show the mean for each group. Data are compiled from two separate experiments consisting of 8 eyes per group. *Statistically significant differences in angiogenesis score ($p < 0.05$) were observed between IL-1 Ra Tg mice to either IL-1 Ra K/O and C57BL/6 mice.

C. At day 20 p. i. extensive growth of blood vessels can be seen in IL-1 Ra -/- and C57BL/6 mice infected with 5×10^6 pfu HSV-1 RE. IL-1 Ra Tg mice show minimum angiogenic sprouts near the limbal ring with the same dose.

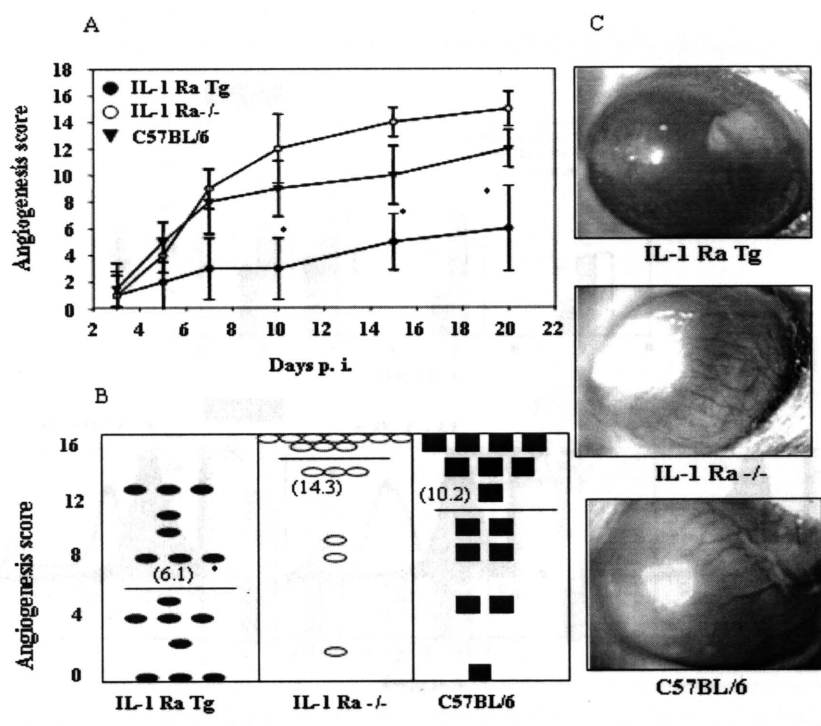


Fig 5. Reduced IL-6 and MCP-1 protein levels in IL-1Ra Tg mice at day 7 p.i.

Fig 4. Presence of abundant Gr-1+ve cells in the cornea of IL-1Ra -/- and IL-1Ra Tg mice.

Fig 3. Presence of abundant Gr-1+ve cells in the cornea of IL-1Ra Tg mice at day 7 p.i.

Fig 2. MIP-2 mRNA levels in corneal tissue at day 7 p.i. in IL-1Ra Tg mice.

Fig 1. Presence of abundant Gr-1+ve cells in the cornea of IL-1Ra Tg mice at day 7 p.i.

Fig 6. Presence of abundant Gr-1+ve cells in the cornea of IL-1Ra Tg mice at day 7 p.i.

Fig 7. Presence of abundant Gr-1+ve cells in the cornea of IL-1Ra Tg mice at day 7 p.i.

Fig 8. Presence of abundant Gr-1+ve cells in the cornea of IL-1Ra Tg mice at day 7 p.i.

Fig 9. Presence of abundant Gr-1+ve cells in the cornea of IL-1Ra Tg mice at day 7 p.i.

Fig 3. *IL-1 Ra Tg mice show reduced viral titers in the cornea following HSV-1 infection at day 20 p. i.*

A. Kinetics of corneal viral titers in *IL-1 Ra Tg* and *IL-1 Ra -/-* mice.

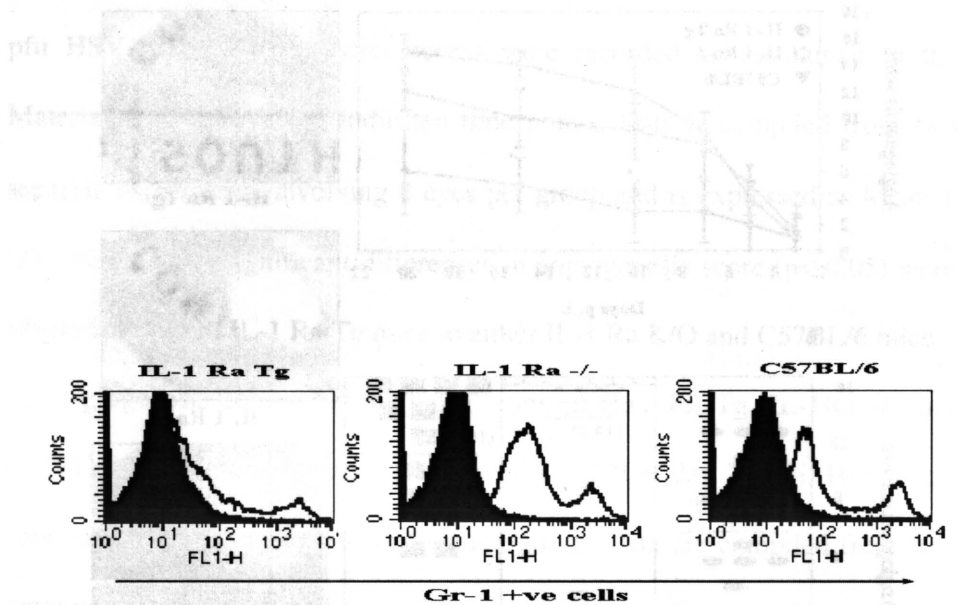


Figure 4. Presence of abundant Gr-1+ve cells in the cornea of *IL-1 Ra -/-* and *C57BL/6* mice but not in *IL-1 Ra Tg* mice at 48 hr p. i.

Fig 4. Presence of abundant Gr-1+ve cells in the cornea of *IL-1 Ra -/-* and *C57BL/6* mice but not in *IL-1 Ra Tg* mice at 48 hr p. i.

Single cell suspensions of corneal cells were prepared from 4 eyes at 24 and 48 hr p. i. The cells were counted and stained with FITC labeled anti Gr-1 antibody and numbers of Gr-1 positive cells were enumerated by FACS. Histogram is representative of one of three separate experiments. Shaded and open histogram represents Gr-1+ve cells at day 2 p. i. from uninfected and infected corneas respectively.

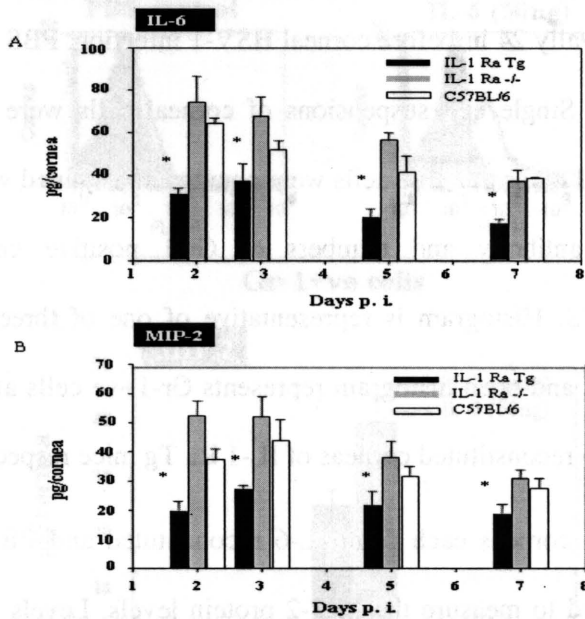


Fig 5. Reduced IL-6 and MIP-2 protein levels in HSV-1 infected corneas of IL-1 Ra Tg mice.

A & B. At indicated time points, 6 corneas /group were processed for measuring the IL-6 and MIP-2 protein levels. Levels of IL-6 and MIP-2 was estimated from supernatants of corneal lysates of mice infected with 5×10^6 pfu HSV-1 RE by an antibody capture ELISA as outlined in materials and methods. Results are expressed as Mean \pm SD of three separate experiments (6 corneas/time point). * Statistically significant differences in IL-6 and MIP-2 level ($p < 0.05$) were observed between IL-1 ra Tg mice to either IL-1 Ra K/O and C57BL/6 mice at all time points analyzed.

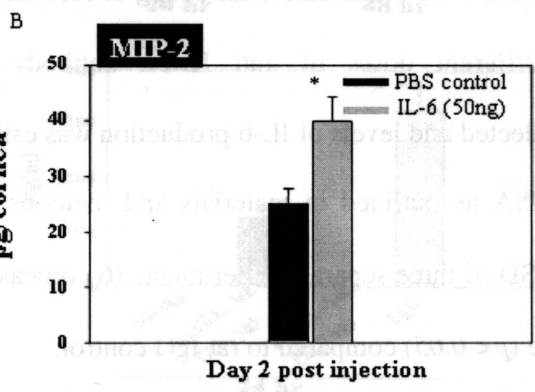
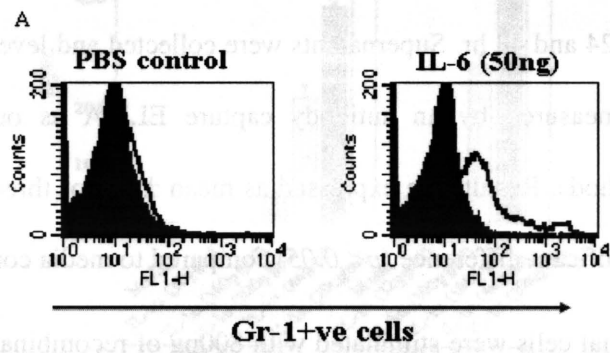
Fig 6. Increased Gr-1+ve cells and MIP-2 levels in recombinant murine IL-6 reconstituted IL-1 Ra Tg corneas at 48 hr p. i.

A. Mice transgenic for IL-1 Ra protein received recombinant murine IL-6 (50ng) subconjunctivally 24 hr before corneal HSV-1 infection. PBS was used as negative control. Single cell suspensions of corneal cells were prepared from 4 eyes at 24 and 48 hr p. i. The cells were counted and stained with FITC labeled anti Gr-1 antibody and numbers of Gr-1 positive cells were enumerated by FACS. Histogram is representative of one of three separate experiments. Shaded and open histogram represents Gr-1+ve cells at day 2 p. i. from PBS and IL-6 reconstituted corneas of IL-1 Ra Tg mice respectively.

B. At 48 hr p. i., 6 corneas each from IL-6 reconstituted and PBS control group were processed to measure the MIP-2 protein levels. Levels of MIP-2 was estimated from supernatants of corneal lysates of mice infected with 5×10^6 pfu HSV-1 RE by an antibody capture ELISA as outlined in materials and methods. Results are expressed as Mean \pm SD of three separate experiments (6 corneas/time point). *Significant difference ($p < 0.05$) compared to PBS treatment.

Fig 7. IL-1-induced IL-6 production from corneal epithelial cells.

A. Corneal epithelial cells were stimulated with different doses of recombinant IL-6 for 24 and 48 hours. Supernatants were collected and levels of IL-6 were measured by ELISA. Error bars represent standard deviation.



* Significant difference ($p < 0.05$) compared to media control.

Fig 7. IL-1 α induced IL-6 production from corneal epithelial cells.

A. Corneal epithelial cells were stimulated with different doses of recombinant murine IL-1 α for 24 and 48 hr. Supernatants were collected and levels of IL-6 production was measured by an antibody capture ELISA as outlined in materials and methods. Results are expressed as mean \pm SD of three separate experiments. *Significant difference ($p < 0.05$) compared to media control.

B. Corneal epithelial cells were stimulated with 800pg of recombinant murine IL-1 α along with different doses of anti IL-1 α antibody for 24 hr. Supernatants were collected and levels of IL-6 production was estimated by an antibody capture ELISA as outlined in materials and methods. Results are expressed as mean \pm SD of three separate experiments (6 corneas/time point).

*Significant difference ($p < 0.05$) compared to rat IgG control.

** Significant difference ($p < 0.05$) compared to media control.

Fig 8. Reduced VEGF protein levels and diminished expression of VEGFR-2

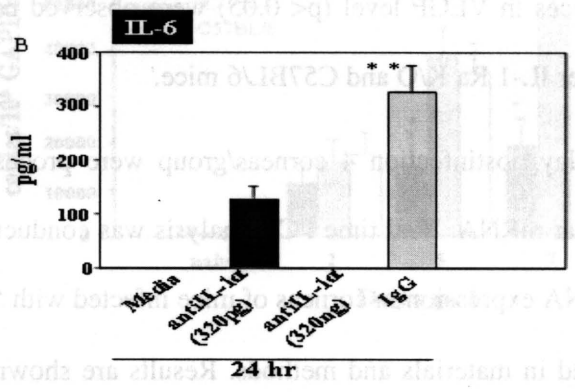
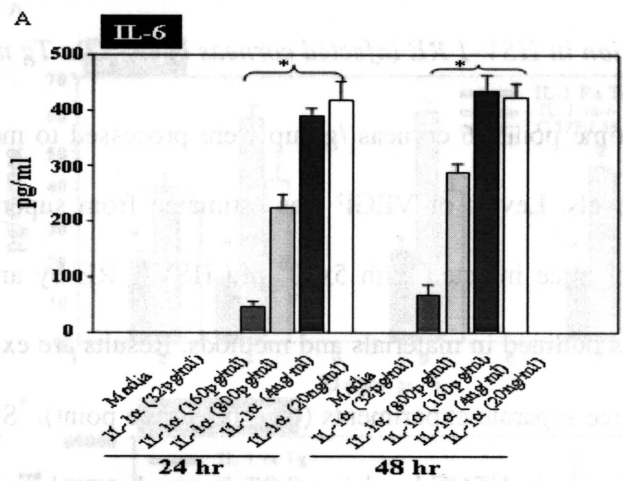


Fig 8. Reduced VEGF protein levels and diminished expression of VEGFR-2 mRNA expression in HSV-1 RE infected corneas of IL-1Ra Tg mice

A. At indicated time points 6 corneas /group were processed to measure the VEGF protein levels. Levels of VEGF was estimated from supernatants of corneal lysates of mice infected with 5×10^6 pfu HSV-1 RE by an antibody capture ELISA as outlined in materials and methods. Results are expressed as mean \pm SD of three separate experiments (6 corneas/time point). *Statistically significant differences in VEGF level ($p < 0.05$) were observed between IL-1 Ra Tg mice to either IL-1 Ra K/O and C57BL/6 mice.

B. At 2, 5 and 7 day postinfection 4 corneas/group were processed for the extraction of cellular mRNA. Real time PCR analysis was conducted to detect the VEGFR-2 mRNA expression in corneas of mice infected with 5×10^6 pfu of HSV-1 as described in materials and methods. Results are shown as mean \pm SD of three separate experiments. *Statistically significant differences ($p < 0.05$) were noted in the expression of VEGFR-2 between IL-1Ra Tg to IL-1 Ra K/O and C57BL/6 mice at 5 and 7 day p. i. ^aCopy number of the target gene was normalized to 10^6 copies of GAPDH.

Fig. 9. IL-1 induces upregulation of a corneal intracellular cytokine cascade

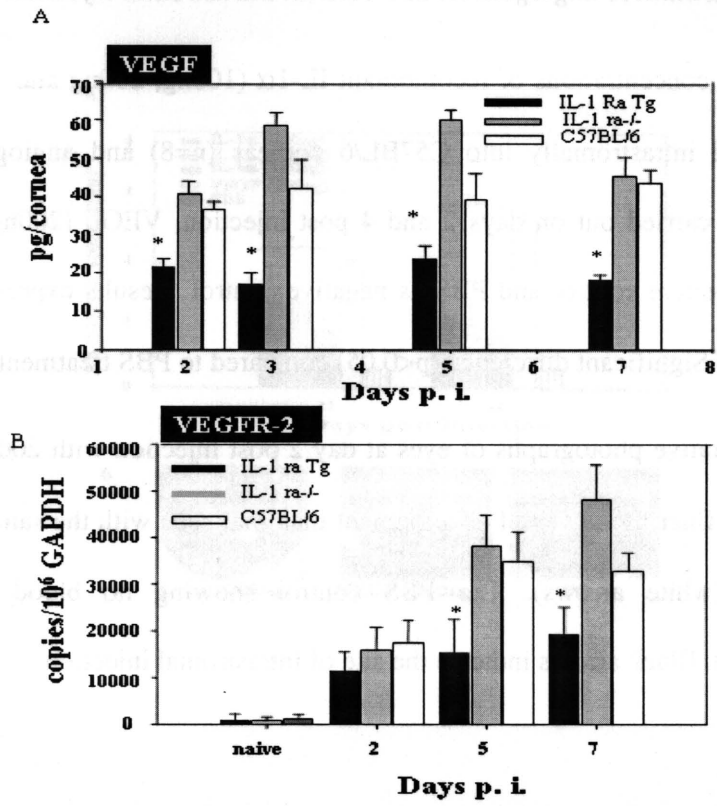
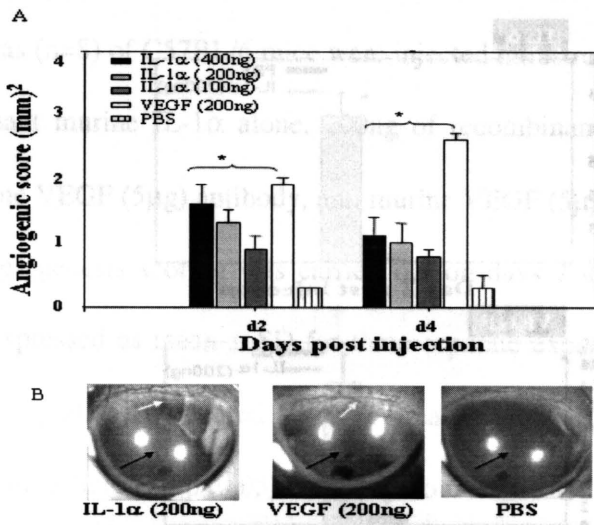


Fig 9. IL-1 α induces angiogenesis in a corneal intrastromal injection assay

A. Different concentrations of recombinant IL-1 α (100ng, 200ng and 400ng) was injected intrastromally into C57BL/6 corneas (n=8) and angiogenesis scoring was carried out on days 2 and 4 post injection. VEGF (200ng) was used as a positive control and PBS as negative control. Results expressed as mean \pm SD. *Significant difference (p<0.05) compared to PBS treatment.

B. Representative photographs of eyes at day 2 post injection with 200ng IL-1 α showing finer blood vessel development than that seen with the same dose of VEGF (white arrows). The PBS control showing no blood vessel development. Black arrows indicate the site of intrastromal injection.

Fig11. Neutralizing antibody against VEGF but not IL-6 can abrogate IL-1 α induced angiogenesis in the cornea.



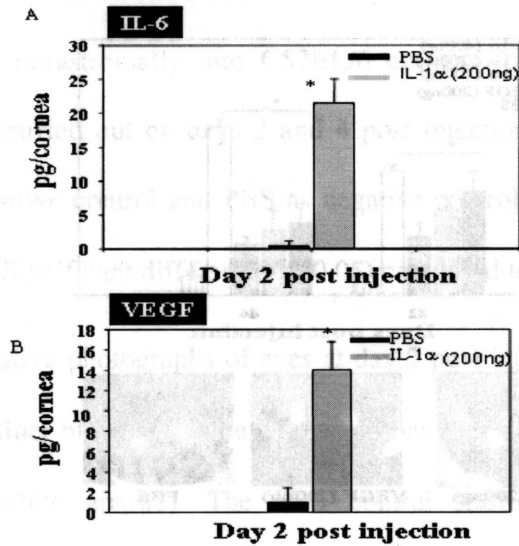
B. Corneas (n=8) of C57BL/6 mice were injected intrastromally with 200ng of recombinant murine IL-1 α alone, 200ng of recombinant murine IL-1 α and anti murine IL-6 (5 μ g) antibody, and murine IL-6 (5 μ g) antibody and PBS. Angiogenesis scoring was carried out on days 2 and 4 post injection. Results expressed as mean \pm SD for three separate experiments. Significant differences were indicated by asterisks.

Fig 10. IL-1 α increases IL-6 and VEGF production in the cornea. A. Significant differences were indicated by asterisks. B. Corneas of C57BL/6 mice were injected intrastromally with 200ng of recombinant murine IL-1 α alone, 200ng of recombinant murine IL-1 α and anti murine IL-6 (5 μ g) antibody, and murine IL-6 (5 μ g) antibody and PBS. Results are expressed as mean \pm SD for three separate experiments involving 6 corneas. Significant differences (p<0.05) compared to

IL-1 α treatment

Fig. 9. *IL-1 α induces angiogenesis in a corneal intrastromal injection assay*

A. Different concentrations of recombinant IL-1 α (100ng, 200ng and 400ng)



development. Black arrows indicate the site of intrastromal injection

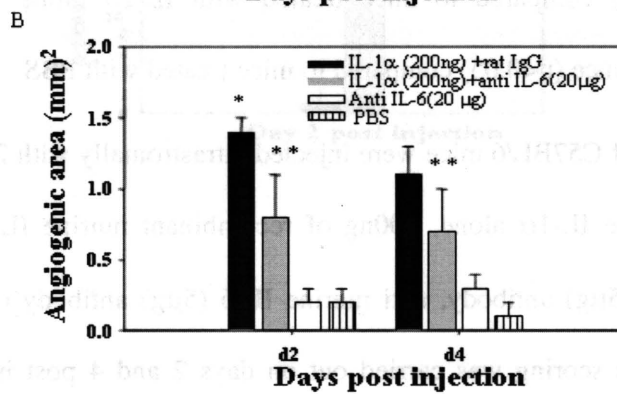
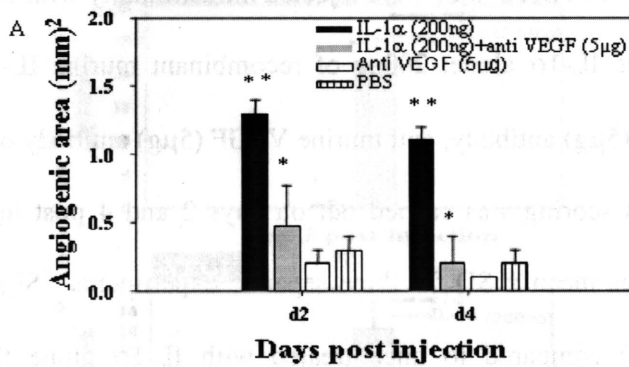
Fig 10. *IL-1 α induces IL-6 and VEGF production in the cornea*

A&B. Corneas of C57BL/6 mice were injected intrastromally with 200ng of recombinant murine IL-1 α . Corneas were excised from mice after 48hr and processed for detection of IL-6 and VEGF from corneal lysates as described in materials and methods. Results are expressed as mean \pm SD for three separate experiments involving 6 corneas. *Significant difference ($p < 0.05$) compared to PBS treatment.

Fig11. Neutralizing antibody against VEGF but not IL-6 can abrogate IL-1 α induced angiogenesis in the cornea.

A. Corneas (n=8) of C57BL/6 mice were injected intrastromally with 200ng of recombinant murine IL-1 α alone, 200ng of recombinant murine IL-1 α and anti murine VEGF (5 μ g) antibody, anti murine VEGF (5 μ g) antibody only and PBS. Angiogenesis scoring was carried out on days 2 and 4 post injection. Results expressed as mean \pm SD for three separate experiments. *Significant difference (p<0.05) compared to mice treated with IL-1 α alone (200ng). **Significant difference (p<0.05) compared to mice treated with PBS.

B. Corneas (n=8) of C57BL/6 mice were injected intrastromally with 200ng of recombinant murine IL-1 α alone, 200ng of recombinant murine IL-1 α and anti murine IL-6 (5 μ g) antibody, anti murine IL-6 (5 μ g) antibody only and PBS. Angiogenesis scoring was carried out on days 2 and 4 post injection. Results expressed as mean \pm SD for three separate experiments. *Significant difference (p<0.05) compared to mice treated with anti IL-6 antibody with IL-1 α . **Significant difference (p<0.05) compared to mice treated with only anti IL-6 antibody or PBS control.



PART III

INVOLVEMENT OF IL-6 IN THE

PARACRINE PRODUCTION OF VEGF IN

OCULAR HSV-1 INFECTION

Research described in this chapter is a slightly modified version of an article submitted for publication in the *Experimental Eye Research* published by Partha Sarathi Biswas, Kaustuv Banerjee, Paul R. Kinchington and Barry T. Rouse.

In this chapter “we” and “our” refers to co-authors and me. My contributions in the paper include (1) selection of the topic (2) data analysis and interpretation (3) planning experiments (4) compiling and interpretation of the literature (5) understanding how results fit with the literature (7) compilation of contributions into one paper (8) providing structure to the paper (9) making graphs, figures and tables (10) writing and editing.

ABSTRACT

Following ocular HSV-1 infection neovascularization of the avascular cornea is a critical event in the pathogenesis of herpetic stromal keratitis. Previous reports indicate an essential role for proinflammatory cytokines in HSV induced angiogenesis. This present study evaluates the role of proinflammatory cytokines such as IL-6 in corneal angiogenesis following virus infection. Our in vivo and in vitro data indicate that IL-6 produced from virus infected cells can stimulate noninfected resident corneal cells and other inflammatory cells in a paracrine manner to secrete VEGF, a potent angiogenic factor. Antibody neutralization of IL-6 results in a significant decrease in the number of VEGF producing cells in the cornea. Thus our result

serve to further demonstrate the close relationship between proinflammatory cytokines and VEGF induced corneal neovascularization.

INTRODUCTION

Ocular Herpes simplex virus 1 (HSV-1) infection may result in a chronic immunoinflammatory lesion in the corneal stroma termed herpetic stromal keratitis (HSK). In the murine model of HSV-1 ocular infection, the pathogenesis of stromal keratitis involves a CD4⁺ T cell mediated destruction of the cornea (1). However, prior to the immunoinflammatory phase, multiple events occur after virus infection that set the stage for the subsequent corneal pathology. These events include the production of proinflammatory cytokines, chemokines and neovascularization of the normally avascular cornea (2, 3). Angiogenesis occurs and new blood vessels sprout from limbal vessels within 24 h of HSV infection that eventually extend to the central cornea within 10–15 days (3). Such angiogenesis impairs vision and appears necessary for the ingress of T cells responsible for orchestrating HSK and impairs vision (1). Thus, neovascularization represents a major step in HSK pathogenesis, and multiple molecules are involved in this process. One of these is vascular endothelial growth factor (VEGF) (4). However, it is not known how HSV infections, which in the mouse model are usually confined to the corneal epithelium, results in VEGF production and initiate the angiogenesis process in the underlying corneal stroma. Previous studies from our group demonstrated that, 24 hr p. i. uninfected corneal resident cells are the principal source of VEGF, indicating a possible paracrine effect. One hypothesis is that

molecules released from infected cells could stimulate other cell types to produce VEGF. After HSV infection, both IL-1 and IL-6 are abundant by day 1 post infection (5, 6). These reach peak levels at day 10, and then diminish over the next few days (5, 6). Interleukin-1 produced from HSV-infected cells has been shown to be a potent VEGF inducer from uninfected resident corneal cells (7).

In addition to IL-1 produced from HSV-infected cells which acts to induce VEGF production, the aim of this study was to determine whether cytokine IL-6 could act as an additional VEGF stimulant. Both in vitro and in vivo observations demonstrate that IL-6 can stimulate uninfected corneal epithelial cells and stromal fibroblast cell line to produce VEGF. In addition, inflammatory cells, a critical component of murine HSK, can also be stimulated to produce VEGF by IL-6. Taken together these results indicate that production of VEGF following HSV infection is a paracrine event with IL-6 produced from virus infected cells acting as one of the factors. Thus IL-6 cause uninfected resident cells and inflammatory cells to produce VEGF which in turn led to corneal angiogenesis.

MATERIALS AND METHODS

Mice

Wild-type female 6-8 weeks old Balb/c mice were purchased from Harlan Sprague Dawley (Indianapolis, IN). Animals were sex and age matched for all experiments. All experimental procedures were in complete agreement with

the Association for Research in Vision and Ophthalmology resolution on the use of animals in research.

Virus

The virus HSV-1 RE-gC-EGFP is a gC-null derivative of the virus strain HSV-1 RE (8) that expresses the EGFP gene under the control of the gC promoter at the gC locus. To construct this virus, a plasmid was derived in which the EGFP gene (obtained as an NheI-XbaI DNA fragment by restriction enzyme digestion of the commercial plasmid pEGFP-N1: Clontech Corp, Palo Alto, CA) was cloned directly into a unique NheI site in the plasmid pUC8-gC. The latter plasmid is a cloned 949 base pair PstI-EcoRI fragment (co-ordinated 95,811 to 96,789, given with respect to the HSV-1 genome sequence) containing the promoter of gC and the first part of the gC open reading frame, all in the vector pUC8. The final resulting construct contains EGFP flanked by gC sequences, with the EGFP gene under control of the gC promoter and fused in the correct reading frame with the first 6 amino acids of gC. In this plasmid, the EGFP gene is followed by part of the gC open reading frame. The flanking gC sequences thus enable genetic recombination of the EGFP into the gC locus of the HSV-1 genome. To derive recombinant virus, the plasmid was linearized and cotransfected with purified HSV-1 RE DNA into vero cells using the calcium phosphate precipitation method. Following four days of incubation at 37°C, progeny virus in which recombination had occurred was identified by screening plaques for

fluorescence under UV illumination. Fluorescent virus was then plaque purified to homogeneity, and grown to stocks. The correct insertion of the EGFP gene and the absence of wild type virus in the final stocks were determined by Southern blot analyses. The virus was propagated and titrated on monolayer of Vero cells (American Type Culture Collection, Manassas, VA; catalogue CCL81) using standard protocols (9). Infected Vero cells were harvested, titrated, and stored in aliquots at -80°C until used.

Cells and Cell lines:

Corneal epithelial cells were isolated from the cornea of Balb/c mice as described with some modifications (10). Briefly, whole eyes were incubated at 37°C in PBS containing 10 mM tetra sodium diaminetetraacetate dehydrate (Sigma-Aldrich, St. Louis, MO) for 45 min. After incubation, the epithelial cell layer was separated from the adjacent corneal tissue by gentle teasing with a fine forceps. The intact epithelial layer was washed several times in PBS, followed by treatment with collagenase D (Roche, Basel, Switzerland) at 37°C for 30 min. The disrupted epithelial cells were then passed through a 40- μ m filter to make a single cell suspension. In some cases, the intact epithelial cell layer was used for the experiments.

The cell lines used for the experiments were MKT-1 (Murine Stromal Fibroblast cell line) (kindly gifted by Dr Winston Kao, Department of Ophthalmology, University of Cincinnati, Cincinnati, OH), J774A.1 (Macrophage cell line) (ATCC, Cat# TIB-67). The DC 2.4 (Dendritic cell line)

was generously provided by Dr. K. L. Rock (Deptt. of Pathology, University of Massachusetts Medical Schools, MA).

Corneal HSV-1 infection

Corneal infections of all mice groups were conducted under deep anesthesia induced by i.p. injection of avertin (Sigma-Aldrich, St. Louis, MO). Mice were scarified on their corneas with a 27-gauge needle, and a 4 μ l drop containing 5×10^5 pfu of virus was applied to the eye and gently massaged with the eyelids.

Subconjunctival injection

Subconjunctival inoculation of murine rIL-6 (BD PharMingen, San-Diego, CA) and anti-murine IL-6 Ab (5 μ g/ μ l) (BD Pharmingen, Rat IgG (5 μ g/ μ l) (R& D Systems) and LPS (1 μ g/ml dissolved in PBS) (Sigma) was performed, as described previously (11). Briefly, subconjunctival inoculations were done using a 2-cm 32-gauge needle and syringe (Hamilton, Reno, NV) to penetrate the perivascular region of conjunctiva and deliver into the subconjunctival space. Control mice received PBS only.

In vitro stimulation of corneal epithelial cell layer and cell lines with IL-6

For corneal epithelial cells, an intact corneal epithelial cell sheet was incubated in DMEM without sera containing various concentrations of recombinant IL-6 at 37° C and 5% CO₂ on a rotator shaker for 24 hrs. After 24 hrs, the cell sheets were spun down and total RNA was extracted. Treatment

with LPS (1 μ g/ml) (Sigma) and DMEM only was used as positive and negative control.

For various cell lines (MKT-1, J774A.1 and DC 2.4), 10⁵ cells/well were grown for 48 hrs in 6 well plate containing 10% FCS-DMEM. After 48 hrs of growth the cells were finally washed and stimulated with various concentrations of recombinant IL-6 in serum-free DMEM for 24 hrs. Following stimulation, the supernatants were collected and stored in -80° C until used. Treatment with DMEM only was used as negative control and LPS (1 μ g/ml) (Sigma) was used as a positive control.

Immunofluorescence staining and confocal microscopy

For immunofluorescence staining, eyes were enucleated at 24 hr. p. i. and snap frozen in OCT compound (Sakura, Torrance CA). Six-micron-thick sections were cut, air dried, and fixed in 4% para-formaldehyde at room temperature for 20 min. Sections were blocked with 3% BSA-PBS containing 0.05% Tween 20 and 1:200 dilution of F_c block (clone 2.4G2; BD PharMingen). Anti VEGF biotinylated antibody (R&D systems, Minneapolis, MN) was diluted (1:100) in 1% BSA-PBS containing 0.1% Triton-X and incubated overnight at 4°C. Sections were then treated with Streptavidin APC (BD Pharmingen) for 45 min. Corneal sections were repeatedly washed in PBS and mounted with Vectashield mounting medium for fluorescence (Vector Laboratories Inc. Burlingame, CA) and visualized with a confocal microscope (Leica, Wetzlar, Germany).

For immunofluorescence staining of IL-6 stimulated J774A.1, the protocol was same except, fixation was done with Acetone-methanol (1:1) at -20° C and Streptavidin Alexa-fluor (Molecular Probes, Eugene, OR) was used in place of Streptavidin APC. Following staining the J774A.1 cells was spun down on microscopic slides using a cytopspin machine. Slides were mounted with Vectashield mounting medium for fluorescence (Vector Laboratories Inc. Burlingame, CA) and visualized with a confocal microscope (Leica, Wetzlar, Germany)

RT-PCR

To detect the presence of IL-6 receptors (gp80 and gp130) on various cell types, total RNA from corneal epithelial cell sheet, MKT-1, J774A.1 and DC2.4 cells was extracted using RNeasy RNA extraction kit (Qiagen, Valencia, CA). Briefly, tissues were lysed in RLT buffer, and RNA was purified following manufacturer's instructions (Qiagen). DNase treatment (Qiagen) was done to remove any contaminating genomic DNA. Total RNA (1 µg) was reverse transcribed using murine leukemia virus reverse transcriptase (Life Technologies, Bethesda, MD) with oligo(dT) as primer (Invitrogen, San Diego, CA). All cDNA samples were aliquoted and stored at -20°C until further use. PCR was performed in PTC-100 Programmable Thermal Controller (MJ Research, Cambridge, MA) using Hot Start PCR Master Mix (Promega, Madison, WI). The primers used were murine GAPDH (forward: CATCCTGCACCACCAACTGCTTAG and reverse: GCCTGCTTCACCACCTTCTTGATG); murine gp80 (forward:

TGTCAACGCCATCTGTGAGTGG reverse:
ACTTTCGTA CTGATCCTCGTGG); murine gp130 (forward:
CAGCGTACACTGATGAAGGTGGGAAAGA reverse:
GCTGACTGCAGTTCTGCTTGA).

Cytokine ELISA of cell culture supernatant

Following 24 hrs of in vitro stimulation, the supernatant was collected and used immediately or stored at -80°C until further use. Lysates were analyzed using a standard sandwich ELISA protocol. Anti-VEGF capture and biotinylated detection Abs and recombinant standards for murine VEGF₁₆₄ were from R&D Systems. The color reaction was developed using 2, 2'-azino-bis-3 ethylbenzthiazoline-6-sulfonic acid) (Sigma-Aldrich) and measured with an ELISA reader (Spectramax 340; Molecular Devices, Sunnyvale, CA) at 405 nm. The detection limit was 2 pg/ml. Quantification was performed with Spectramax ELISA reader software version 1.2.

Intracellular staining and flow cytometry

Single cell suspensions were prepared from four corneas at 12 and 24 h post injection, as described elsewhere (12), with some modifications. Briefly, corneal buttons were incubated with collagenase D (Roche) for 60 min at 37°C in a humidified atmosphere at 5% CO₂. After incubation, corneas were disrupted by grinding with a syringe plunger and passing through a cell strainer. Cells were washed and suspended in RPMI 1640 with 10% FBS. The Fc

receptors on the cells were blocked with unconjugated anti-CD16/32 (BD PharMingen) for 30 min. Intracellular staining of VEGF was done as described before (4). All samples were collected on a FACScan (BD Biosciences, San Diego, CA), and data were analyzed using CellQuest 3.1 software (BD Biosciences).

Quantitative real-time PCR

Total RNA from four corneas per time point was extracted by using RNeasy RNA extraction kit (Qiagen, Valencia, CA). Briefly, tissues were lysed in RLT buffer, and RNA was purified following manufacturer's instructions (Qiagen). DNase treatment (Qiagen) was done to remove any contaminating genomic DNA. To generate cDNA, 1 μ g of total RNA was reverse transcribed using murine leukemia virus reverse transcriptase (Life Technologies) with oligo(dT) as primer (Invitrogen), according to manufacturer's instructions. All cDNA samples were aliquoted and stored at -20°C until further use.

Real-time PCR was performed using a DNA Engine Opticon (MJ Research Inc.). PCR was performed using SYBR Green I reagent (Qiagen), according to manufacturer's protocol. PCR amplification of housekeeping gene, murine GAPDH, was done for each sample as a control for sample loading and to allow normalization between samples. During the optimization procedures of the primers, 1% agarose gel analysis verified the amplification of one of the product of the predicted size with no primer-dimer bands. The absence of primer-dimer formation for each oligonucleotide set was also

validated by establishing the melting curve profile. The semiquantitative comparison between samples was calculated as follows: the data were normalized by subtracting the differences of the threshold cycles (C_T) between the gene of interest's C_T and the "house keeping" gene GAPDH's C_T (gene of interest $C_T - \text{GAPDH } C_T = \Delta C_T$) for each sample. The ΔC_T was then compared to the expression levels of the negative control sample (sample $\Delta C_T - \text{negative control } \Delta C_T$) (negative control samples include PBS injected eyes in case of in vivo experiments and media only in case of in vitro experiments). To determine the relative enhanced expression of the gene of interest, the following calculation was made: fold change = $2^{(-\text{sample } \Delta C_T - \text{negative control } \Delta C_T)}$. The primers used for murine VEGF₁₆₄ were, forward GCCAGCACATAGAGAAATGAGC and reverse CAAGGCTCACAGTGATTTTCTGG

Statistical analysis

Unless specified, a one-tailed, paired Student's *t*-test has been used.

RESULTS

Uninfected resident corneal cells act as a source of VEGF at an early stage of viral infection

To determine and characterize the cellular source of VEGF following virus infection, mice were infected with HSV-1 RE expressing EGFP under the control of gC promoter (HSV-1-RE-pgC-EGFP). At 24 hr p. i., corneas were

stained for VEGF. As demonstrated in Fig 1A, it is clearly evident that uninfected corneal epithelial cells surrounding the infected ones stained positive for VEGF. However, no double staining was observed in the infected cells. In addition, in the single cell suspension of cornea infected with HSV-1 RE pgC-EGFP, uninfected resident corneal cells (GFP⁻) and not infected cells (GFP⁺) were stained positive for VEGF at 24 hr p. i. (Fig. 1B and 1C). These results indicate that production of VEGF at an early time point was a product of uninfected resident corneal cells.

Subconjunctival injection of recombinant murine IL-6 induces VEGF in a dose dependent manner

To establish the role of IL-6 in paracrine production of VEGF, various doses (50ng, 100ng, 200ng and 400ng) of recombinant murine IL-6 was injected subconjunctivally (3 mice/group). At 24 hr post injection, an approximately an 8-10 fold increase in the VEGF transcript level was detectable by Real Time PCR (Fig. 2A). In addition, a dose dependent increase in the VEGF transcript level also occurred following IL-6 administration (Fig. 2A). At this time point, the VEGF transcript level was 1.8 fold (50ng), 5.9 fold (100ng), 9.8 fold (200ng) and 10.1 fold (400ng) higher in comparison to the PBS control. Antibody neutralization of recombinant IL-6 resulted in a dose dependent decrease in VEGF transcript levels (Fig. 2B). In addition, at an antibody concentration of 500ng (3.5 fold) and 5 μ g (1.4 fold) was significantly decreased ($p < 0.05$) in comparison to rat the IgG control (Fig. 2B).

In additional experiments, the number of resident corneal cells producing VEGF in response to subconjunctival injection of murine IL-6 (200ng) was quantified. As demonstrated in Fig. 2C, $0.9 \pm 0.3\%$ and $1.5 \pm 0.2\%$ of cells were VEGF⁺ at 12 and 24 hr post injection respectively. In addition antibody neutralization of IL-6 resulted in a significant ($p < 0.05$) decrease in the number of VEGF⁺ cells in comparison to the rat IgG control. These experiments suggest that IL-6, normally produced post HSV-1 infection, can in itself induce the production of VEGF from resident corneal cells.

To further delineate the possible cellular sources of VEGF following IL-6 stimulation primary corneal epithelial cells and various cell lines that represent cellular components of the cornea were stimulated in vitro with various doses of recombinant IL-6 for 24 hrs. All the cells investigated expressed both the gp80 and gp130 transcripts of the IL-6 receptor (Fig 3).

As shown in Fig 4A and B, corneal epithelial cells and stromal fibroblast cells respond to recombinant murine IL-6 result in a dose dependent manner to express VEGF transcript and protein levels respectively. In sharp contrast, there was no significant increase in the amount of VEGF produced from a dendritic cell line (DC 2.4) following stimulation with IL-6 for 24 hrs (Fig 5B).

To find out whether in addition to resident corneal cells, inflammatory cells can also produce VEGF in response to IL-6 stimulation, the macrophage cell line (J774A.1) was stimulated with various concentrations of recombinant murine IL-6. As evident from Fig. 5A, C, following 24hrs of stimulation, there

was a dose dependent increase in the VEGF label in cell culture supernatant. The VEGF level was significantly higher ($p < 0.05$) than the media control. Intracellular staining of some of these stimulated cells revealed positive staining for VEGF in the cytoplasm.

DISCUSSION

This present study evaluates the role of IL-6 in the initiation of corneal angiogenesis following virus infection. Both in vivo and in vitro data indicate that IL-6 produced from virus infected cells can stimulate noninfected resident corneal cells and other inflammatory cells in a paracrine manner to secrete VEGF, a potent angiogenic factor. Thus, our data substantiates the close relationship between proinflammatory cytokines and VEGF induced corneal neovascularization.

In HSK, angiogenesis is a prominent and early feature of the pathogenesis, with VEGF mRNA detectable by 12 hr p.i. and proteins detectable by 24 h p.i. (3, 4). Interestingly only a replication competent and not an incompetent virus have been shown to induce VEGF expression in the cornea, indicating the essential role of viral replication in the corneal epithelium to initiate this process (13). However, the production of VEGF seems to be the consequence of a paracrine effect of molecules released from a virus infected cell, as uninfected corneal cells and not infected cells stained positive for VEGF. The above observations raise the question as to the mechanism by which HSV infection of a cell triggers another cell to turn on VEGF gene expression. Although productive HSV infection by virtue of virion

host shutoff protein eliminates most host cell protein synthesis (14), evidence suggests that some proinflammatory cytokine gene such as IL-1 and IL-6 are upregulated (15, 16, 17). Supporting this scheme, previous studies demonstrated that shortly after HSV infection, both IL-1 and IL-6 are abundant by day 1 post infection. (5, 6). It is presently unclear as to whether, during a corneal infection, one of two cytokines precedes the other or whether they are both produced at the same time. However, based on the generally accepted fact that IL-1 precedes IL-6 in inflammatory cascade of events and our previous results (7), we believe that IL-1 is a critical cytokines and is presumably upregulated very early after infection of the cornea and induces the production of IL-6 from resident corneal cells (7). However, these cytokines are potent stimulators of VEGF production (18, 19). Previous study from our group demonstrated the essential role of IL-1 α in VEGF production from corneal epithelial cells (7). In addition, intrastromal injection of IL-6 results in corneal neovascularization in a VEGF dependent process (20). Specifically, IL-6 produced from a virus infected cell can stimulate surrounding noninfected cells to produce VEGF.

In our study the VEGF producers appeared to be two major cell types, noninflammatory residential corneal cells and inflammatory cells. Previous investigations have demonstrated that inflammatory cells start infiltrating corneal stroma 48 hr p.i. onwards (21). Thus, it can be assumed that early after infection most VEGF producing cells were noninflammatory resident corneal epithelial and stromal cells. Supporting this scheme we were able to demonstrate that both corneal epithelium and stromal cells can produce VEGF

in response to IL-6. The second VEGF-producing cell type was inflammatory cells in the corneal stroma. These were the major VEGF producers in the clinical phase, with both PMN and macrophage-like cells involved. Since virus is usually undetectable in the stroma and is absent in the cornea after the first few days of infection, virus itself, would seem not to be the stimulus for VEGF production. As macrophages are seen in the clinical phase, our data along with other findings (4) indicate that the predominant producer cell type appeared to be noninflammatory cells in the preclinical phase, but subsequently, in the clinical phase, macrophages and probably stromal fibroblast in the stroma were the sites of VEGF production. In addition, neutrophils also contribute significantly to VEGF induced angiogenesis process by carrying preformed VEGF in their vesicles (22, 23). However, it is not known whether IL-6 influence the neutrophil degranulation process and thereby causing release of preformed VEGF. This issue is currently under investigation.

Taken together, this study support the hypothesis that cytokines induced as a consequence of viral replication play an essential role in VEGF induced corneal neovascularization process. An important component of this cytokine milieu, as demonstrated in this present report is IL-6. Our results indicate that the control of angiogenesis by limiting the virus induced inflammatory response represents a useful therapy of herpetic ocular disease, an important cause of human blindness.

LIST OF REFERENCES

LIST OF REFERENCES

1. Deshpande, S., K. Banerjee, P. S. Biswas, and B. T. Rouse. 2004. Herpetic eye disease: immunopathogenesis and therapeutic measures. *Expert Rev. Mol. Med.* 30:1.
2. Kumaraguru, U., I. Davis, and B. T. Rouse. 1999. Chemokines and ocular pathology caused by corneal infection with herpes simplex virus. *J Neurovirol.* 5: 42.
3. Zheng, M., M. A. Schwarz, S. Lee, U. Kumaraguru, and B. T. Rouse. 2001a. Control of stromal keratitis by inhibition of neovascularization. *Am. J. Pathol.* 159:1021.
4. Zheng, M., S. Deshpande, S. Lee, N. Ferrara, and B. T. Rouse. 2001b. Contribution of vascular endothelial growth factor in the neovascularization process during the pathogenesis of herpetic stromal keratitis. *J. Virol.* 75:9828.
5. Staats, H. F., and R. N. Lausch. 1993. Cytokine expression in vivo during murine herpetic stromal keratitis. Effect of protective antibody therapy. *J. Immunol.* 151: 277.
6. Thomas, J., S. Kanangat, and B. T. Rouse. 1998. Herpes simplex virus replication-induced expression of chemokines and proinflammatory cytokines in the eye: implications in herpetic stromal keratitis. *J. Interferon Cytokine Res.* 18: 681.
7. Biswas, P. S., K. Banerjee, B. Kim, and B. T. Rouse. 2004. Mice transgenic for IL-1 receptor antagonist protein are resistant to herpetic

- stromal keratitis: possible role for IL-1 in herpetic stromal keratitis pathogenesis. *J. Immunol.* 172: 3736.
8. Liu, T., K. M. Khanna, X. Chen, D. J. Fink, and R. L. Hendricks. 2000. CD8(+) T cells can block herpes simplex virus type 1 (HSV-1) reactivation from latency in sensory neurons. *J. Exp. Med.* 191:1459.
 9. Spear, P. G., and B. Roizman. 1972. Proteins specified by herpes simplex virus. V. Purification and structural proteins of the herpes virion. *J. Virol.* 9:143.
 10. Lausch, R. N., S. H. Chen, S. H. Tumpey, Y. H. Su, and Y. H. Oakes. 1996. Early cytokine synthesis in the excised mouse cornea. *J. Interferon Cytokine Res.* 16: 35.
 11. Fenton, R. R., S. Molesworth-Kenyon, J. E. Oakes, and R. N. Lausch. 2002. Linkage of IL-6 with neutrophil chemoattractant expression in virus-induced ocular inflammation. *Invest. Ophthalmol. Vis. Sci.* 43:737.
 12. Deshpande, S., M. Zheng, S. Lee, K. Banerjee, S. Gangappa, U. Kumaraguru, and B. T. Rouse. 2001. Bystander activation involving T lymphocytes in herpetic stromal keratitis. *J. Immunol.* 167:2902.
 13. Babu, J. S., J. Thomas, S. Kanangat, L. A. Morrison, D. M. Knipe, and B. T. Rouse. 1996. Viral replication is required for induction of ocular immunopathology by herpes simplex virus. *J. Virol.* 70:101.
 14. Kwong, A. D., J. A. Kruper, and N. Frenkel. 1988. Herpes simplex virus virion host shutoff function. *J. Virol.* 62:912.

15. Kanangat, S., J. S. Babu, D. M. Knipe, and B. T. Rouse. 1996. HSV-1-mediated modulation of cytokine gene expression in a permissive cell line: selective upregulation of IL-6 gene expression. *Virology* 219:295.
16. Tran, M. T., D. A. Dean, R. N. Lausch, and J. E. Oakes. 1998. Membranes of herpes simplex virus type-1-infected human corneal epithelial cells are not permeabilized to macromolecules and therefore do not release IL-1alpha. *Virology* 244: 74.
17. Paludan, S. R. 2001. Requirements for the induction of interleukin-6 by herpes simplex virus-infected leukocytes. *J Virol.* 75: 8008.
18. Nakahara, H., J. Song, M. Sugimoto, K. Hagihara, T. Kishimoto, K. Yoshizaki, N. Nishimoto. 2003. Anti-interleukin-6 receptor antibody therapy reduces vascular endothelial growth factor production in rheumatoid arthritis. *Arthritis. Rheum.* 48:1521.
19. Wei, L. H., M. L. Kuo, C. A. Chen, C. A. Chou, K. B. Lai, C. N. Lee, and C. Y. Hsieh. 2003. Interleukin-6 promotes cervical tumor growth by VEGF-dependent angiogenesis via a STAT3 pathway. *Oncogene* 22:1517.
20. Banerjee, K., P. S. Biswas, B. Kim, S. Lee, and B. T. Rouse. 2004. CXCR2^{-/-} mice show enhanced susceptibility to herpetic stromal keratitis: a role for IL-6-induced neovascularization. *J. Immunol.* 172:1237.
21. Thomas, J., S. Gangappa, S. Kanangat, B. T. Rouse. 1997. On the essential involvement of neutrophils in the immunopathologic disease: herpetic stromal keratitis. *J. Immunol.* 158:1383.

22. Scapini, P., F. Calzetti, and M. A. Cassatella. 1999. On the detection of neutrophil-derived vascular endothelial growth factor (VEGF). *J. Immunol. Methods* 232:121.
23. Kasama, T., K. Kobayashi, N. Yajima, F. Shiozawa, Y. Yoda, H. T. Takeuchi, Y. Mori, M. Negishi, H. Ide, and M. Adachi. 2000. Expression of vascular endothelial growth factor by synovial fluid neutrophils in rheumatoid arthritis (RA). *Clin. Exp. Immunol.* 121:533.

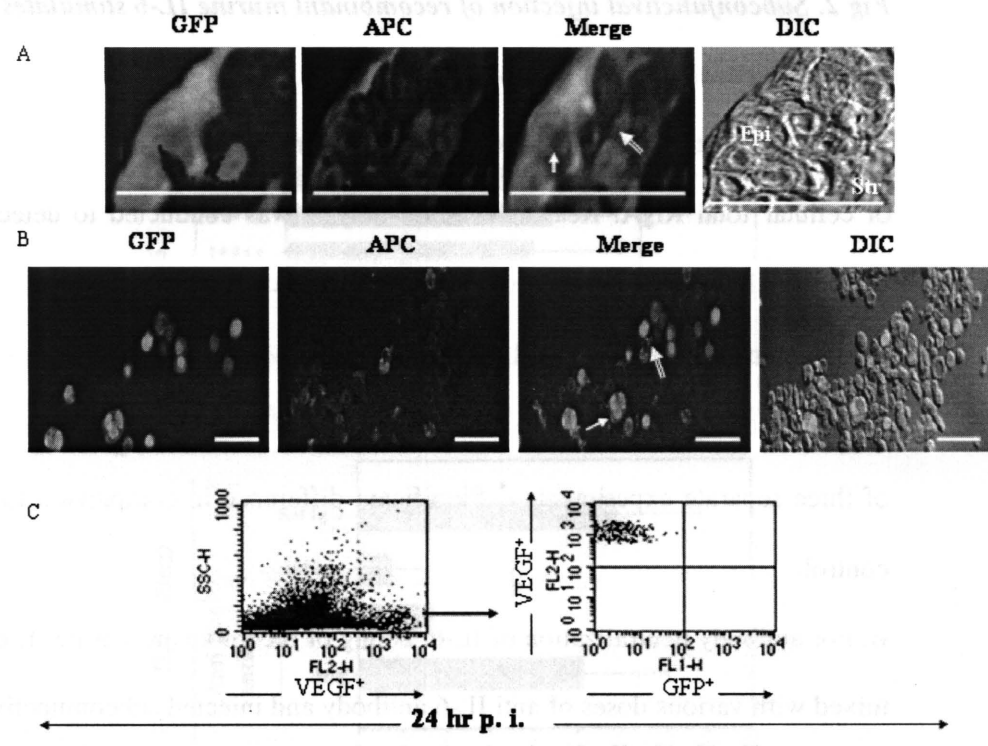
APPENDIX

Fig 1. Uninfected and not infected corneal epithelial cells express VEGF following ocular infection with HSV-1 following 24 hr post infection

A. Mice were infected with HSV-1-RE-pgC-GFP. At 24 hr p. i. eyes were frozen in OCT compound and six micron sections were made. The slides were stained with monoclonal anti mouse biotinylated VEGF antibody and Streptavidin APC. The slides were visualized under a confocal laser scanning microscope (Leica, Wetzlar, Germany). Original bar 80µm. The single arrow indicates the HSV-1 RE gC-GFP infected corneal epithelial cells and the double arrow indicates VEGF⁺ cells. Epi: Epithelium; Str: Stroma

B. Mice were infected with HSV-1-RE-pgC-GFP. At 24 hr p. i. corneas were digested and single cell suspension was made as described in *Materials and Methods*. The cells were stained with monoclonal anti mouse biotinylated VEGF antibody and Streptavidin APC. The slides were visualized under a confocal laser scanning microscope (Leica, Wetzlar, Germany). Original bar 80µm. The single arrow indicates the HSV-1-RE-pgC-GFP infected resident corneal cells and the double arrow indicates VEGF⁺ cells.

C. At 24 hr p. i. single cell suspensions were made from HSV-1-RE-pgC-GFP infected corneas. Numbers of cells expressing GFP (virus infected) out of total VEGF⁺ cells were enumerated by FACS analysis. The dot plot represents one of three separate experiments.



...the best interaction between VEGF and VEGFR-2 was observed for the extraction of cellular mRNA. Real time PCR analysis was conducted to quantify the VEGF mRNA in various of these tissues. The results are shown in Figure 2. The data described in Materials and Methods. Results are shown as mean \pm SD of three independent experiments. The number in the right hand represents one of the three separate experiments. The number in the right hand ...

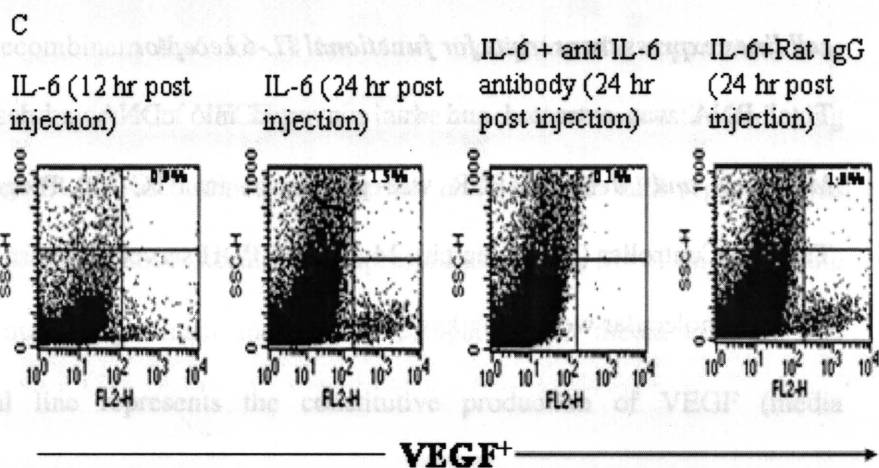
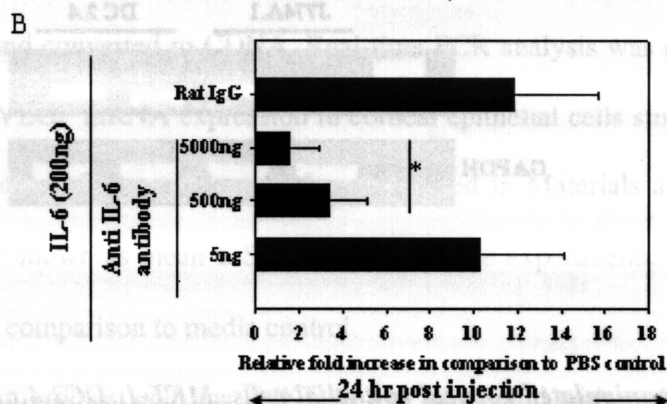
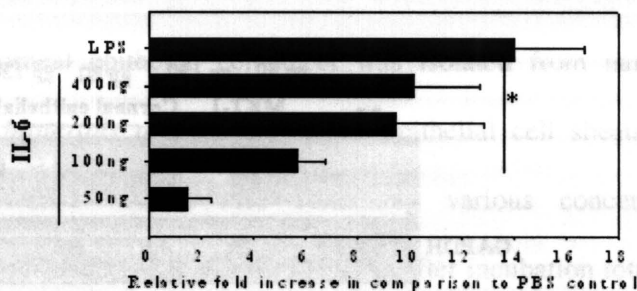
Fig 2. Subconjunctival injection of recombinant murine IL-6 stimulates resident corneal cells to produce VEGF

A. At 24 hr post injection four corneas/group were processed for the extraction of cellular total RNA. Real-time PCR analysis was conducted to detect the VEGF mRNA expression in corneas of mice injected with different doses of recombinant IL-6 as described in *Materials and Methods*. LPS (1µg/ml) was injected subconjunctivally as positive control. Results are shown as mean ± SD of three separate experiments. * Significant difference in comparison to PBS control.

B. For antibody neutralization of IL-6, 200ng of recombinant murine IL-6 was mixed with various doses of anti IL-6 antibody and injected subconjunctivally. At 24 hr post injection four corneas/group were processed for the extraction of cellular mRNA. Real-time PCR analysis was conducted to quantify the VEGF mRNA in corneas of mice injected with different doses of recombinant IL-6 as described in *Materials and Methods*. Results are shown as mean ± SD of three separate experiments. *Significant differences in comparison to rat IgG control.

C. At 24 hr post injection 6 corneas/ group were collected and made into single cell suspension. The cells were counted and intracellular staining was done with anti murine biotinylated VEGF antibody and streptavidin PE. The number of VEGF⁺ cells was enumerated by FACS analysis. The dot plot represents one of the three separate experiments. The number in the right hand corner represents percentage of VEGF⁺ cells out of total corneal cells.

Fig 4. Interleukin 6 stimulation of corneal epithelial cells and stromal fibroblast result in the expression of VEGF transcript and protein respectively. A



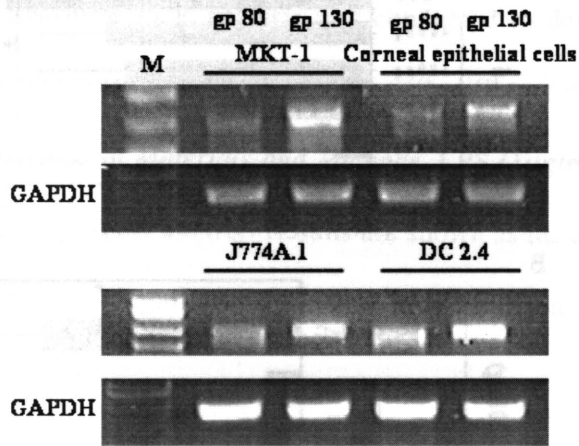


Fig 3. Unmanipulated corneal epithelial cells, MKT-1, DC2.4 and J774A.1 cell lines express transcripts for functional IL-6 receptor

Total RNA was extracted and was converted into cDNA, as described in *Materials and Methods*. PCR was performed in PTC-100 Programmable Thermal Controller (MJ Research). Murine GAPDH served as internal control.

Lane M: molecular weight marker.

Fig 4. Interleukin 6 stimulation of corneal epithelial cells and stromal fibroblast result in the expression of VEGF transcript and protein respectively

A. Murine corneal epithelial cell sheet was isolated from naïve mice as described in *Materials and Methods*. The epithelial cell sheets were then placed in DMEM without sera containing various concentrations of recombinant murine IL-6 for 24 hrs at 37° C. After incubation total RNA was extracted and converted to CDNA. Real-time PCR analysis was conducted to detect the VEGF mRNA expression in corneal epithelial cells stimulated with different doses of recombinant IL-6 as described in *Materials and Methods*. Results are shown as mean \pm SD of three separate experiments. * Significant increase in comparison to media control.

B. Stromal fibroblast cell line (MKT-1) was stimulated with various doses of murine recombinant IL-6 for 24 hrs. After incubation the supernatant was collected and amount of VEGF protein in the supernatant was estimated using a sandwich ELISA as outlined in *Materials and Methods*. LPS (1 μ g/ml) was used as positive control. Results are expressed as mean \pm SD of three separate experiments. * Significant increase in comparison to media control. The horizontal line represents the constitutive production of VEGF (media control).

Fig 4. Interleukin 6 stimulation of corneal epithelial cells and treatment
 fibroblast results in the expression of VEGF transcript and protein
 respectively

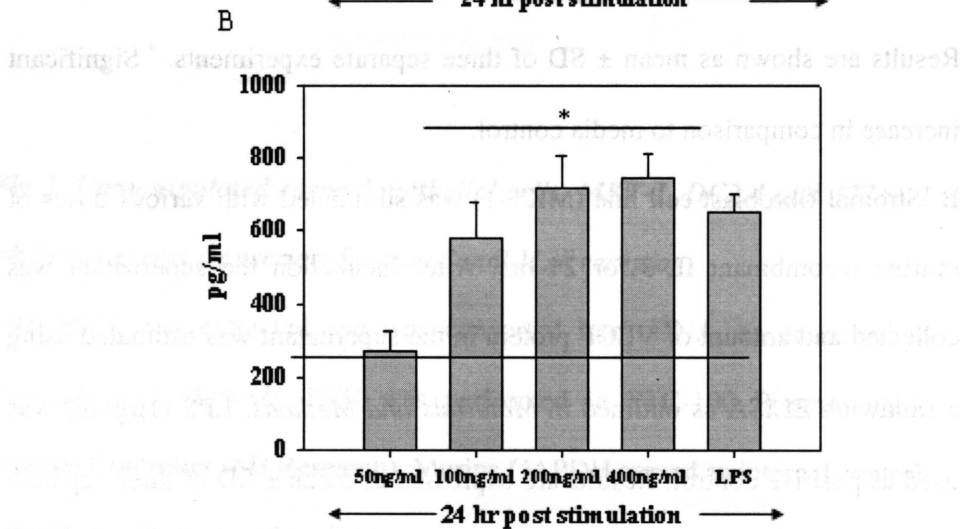
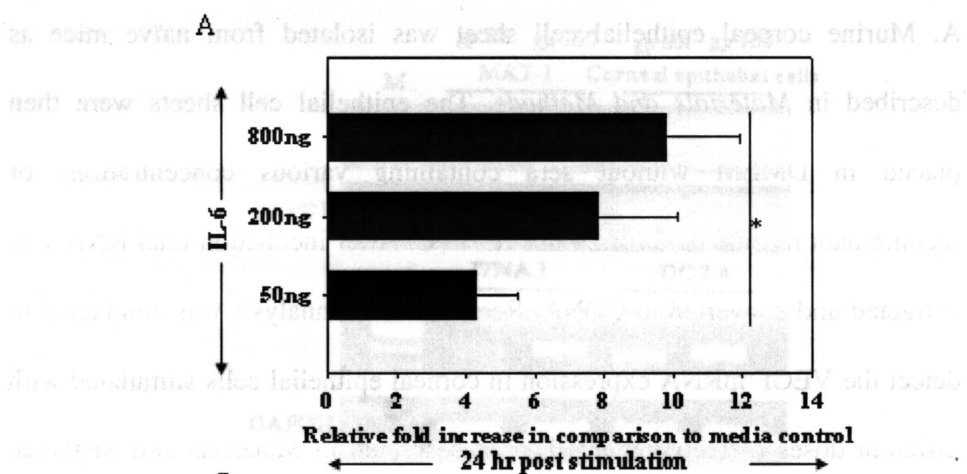


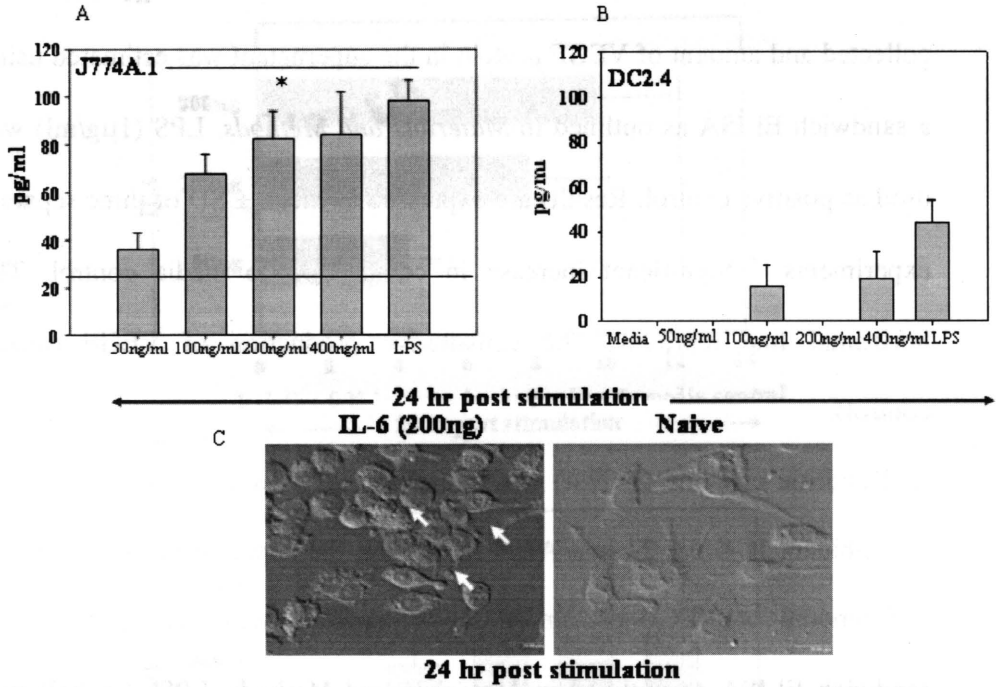
Fig 5. Macrophage cell line (J774A.1) produces VEGF following in vitro stimulation with various doses of recombinant murine IL-6

A. Macrophage cell line (J774A.1) was stimulated with various doses of murine recombinant IL-6 for 24 hrs. After incubation the supernatant was collected and amount of VEGF protein in the supernatant was estimated using a sandwich ELISA as outlined in *Materials and Methods*. LPS (1µg/ml) was used as positive control. Results are expressed as mean ± SD of three separate experiments. * Significant increase in comparison to media control. The horizontal line represents the constitutive production of VEGF (media control).

B. Dendritic cell line (DC2.4) was stimulated with various doses of murine recombinant IL-6 for 24 hrs. After incubation the supernatant was collected and amount of VEGF protein in the supernatant was estimated using a sandwich ELISA as outlined in *Materials and Methods*. LPS (1µg/ml) was used as positive control. Results are expressed as mean ± SD of three separate experiments.

C. Macrophage cell line (J774A.1) was stimulated with 200ng of murine recombinant IL-6 for 24 hrs. Following incubation intracellular staining was done to detect the VEGF using anti murine biotinylated VEGF antibody and streptavidin Alexa-flour. A total volume of 100µl cell suspension containing 5×10^4 cells was spun down using a cytopspin. The slides were visualized under a confocal microscope (Leica, Wetzlar, Germany). Original magnification x 200

Fig. 5. Macrophage cell line (J774A.1) produces VEGF following *in vitro* stimulation with various doses of recombinant murine IL-6. A Macrophage cell line (J774A.1) was stimulated with various doses of murine recombinant IL-6 for 24 hr. After incubation the supernatant was



Macrophage cell line (J774A.1) was stimulated with 200ng of murine recombinant IL-6 for 24 hr. Following incubation intracellular staining was done to detect the VEGF using anti murine biotinylated VEGF antibody and streptavidin Alexa-fluor. A total volume of 100µl cell suspension containing 2×10^5 cells was spun down using a cyto spin. The slides were visualized under a confocal microscope (Leica, Wetzlar, Germany). Original magnification x

PART IV

**ROLE OF IL-1 INDUCED COX-2 IN OCULAR
IMMUNOPATHOLOGIC DISEASE;
HERPETIC STROMAL KERATITIS**

Research described in this chapter is a slightly modified version of an article submitted for publication in The Journal of Immunology by Partha Sarathi Biswas, Kaustuv Banerjee, Bumseok Kim, Paul R. Kinchington and Barry T. Rouse.

In this chapter “we” and “our” refers to co-authors and me. My contributions in the paper include (1) selection of the topic (2) data analysis and interpretation (3) planning experiments (4) compiling and interpretation of the literature (5) understanding how results fit with the literature (7) compilation of contributions into one paper (8) providing structure to the paper (9) making graphs, figures and tables (10) writing and editing.

ABSTRACT

Ocular infection with Herpes simplex virus (HSV) results in a blinding immuno-inflammatory lesion known as herpetic stromal keratitis (SK). Early preclinical events include PMN infiltration and neovascularization in the corneal stroma. In this report, we demonstrate that HSV infection of the cornea results in the upregulation of the Cyclooxygenase 2 enzyme (COX-2). The likely source of COX-2, at least initially after infection, was stromal fibroblasts. This enzyme was shown to contribute to the early inflammatory and neovascularization process in response to HSV infection through upregulation of prostanoids. Inhibition of COX-2 with a selective inhibitor was shown to reduce corneal angiogenesis and HSK severity. The administration of a COX-2 inhibitor resulted compromised PMN infiltration

into the cornea. In addition, the treatment diminished corneal vascular endothelial growth factor levels, likely accounting for the reduced angiogenic response. Since early proinflammatory events and angiogenesis appears to represent a critical step in the pathogenesis of SK, these results indicate that targeting COX-2 for inhibition should prove useful for the therapy of herpetic SK.

INTRODUCTION

Herpetic stromal keratitis (HSK) is a blinding immunopathological reaction that results from ocular infection with Herpes simplex virus 1 (HSV-1) (1). This results mainly from a chronic inflammatory reaction in the normally transparent and avascular cornea. Studies with the murine model have revealed a complicated pathogenesis, the critical event being the influx of CD4⁺ T cells (2, 3). Prior to the T cell-mediated immunoinflammatory phase, multiple events occur after virus infection that set the stage for the subsequent pathology. These events include the production of proinflammatory mediators, prominent invasion of the cornea by polymorphonuclear leukocytes (PMN) and corneal angiogenesis (4). However the factors responsible to initiate the inflammatory and angiogenic events in the corneal stroma following virus infection remain poorly understood. Previous studies demonstrated that HSV replication, which in the mouse model is usually confined to the corneal epithelium, results in the production of proinflammatory cytokines and chemokines, creating an environment favorable for cell influx and angiogenesis in corneal stroma (4). Thus understanding these early

inflammatory mediators that determine the subsequent outcome of this immunopathological condition is crucial for designing potential therapeutic approaches to counteract this blinding disease in humans.

Arachidonic acid (AA), an unsaturated fatty acid is a normal constituent of membrane phospholipids and is released by the actions of phospholipase A₂. AA is converted to prostaglandins (PGs) by cyclooxygenase (COX) and to leukotrienes (LTs) by 5-lipoxygenase metabolites that are biologically very active and modulate cellular functions (5). The two isoforms of COX, COX-1 and COX-2 are encoded by two separate genes and exhibit distinct cell specific expression, regulation and subcellular localization (5). COX-1 is a constitutive enzyme and is essential for various physiological functions (5). In contrast, COX-2 is an inducible enzyme that is induced in a variety of cell types by diverse stimuli (5). COX-2 induced production of prostanoids is often implicated in chronic inflammatory diseases, characterized by edema, chemotactic factors, prostanoids, leukotrienes and phospholipase (6, 7). Increased COX-2 induced synthesis of prostaglandins stimulates cancer cell proliferation (8), promotes angiogenesis (9, 10), inhibits apoptosis (11) and increases metastatic potential (12). In addition, recent studies demonstrated the essential role of COX-2 mediated up regulation of prostanoids in various ocular inflammatory models (13-15).

The aim of this study was to determine whether inhibition of COX-2, as could be achieved by using a selective COX-2 blocker, had an effect on SK pathogenesis. Our results with ocular infection with HSV demonstrate that selective inhibition of COX-2, but not COX-1, resulted in significantly milder

disease and reduced corneal angiogenesis compared to control mice. This difference in disease phenotype was an indirect event and was shown to be the consequence of a compromised early inflammatory response. Taken together, our results demonstrate that COX-2 mediated prostanoids production is critical in SK pathogenesis, and that the use of NSAIDs to inhibit COX-2 represents a valuable approach for disease control.

MATERIALS AND METHODS

Mice

Wild-type, female, 6 to 8 week old, Balb/c and C57BL/6 mice were purchased from Harlan Sprague-Dawley (Indianapolis, IN). Animals were sex- and age-matched for all experiments. Mice transgenic (Tg) for IL-1 α protein (T14 hemizygous line) were kindly provided by Dr. David Hirsh (Department of Biochemistry and Molecular Biophysics, College of Physician and Surgeons, Columbia University, New York, NY). All manipulations involving the immunocompromised mice were performed in a laminar flow hood. All experimental procedures were in complete agreement with the Association for Research in Vision and Ophthalmology resolution on the use of animals in research.

Virus

HSV-1 RE (obtained from Dr. Robert Hendricks Laboratory, University of Pittsburgh School of Medicine, PA) was used in the present study. HSV-1 RE-pgC-GFP was derived in the RE strain background of HSV-1, detailed by

Hendricks group (16) and is a null mutant at the gC locus. For construction, a cloned PstI-EcoRI fragment (sequences from 95811 to 96789 in wild type HSV-1 genome) containing the gC promoter and first part of the gC open reading frame (ORF) in the corresponding sites of puc8, was first collapsed by digestion, blunt end generation and religation to remove PstI, HindIII and sites between. A NheI-XbaI fragment derived from pEGFP-N1 (Clontech, Palo Alto, CA) was then inserted into the unique NheI site located at the sequence encoding residue 6 of gC, resulting in an in-frame placement of the EGFP gene immediately following the glycoprotein C first 6 residues and gC promoter. This plasmid was linearized, co-transfected with purified HSV-1 RE DNA into vero cells using calcium phosphate coprecipitation, and progeny virus with EGFP driven by the native gC promoter were identified by fluorescence, plaque purified and insert confirmed by Southern blot analysis. The virus was propagated and titrated on a monolayer of Vero cells (American Type Culture Collection, Manassas, VA, Cat. No. CCL81) using standard protocols (17). Infected Vero cells were harvested, titrated, and stored in aliquots at -80°C until used.

Corneal HSV-1 infection

Mice were ocularly infected with HSV-1 RE (5×10^5 pfu for Balb/c and 5×10^6 pfu for C57BL6) under deep anesthesia induced by intraperitoneal injection of Avertin (Sigma-Aldrich, St. Louis, MO). Mice were lightly scarified on their corneas with a 27-gauge needle, and a 4- μl drop containing the required dose of virus was applied to the eye and gently massaged with the eyelids.

Clinical observations and angiogenesis scoring

The eyes were examined on different days post infection (p. i.) by a slit-lamp biomicroscope (Kowa Co., Nagoya, Japan), and the clinical severity of keratitis of individually scored mice was recorded as described previously (18). Briefly, the clinical lesion score of SK was described as 0, normal cornea; 1, mild haze; 2, moderate haze, iris visible; 3, severe haze, iris not visible; 4, severe haze and corneal ulcer; and 5, corneal rupture. Angiogenesis severity was measured as described previously (19). According to this system, a grade of 4 for a given quadrant of the circle represents a centripetal growth of 1.5 mm toward the corneal center. The score of the four quadrants of the eye was then summed to derive the neovessel index (range, 0–16) for each eye at a given time-point.

Administration of COX-1 and COX-2 inhibitors

For COX inhibition experiments, Balb/c and C57BL6 mice were treated with COX-1 inhibitor SC-560 (10 mg/kg/day) (Upjohns and Pharmacia, a division of Pfizer) and COX-2 inhibitor SC-236 (10 mg/kg/day) (Upjohns and Pharmacia, a division of Pfizer) or vehicle 0.5% methylcellulose, 0.025% Tween 80 (Sigma) by gavages. The treatment was started a day before corneal infection and continued till day 10 p. i. These doses were recommended by the manufacturer as being selective for effective inhibition of COX-1 and COX-2 and have been used previously (20, 21).

In vitro stimulation of murine stromal fibroblast cell line with various recombinant murine cytokines

For stimulation of murine stromal fibroblast cell line (MKT-1) (kindly provided by Dr. W. Kao, Department of Ophthalmology, University of Cincinnati, Cincinnati, OH), 10^5 cells/well were grown for 48 hrs in 6 well plate containing 10% FCS-DMEM. After 48 hrs of growth the cells were finally washed and stimulated with various concentrations of recombinant IL-1 α , IL-1 β , TNF- α , IL-6, IL-18, IFN- γ , IL-2 and VEGF in sera free DMEM for 24 hrs. Following stimulation, total RNA was extracted and stored at -80° C till further use. LPS was used as positive control and only media was used as negative control.

Corneal micropocket assay

The murine corneal micropocket assay was done as described previously (22). Various doses (50ng and 200ng) of recombinant murine IL-1 β (R&D systems) were added to these pellets before insertion into corneal pockets (four eyes per group). In some experiments, mice were treated with COX-2 inhibitors before corneal micropocket assay was performed. Angiogenesis was quantitated at day 3 post implantation under stereomicroscopy as described previously (23).

Histopathology

For histopathological analysis, eyes were extirpated at day 20 p.i. and fixed in 10% buffered neutral formalin. Staining was performed with hematoxylin and eosin (H&E; Richard Allen Scientific, Kalamazoo, MI).

Immunofluorescence and Immunohistochemistry staining

For immunofluorescence staining of Gr-1⁺ cells, at day 2 p. i., eyes were frozen in optimum cutting temperature (OCT) compound (Miles, Elkart, IN). Sections were stained for Gr-1⁺ cells with fluorescein isothiocyanate (FITC)-labeled anti-mouse Gr-1⁺ antibody (clone RB6-8C5, BD PharMingen) and counterstained with Vectashield mounting medium for fluorescence with propidium iodide (Vector Laboratories, Burlingame, CA) and visualized under a fluorescence microscope (Leica, Wetzlar, Germany).

For immunohistochemistry eyes were enucleated at the indicated time points and snap frozen in OCT compound (Miles, Elkart, IN). Six-micron-thick sections were cut, air dried, and fixed in acetone:methanol (1:1) at -20°C for 10 min. Endogenous peroxidase activity was blocked using a 50% alcohol solution containing 0.3% hydrogen peroxide for 15 min, and sections were blocked with 3% BSA-PBS. For detection of COX-2, Goat Anti-Cox2 (M-19) (Santa Cruz Biotechnology, Santa Cruz, CA) was diluted 1/100 and incubated for 1 hr at room temperature. Sections were then treated with Rabbit Anti-Goat IgG biotinylated antibody (1/200) (Vector Laboratories, Burlingame, CA) followed by HRP-conjugated streptavidin for 45 min (1/1000 dilution; Jackson

ImmunoResearch Laboratories, West Grove, PA) and 3, 3'-diaminobenzidine substrate (Biogenex, San Ramon, CA), and counterstained with hematoxylin (Richard Allen Scientific, Kalamazoo, MI). Irrelevant biotinylated antibody was used as negative controls.

Enzyme-linked immunosorbent assay (ELISA) of corneal lysate

For preparation of corneal lysates, six corneas per time-point were pooled and processed as described previously (24). Lysates were analyzed using a standard sandwich ELISA protocol. Anti-IL-6 capture and biotinylated detection antibodies were from BD PharMingen (clone MP5-20F3), and standard recombinant murine (rm)IL-6 was from R&D Systems (Minneapolis, MN). Anti-IL-1 α , anti-MIP-2, anti-VEGF, anti IL-1 β and anti TNF- α capture, biotinylated detection antibodies and recombinant standards were from R&D Systems. The color reaction was developed using 2,2'-azinobis(3-ethylbenzothiazoline-6-sulfonic acid diammonium salt) (Sigma-Aldrich) and measured with an ELISA reader (Spectramax 340, Molecular Devices, Sunnyvale, CA) at 405 nm. Quantification was performed with Spectramax ELISA reader software version 1.2.

Prostaglandin E₂ extraction and quantification was done as per manufacturer's protocol. Briefly, six corneas per time point were dissected under a microscope, dipped briefly in 100 μ M indomethacin in saline to stop prostaglandin synthesis and wash off excess blood, and placed in a homogenizer tube containing garnet beads, and 0.5 ml of ethanol. The corneas

were homogenized using a tissue homogenizer (PRO Scientific Inc., Monroe, CT). Protein precipitate was pelleted in a microcentrifuge, and the ethanol layer was removed to a clean tube. The ethanol was evaporated by vacuum centrifugation, the residue was redissolved in enzyme immunoassay (EIA) buffer (Cayman Chemical, Ann Arbor, MI), and samples were analyzed for PGE₂ and LTB₄ using an EIA kit (Cayman Chemical).

Flow cytometry

Single cell suspensions were prepared from four corneas at 48 h post infection, as described elsewhere (25). The Fc receptors on the cells were blocked with unconjugated anti-CD16/32 (BD PharMingen) for 30 min. Samples were incubated with FITC-labeled anti-Gr-1 Ab (clone RB6-8C5; BD PharMingen) and isotype controls for 30 min. All samples were collected on a FACScan (BD Biosciences, San Diego, CA), and data were analyzed using CellQuest 3.1 software (BD Biosciences).

Reverse transcriptase Polymerase chain reaction

Total RNA from MKT-1 cells was extracted by using Tri-reagent (Molecular Biology, Cincinnati, OH). Total RNA (1 μ g) was reverse transcribed using murine leukemia virus reverse transcriptase (Life Technologies, Bethesda, MD) with oligo(dT) as primer (Invitrogen, San Diego, CA). All cDNA samples were aliquoted and stored at -20°C until further use. PCR was performed in PTC-100 Programmable Thermal Controller (MJ Research,

Cambridge, MA) using Hot Start PCR Master Mix (Promega, Madison, WI).

The primers used were murine GAPDH Forward
CATCCTGCACCACCAACTGCTTAG, Reverse
GCCTGCTTCACCACCTTCTTGATG; murine IL-1 β Forward
CAACCAACAAGTGATAT, Reverse GATCCAGAGTCTCCAGCTGCA;
murine COX-2 Forward TTCGGGAGCACAACAGAGTG; Reverse
TAACCGCTCAGGTGTTGCAC.

Quantitative real-time PCR

Total RNA from four corneas per time point was extracted by using RNeasy RNA extraction kit (Qiagen, Valencia, CA) according to manufacturer's instructions. To generate cDNA, 1 μ g of total RNA was reverse transcribed using murine leukemia virus reverse transcriptase (Life Technologies) with oligo(dT) as primer (Invitrogen), according to manufacturer's instructions. All cDNA samples were aliquoted and stored at -20°C until further use.

Real-time PCR was performed using a DNA Engine Opticon (MJ Research Inc.). PCR was performed using SYBR Green I reagent (Qiagen), according to manufacturer's protocol. PCR amplification of housekeeping gene, murine GAPDH, was done for each sample as a control for sample loading and to allow normalization between samples. During the optimization procedures of the primers, 1% agarose gel analysis verified the amplification of one of the product of the predicted size with no primer-dimer bands. The absence of primer-dimer formation for each oligonucleotide set was also

validated by establishing the melting curve profile. The semiquantitative comparison between samples was calculated as follows: the data were normalized by subtracting the differences of the threshold cycles (C_T) between the gene of interest's C_T and the "house keeping" gene GAPDH's C_T (gene of interest $C_T - \text{GAPDH } C_T = \Delta C_T$) for each sample. The ΔC_T was then compared to the expression levels of the vector control sample (sample $\Delta C_T - \text{vector } \Delta C_T$). To determine the relative enhanced expression of the gene of interest, the following calculation was made: fold change = $2^{-(\text{sample } \Delta C_T - \text{vector } \Delta C_T)}$. The primers used were murine GAPDH Forward CATCCTGCACCACCAACTGCTTAG, Reverse GCCTGCTTCACCACCTTCTTGATG; HSV polymerase Forward CCGTACATGTCGATGTTACC, Reverse ATCAACTTCGACTGGCCCTTC; HSV gB Forward: CGTTTCGCAGGTGTGGTTC, Reverse: ATGTCGGTCTCGTGGTGC. murine COX-2 Forward TTCGGGAGCACAACAGAGTG; Reverse TAACCGCTCAGGTGTTGCAC; murine COX-1 Forward ACT CAC TCA GTT TGT TGA GTC ATT C, Reverse TTT GAT TAG TAC TGT AGG GTT AAT G.

Statistical analysis

Unless specified, a one-tailed, paired Student's *t*-test has been used.

RESULTS

Mice treated with COX-2 inhibitor demonstrated diminished SK severity and corneal angiogenesis following ocular HSV-1 infection

Mice (Balb/c and C57BL6) were ocularly infected with HSV-1 RE and at different days post infection and corneal levels of COX-1, COX-2 mRNA and PGE₂ protein were measured by Real Time PCR and ELISA respectively. As demonstrated in Fig. 1, the kinetic study revealed a steady increase in the COX-2 mRNA and PGE₂ protein levels during the preclinical phase (till day 7 p. i.) of SK. The levels of COX-2 mRNA and PGE₂ protein were below the limit of detection in naïve corneas. However, COX-1 mRNA was found to be constitutively expressed in naïve corneas and following HSV infection no significant ($p < 0.05$) increase in the expression level was observed (data not shown). Taken together these data indicate that corneal inflammation during the preclinical phase is associated with a prompt increase in the COX-2 expression, an enzyme essential for the synthesis of various proinflammatory prostanoids such as PGE₂.

To elucidate the essential role of COX-2 in HSK pathogenesis, three groups of Balb/c (5×10^5 pfu) and C57BL6 (5×10^6 pfu) mice were treated (till day 10 p. i.) with COX-2 inhibitor (SC-260), COX-1 inhibitor (SC-536) or vehicle respectively. These mice were evaluated clinically for the development of SK following ocular HSV-1RE infection over a 20 days test period. As shown in Fig. 2A and 2C, groups of Balb/c and C57BL6 mice receiving COX-2 inhibitor demonstrated significantly ($p < 0.05$) reduced SK severity [mean

score 1.4 ± 0.7 (Balb/c) and 1.0 ± 0.8 (C57BL6)] in comparison to COX-1 [mean score 2.9 ± 0.8 (Balb/c) and 2.8 ± 0.9 (C57BL6)] and vehicle control [mean score 3.4 ± 0.6 (Balb/c) and 2.7 ± 0.9 (C57BL6)] groups. In addition, while 87.5% (Balb/c) and 62.5% (C57BL6) eyes demonstrated clinically evident lesions (score 3 or more), only 25% (Balb/c) and 12.5% (C57BL6) COX-2 inhibitor treated eyes developed such lesions (Fig. 2B and D). Attempts to infect mice with a higher virus dose resulted in lethality, but still few developed a SK score of greater than or equal to 3 in COX-2 inhibitor treated mice (data not shown). Histopathological analysis of representative eyes of vehicle and COX-1 inhibitor treated mice revealed severe inflammatory changes and cellular infiltration in the corneal stroma at day 20 p. i. (Fig 2E). However, in mice, treated with COX-2 inhibitor protein, only mild, inflammatory changes and cellular infiltrations were evident (Fig 2E).

In concurrence with lesion incidence and severity, significant differences were apparent in the average extent of angiogenesis in mice treated with COX-2 inhibitor and vehicle only following ocular infection with HSV-1 RE (5×10^5 pfu for Balb/c and 5×10^6 pfu for C57BL6) at day 20 p. i. (Fig 3B and D). At day 20 p. i., 10 of 16 eyes (Balb/c) and 8 of 16 eyes (C57BL6) of vehicle treated mice had developed an angiogenesis score of greater than 10 (Fig.3A and C). In marked contrast, no eyes of COX-2 inhibitor treated BALB/c and C57BL6 mice developed equivalent scores (Fig. 3A and C). When the overall angiogenesis was compared in the groups of vehicle treated and COX-2 inhibitor treated mice (Balb/c and C57BL6), vehicle control mice

showed 3-4 times (day 20 p. i.) more angiogenesis than COX-2 inhibitor treated mice (Fig. 3A and C).

IL-1 β induces COX-2 expression in murine cornea following ocular HSV-1 infection

To evaluate the cellular source of COX-2 at an early stage of virus infection, Balb/c corneas were infected with HSV-1-pgC-GFP. After 24hr p. i., corneas were isolated and GFP⁺ (infected) and GFP⁻ (uninfected) corneal cells were sorted by FACS and analyzed for COX-2 mRNA expression by Real Time PCR analysis. Interestingly, uninfected corneal cells expressed significantly ($p < 0.05$) higher COX-2 mRNA in comparison to infected cells (Fig 4A). Polymerase chain reaction of GFP⁻ (uninfected) corneal cells revealed 3000-4000 fold lesser viral mRNA (gB, tk) in comparison to GFP⁺ (infected) at this time point (data not shown). In addition, by immunohistochemically we were able to demonstrate that corneal stromal fibroblasts and few corneal epithelial cells expressed COX-2 at 24 hr p. i. (Fig 4B).

Additional experiments were carried out to detect the factors responsible for inducing COX-2 expression in corneal stromal fibroblasts following viral infection. Based on previous findings, potential candidates for inducing COX-2 were proinflammatory cytokines. Thus a murine stromal fibroblast cell line was stimulated in vitro by various doses of proinflammatory cytokines known to be upregulated in murine corneas following HSV infection (IL-1 α , IL-1 β , TNF- α , IL-6, IL-18, IFN- γ , IL-2 and

VEGF). Interestingly, only IL-1 β (in all the doses used) and TNF- α (only at the highest dose used) induced COX-2 mRNA expression at 24 hr p. i. as revealed by RT-PCR (data not shown). Quantitatively, Real Time PCR analysis revealed a significant ($p < 0.05$) and dose dependent increase in COX-2 mRNA expression in IL-1 β treated cells (Fig. 5A). Hence, IL-1 β produced as consequence of corneal HSV infection (Fig. 5B) may serve as a potential molecule to induce COX-2 and drive the early inflammatory process. Supporting this notion, we were able to demonstrate that administration of IL-1 β in the murine cornea by micropocket assay resulted in a significant ($p < 0.05$) and dose dependent increase in COX-2 mRNA level (Fig 5C). Blocking of IL-1 β activity using IL-1 receptor antagonist transgenic mice resulted in a significantly ($p < 0.05$) diminished COX-2 mRNA and PGE₂ levels in murine cornea following ocular HSV-1 infection (Fig 5D and E).

Diminished inflammatory response in mice treated with COX-2 inhibitor during the preclinical phase of HSK

Normally, after corneal HSV-1 infection, PMN infiltrate the corneal stroma at 48 hr p. i. (26). However, in mice treated with COX-2 inhibitor and eventually showing a reduction in SK severity, the influx of PMN was severely compromised (Fig 6). As revealed by FACS analysis at 48 hr p. i., there was approximately 5-6 fold reduction in the number of PMN in COX-2 treated corneas in comparison to vehicle controls. (Fig 6).

We reasoned that the scarce cellular influx in the treated group was a result of a block in the induction of proinflammatory cytokines and chemokines, as a consequence of impaired COX-2 activity. As demonstrated in Fig 7, indeed there was a significant reduction ($p < 0.05$) in IL-6, IL-1 α , MIP-2 and PGE₂ levels during the preclinical phase. However no significant difference was observed in IL-1 β and TNF- α levels at these time points (data not shown). Although the LTB₄ level was reduced at day 1 p. i., there was no significant ($p < 0.05$) reduction at 3 and 7 days p. i. (data not shown).

Compromised angiogenic response following ocular HSV infection in COX-2 inhibitor treated mice

As stated above, groups of mice treated with COX-2 inhibitor showed diminished angiogenic responses in comparison to vehicle treated controls. These mice when tested for corneal VEGF level during the preclinical phase, demonstrated significantly ($p < 0.05$) reduced levels of VEGF at 3 and 7 days p. i. in comparison to vehicle controls (Fig 8A). Previous studies in tumor systems demonstrated that IL-1 β can induce VEGF production through upregulation of COX-2 and prostanoids (27). To demonstrate the angiogenic activity of COX-2 induced prostanoids in murine corneas, different doses of murine rIL-1 β were administered by corneal micropocket assay, and the extent of angiogenesis was measured at day 3 post implantation. Interestingly, IL-1 β induced a dose-dependent angiogenic response (Fig. 8B). In such eyes, COX-2 protein was readily detectable by immunohistochemistry around the pellet containing recombinant IL-1 β protein (200ng) in corneal stroma at day 4 post

implantation (Fig 8C). In addition, IL-1 β (200ng) implanted eyes demonstrated a significant ($p < 0.05$) increase in the corneal PGE₂ and VEGF protein levels in comparison to pellet only at this time point (Fig. 8E). Administration of COX-2 inhibitor in those mice resulted in a significant ($p < 0.05$) decrease in the angiogenic response (Fig 8D). This decrease in angiogenic response was associated with a reduction in corneal PGE₂ and VEGF protein levels in those corneas (Fig 8E).

DISCUSSION

This study focuses on the early events in the pathogenesis of the blinding immunoinflammatory lesion SK caused by ocular infection with HSV. In this report, we demonstrate that HSV infection of the cornea results in the upregulation of the COX-2 enzyme. This enzyme was shown to contribute to the inflammatory and neovascularization process in the corneal stroma through upregulation of prostanoids. The likely source of COX-2, at least initially after infection was corneal stromal fibroblasts. Interleukin-1 β , a proinflammatory cytokine produced as a consequence of HSV replication stimulates stromal fibroblasts to produce COX-2. The present study demonstrates for the first time, the critical role of COX-2 for herpetic SK lesion development. Accordingly, selective inhibition of COX-2 and not COX-1 results in significantly milder disease and reduced corneal angiogenesis compared to control mice. This difference in disease phenotype was an indirect event and was shown to be the consequence of a compromised inflammatory and angiogenic response. Thus our results imply that COX-2

plays an important role in early inflammatory phase and blocking COX-2 activity using NSAIDS could represent a valuable therapeutic approach to control HSK.

Early after ocular HSV infection the cellular source of COX-2 was shown to be the stromal fibroblasts. It is not clear how COX-2 expression is induced in stromal fibroblasts following HSV replication, since the infection appears confined to the corneal epithelium (4). Our study demonstrated that IL-1 β , and to some extent TNF- α , produced as a consequence of HSV replication, may stimulate stromal fibroblasts to produce COX-2. Blocking IL-1 β by IL-1 receptor antagonist protein resulted in a diminished COX-2 expression. This study, as well as others (28-30), indicated that IL-1 β stimulated fibroblasts are potent producers of COX-2. The above observations thus delineate the mechanism by which HSV infection of a cell triggers another cell to turn on COX-2 gene expression. However previous studies revealed that virus reactivation in the trigeminal ganglion is associated with upregulation of COX-2 transcript expression (31). Thus it is unclear whether upregulation of COX-2 is also mediated by some HSV-encoded components released from infected cells. We are currently analyzing the role of some of these viral encoded proteins as candidates to explain COX-2 triggering.

A prominent early event after virus infection of the cornea is the influx of inflammatory cells into the avascular stroma, primarily PMN (26). This influx occurs promptly after infection and most likely serves several functions. These include antiviral effects (26, 32) and an involvement in neovascularization (33). Our result showed that mice treated with selective

COX-2 inhibitor have compromised neutrophil influx. This observation is in concordance with previous findings demonstrating the essential role of COX-2 induced prostanoids in neutrophil influx and activation in various inflammatory models such as rheumatoid arthritis, dermatitis, periodontitis and pancreatitis (34-36). How COX-2 induced prostanoids in infected mice cornea causes PMN influx remains unclear.

The possible signals responsible for the PMN influx are most likely multiple and nonviral derived. Previous observations demonstrated that MIP-2, IL-6 and IL-1 are critical in early influx of PMN in the murine cornea following virus infection (24, 37, 38) and the level of COX-2 correlates with the expression patterns of these cytokines and chemokines (39). Thus, it is highly likely that COX-2 induced prostanoid synthesis aid PMN influx through upregulation of IL-1, IL-6 and MIP-2. Supporting this scheme, we could show that mice treated with selective COX-2 inhibitors and having compromised neutrophil influx had lower levels of corneal IL-1, IL-6 and MIP-2. Previous observations demonstrated that in humans selective inhibition of COX-2 can prevent IL-8 mediated PMN chemotaxis at the inflammatory site (40). This observation along with ours further strengthens the notion that COX-2 plays a critical role in PMN chemotaxis by upregulating various proinflammatory cytokines and chemokines. In addition, PMN and macrophages themselves serve as an additional source of COX-2 induced prostanoids at the inflammatory site (41, 42). We anticipate that, early after infection, COX-2 produced from stromal fibroblasts facilitates the influx of

PMN, which in turn now acts as an additional source of prostanoids, thus setting the stage for the chronic immuno-inflammatory phase.

Early PMN invasion contributes to corneal pathology because the cells are a major source of angiogenesis factors (33, 43) and perhaps also tissue damaging factors such as NO (44). Thus, in line with the minimal early PMN response noted in COX-2 inhibitor treated mice, such animals showed a marked reduction in angiogenesis. One factor derived from PMN, as well as from other cell types involved in neovascularization, is VEGF (43). We demonstrated that VEGF was significantly down-regulated in COX-2 inhibitor treated mice in comparison to control animals. This observation is in accord with previous findings in rheumatoid synoviocyte and tumour models (9, 10). How COX-2 induces VEGF production is not known. One explanation for diminished angiogenic response in COX-2 inhibitor treated mice is, COX-2 induced PGE₂ itself has been shown to be proangiogenic (45). PGE₂ along with other prostanoids can stimulate the production of VEGF (39). However, it is not clear whether this effect is direct or mediated by upregulation of other cytokines such as IL-6, IL-1 and chemokines containing E-L-R motifs. We are currently testing such notions in our HSV angiogenesis model.

COX-2 represents a logical target for therapy, since this component acts as a principal inflammatory and angiogenic factor in HSV induced corneal inflammation. However, COX-2 inhibitors should be used with a word of caution. Previous studies in Endotoxin induced uveitis (EIU) model suggested that disturbance of the AA pathway exacerbates EIU in COX-2-deficient mice (46). This was caused by elevated LTB₄ and 5-LO metabolized

from arachidonic acid via the lipoxygenase pathway. At least, in our system we were able to demonstrate that inhibition of COX-2 is not associated with an increase in LTB₄, thus justifying our approach in counteracting corneal immunoinflammatory lesion with COX-2 inhibitors.

Taken together, our results support the hypothesis that the inflammatory milieu and angiogenic stimuli created early after infection play an important role in HSV-induced ocular lesions. An important participant of this environment is COX-2 induced prostanoid synthesis. Blocking the effect of COX-2 by a specific COX-2 inhibitor abrogates the cascade of events that culminate in HSK. This regulation is indirectly mediated by down-regulating various signaling molecules previously known to be important in HSK pathogenesis and corneal angiogenesis. Thus targeting COX-2 could prove to be a worthwhile therapeutic approach to control SK, an important cause of human blindness.

LIST OF REFERENCES

LIST OF REFERENCES

1. Streilein, J. W., M. R. Dana, and B. R. Ksander. 1997. Immunity causing blindness: five different paths to herpes stromal keratitis. *Immunol Today* 18:443.
2. Metcalf, J. F., D. S. Hamilton, and R. W. Reichert. 1979. Herpetic keratitis in athymic (nude) mice. *Infect Immun* 26:1164.
3. Russell, R. G., M. P. Nasisse, H. S. Larsen, and B. T. Rouse. 1984. Role of T-lymphocytes in the pathogenesis of herpetic stromal keratitis. *Invest Ophthalmol Vis Sci* 25:938.
4. Deshpande, S., K. Banerjee, P. S. Biswas, and B. T. Rouse. 2004. Herpetic eye disease: immunopathogenesis and therapeutic measures. *Expert Rev Mol Med* 2004:1.
5. Williams, C. S., and R. N. DuBois. 1996. Prostaglandin endoperoxide synthase: why two isoforms? *Am J Physiol* 270:G393.
6. Arslan, A., and H. H. Zingg. 1996. Regulation of COX-2 gene expression in rat uterus in vivo and in vitro. *Prostaglandins* 52:463.
7. Tanaka, Y., M. Takahashi, M. Kawaguchi, and F. Amano. 1997. Delayed release of prostaglandins from arachidonic acid and kinetic changes in prostaglandin H synthase activity on the induction of prostaglandin H synthase-2 after lipopolysaccharide-treatment of RAW264.7 macrophage-like cells. *Biol Pharm Bull* 20:322.

8. Sheng, H., J. Shao, M. K. Washington, and R. N. DuBois. 2001. Prostaglandin E2 increases growth and motility of colorectal carcinoma cells. *J Biol Chem* 276:18075.
9. Ben-Av, P., L. J. Crofford, R. L. Wilder, and T. Hla. 1995. Induction of vascular endothelial growth factor expression in synovial fibroblasts by prostaglandin E and interleukin-1: a potential mechanism for inflammatory angiogenesis. *FEBS Lett* 372:83.
10. Tsuji, S., S. Kawano, M. Tsujii, T. Michida, E. Masuda, E. S. Gunawan, and M. Hori. 1998. [Mucosal microcirculation and angiogenesis in gastrointestinal tract]. *Nippon Rinsho* 56:2247.
11. Sheng, H., J. Shao, J. D. Morrow, R. D. Beauchamp, and R. N. DuBois. 1998. Modulation of apoptosis and Bcl-2 expression by prostaglandin E2 in human colon cancer cells. *Cancer Res* 58:362.
12. Kakiuchi, Y., S. Tsuji, M. Tsujii, H. Murata, N. Kawai, M. Yasumaru, A. Kimura, M. Komori, T. Irie, E. Miyoshi, Y. Sasaki, N. Hayashi, S. Kawano, and M. Hori. 2002. Cyclooxygenase-2 activity altered the cell-surface carbohydrate antigens on colon cancer cells and enhanced liver metastasis. *Cancer Res* 62:1567.
13. Takahashi, K., Y. Saishin, K. Mori, A. Ando, S. Yamamoto, Y. Oshima, H. Nambu, M. B. Melia, D. P. Bingaman, and P. A. Campochiaro. 2003. Topical nepafenac inhibits ocular neovascularization. *Invest Ophthalmol Vis Sci* 44:409.

14. Sennlaub, F., F. Valamanesh, A. Vazquez-Tello, A. M. El-Asrar, D. Checchin, S. Brault, F. Gobeil, M. H. Beauchamp, B. Mwaikambo, Y. Courtois, K. Geboes, D. R. Varma, P. Lachapelle, H. Ong, F. Behar-Cohen, and S. Chemtob. 2003. Cyclooxygenase-2 in human and experimental ischemic proliferative retinopathy. *Circulation* 108:198.
15. Sarlos, S., B. Rizkalla, C. J. Moravski, Z. Cao, M. E. Cooper, and J. L. Wilkinson-Berka. 2003. Retinal angiogenesis is mediated by an interaction between the angiotensin type 2 receptor, VEGF, and angiopoietin. *Am J Pathol* 163:879.
16. Liu, T., K. M. Khanna, X. Chen, D. J. Fink, and R. L. Hendricks. 2000. CD8(+) T cells can block herpes simplex virus type 1 (HSV-1) reactivation from latency in sensory neurons. *J Exp Med* 191:1459.
17. Spear, P. G., and B. Roizman. 1972. Proteins specified by herpes simplex virus. V. Purification and structural proteins of the herpesvirion. *J Virol* 9:143.
18. Banerjee, K., S. Deshpande, M. Zheng, U. Kumaraguru, S. P. Schoenberger, and B. T. Rouse. 2002. Herpetic stromal keratitis in the absence of viral antigen recognition. *Cell Immunol* 219:108.
19. Dana, M. R., S. N. Zhu, and J. Yamada. 1998. Topical modulation of interleukin-1 activity in corneal neovascularization. *Cornea* 17:403.

20. Johnson, P. M., S. K. Vogt, M. W. Burney, and L. J. Muglia. 2002. COX-2 inhibition attenuates anorexia during systemic inflammation without impairing cytokine production. *Am J Physiol Endocrinol Metab* 282:E650.
21. Masferrer, J. L., B. S. Zweifel, P. T. Manning, S. D. Hauser, K. M. Leahy, W. G. Smith, P. C. Isakson, and K. Seibert. 1994. Selective inhibition of inducible cyclooxygenase 2 in vivo is antiinflammatory and nonulcerogenic. *Proc Natl Acad Sci U S A* 91:3228.
22. Kenyon, B. M., E. E. Voest, C. C. Chen, E. Flynn, J. Folkman, and R. J. D'Amato. 1996. A model of angiogenesis in the mouse cornea. *Invest Ophthalmol Vis Sci* 37:1625.
23. Zheng, M., D. M. Klinman, M. Gierynska, and B. T. Rouse. 2002. DNA containing CpG motifs induces angiogenesis. *Proc Natl Acad Sci U S A* 99:8944.
24. Banerjee, K., P. S. Biswas, B. Kim, S. Lee, and B. T. Rouse. 2004. CXCR2^{-/-} mice show enhanced susceptibility to herpetic stromal keratitis: a role for IL-6-induced neovascularization. *J Immunol* 172:1237.
25. Deshpande, S., M. Zheng, S. Lee, K. Banerjee, S. Gangappa, U. Kumaraguru, and B. T. Rouse. 2001. Bystander activation involving T lymphocytes in herpetic stromal keratitis. *J Immunol* 167:2902.

26. Thomas, J., S. Gangappa, S. Kanangat, and B. T. Rouse. 1997. On the essential involvement of neutrophils in the immunopathologic disease: herpetic stromal keratitis. *J Immunol* 158:1383.
27. Kuwano, T., S. Nakao, H. Yamamoto, M. Tsuneyoshi, T. Yamamoto, M. Kuwano, and M. Ono. 2004. Cyclooxygenase 2 is a key enzyme for inflammatory cytokine-induced angiogenesis. *Faseb J* 18:300.
28. Mifflin, R. C., J. I. Saada, J. F. Di Mari, P. A. Adegboyega, J. D. Valentich, and D. W. Powell. 2002. Regulation of COX-2 expression in human intestinal myofibroblasts: mechanisms of IL-1-mediated induction. *Am J Physiol Cell Physiol* 282:C824.
29. Di Mari, J. F., R. C. Mifflin, P. A. Adegboyega, J. I. Saada, and D. W. Powell. 2003. IL-1 α -induced COX-2 expression in human intestinal myofibroblasts is dependent on a PKC ζ -ROS pathway. *Gastroenterology* 124:1855.
30. Tipton, D. A., J. C. Flynn, S. H. Stein, and M. Dabbous. 2003. Cyclooxygenase-2 inhibitors decrease interleukin-1 β -stimulated prostaglandin E₂ and IL-6 production by human gingival fibroblasts. *J Periodontol* 74:1754.
31. Hill, J. M., W. J. Lukiw, B. M. Gebhardt, S. Higaki, J. M. Loutsch, M. E. Myles, H. W. Thompson, B. S. Kwon, N. G. Bazan, and H. E. Kaufman. 2001. Gene expression analyzed by microarrays in HSV-1

- latent mouse trigeminal ganglion following heat stress. *Virus Genes* 23:273.
32. Tumpey, T. M., S. H. Chen, J. E. Oakes, and R. N. Lausch. 1996. Neutrophil-mediated suppression of virus replication after herpes simplex virus type 1 infection of the murine cornea. *J Virol* 70:898.
33. Lee, S., M. Zheng, B. Kim, and B. T. Rouse. 2002. Role of matrix metalloproteinase-9 in angiogenesis caused by ocular infection with herpes simplex virus. *J Clin Invest* 110:1105.
34. Puignero, V., and J. Queralt. 1997. Effect of topically applied cyclooxygenase-2-selective inhibitors on arachidonic acid- and tetradecanoylphorbol acetate-induced dermal inflammation in the mouse. *Inflammation* 21:431.
35. Bezerra, M. M., V. de Lima, V. B. Alencar, I. B. Vieira, G. A. Brito, R. A. Ribeiro, and F. A. Rocha. 2000. Selective cyclooxygenase-2 inhibition prevents alveolar bone loss in experimental periodontitis in rats. *J Periodontol* 71:1009.
36. Song, A. M., L. Bhagat, V. P. Singh, G. G. Van Acker, M. L. Steer, and A. K. Saluja. 2002. Inhibition of cyclooxygenase-2 ameliorates the severity of pancreatitis and associated lung injury. *Am J Physiol Gastrointest Liver Physiol* 283:G1166.

37. Biswas, P. S., K. Banerjee, M. Zheng, and B. T. Rouse. 2004. Counteracting corneal immunoinflammatory lesion with interleukin-1 receptor antagonist protein. *J Leukoc Biol* 76:868.
38. Fenton, R. R., S. Molesworth-Kenyon, J. E. Oakes, and R. N. Lausch. 2002. Linkage of IL-6 with neutrophil chemoattractant expression in virus-induced ocular inflammation. *Invest Ophthalmol Vis Sci* 43:737.
39. Kyrkanides, S., A. H. Moore, J. A. Olschowka, J. C. Daeschner, J. P. Williams, J. T. Hansen, and M. Kerry O'Banion. 2002. Cyclooxygenase-2 modulates brain inflammation-related gene expression in central nervous system radiation injury. *Brain Res Mol Brain Res* 104:159.
40. Bizzarri, C., S. Pagliei, L. Brandolini, P. Mascagni, G. Caselli, P. Transidico, S. Sozzani, and R. Bertini. 2001. Selective inhibition of interleukin-8-induced neutrophil chemotaxis by ketoprofen isomers. *Biochem Pharmacol* 61:1429.
41. He, L. K., L. H. Liu, E. Hahn, and R. L. Gamelli. 2001. The expression of cyclooxygenase and the production of prostaglandin E2 in neutrophils after burn injury and infection. *J Burn Care Rehabil* 22:58.
42. Bowman, C. C., and K. L. Bost. 2004. Cyclooxygenase-2-mediated prostaglandin E2 production in mesenteric lymph nodes and in cultured macrophages and dendritic cells after infection with *Salmonella*. *J Immunol* 172:2469.

43. Scapini, P., F. Calzetti, and M. A. Cassatella. 1999. On the detection of neutrophil-derived vascular endothelial growth factor (VEGF). *J Immunol Methods* 232:121.
44. Daheshia, M., S. Kanangat, and B. T. Rouse. 1998. Production of key molecules by ocular neutrophils early after herpetic infection of the cornea. *Exp Eye Res* 67:619.
45. Gately, S., and W. W. Li. 2004. Multiple roles of COX-2 in tumor angiogenesis: a target for antiangiogenic therapy. *Semin Oncol* 31:2.
46. Tuo, J., N. Tuailon, D. Shen, and C. C. Chan. 2004. Endotoxin-induced uveitis in cyclooxygenase-2-deficient mice. *Invest Ophthalmol Vis Sci* 45:2306.

APPENDIX

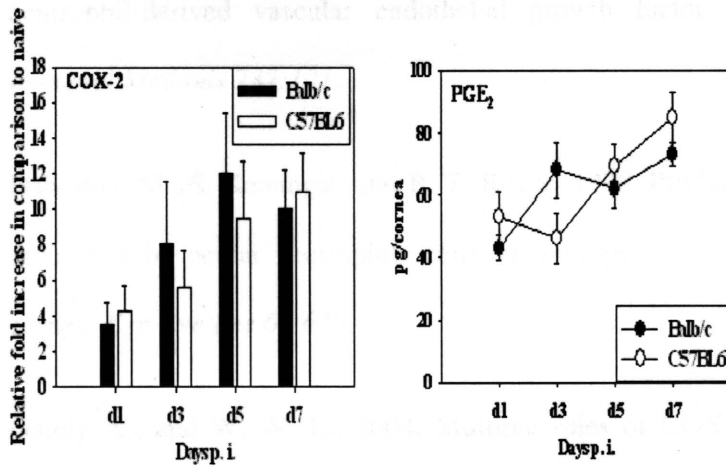


Fig 1. Kinetics of COX-2 mRNA and PGE₂ levels in HSV-1 infected corneas of Balb/c and C57BL6 mice

- A. At 1, 3, and 7 days postinfection, four corneas/group were processed for the extraction of cellular mRNA. Real-time PCR analysis was conducted to detect the COX-2 mRNA expression in corneas of mice infected HSV-1, as described in *Materials and Methods*. Results are shown as mean \pm SD of three separate experiments.
- B. Levels of PGE₂ were estimated from corneas (6 corneas/ time point) of mice infected with HSV-1 RE by a competitive ELISA, as outlined in *Materials and Methods*. Results are expressed as mean \pm SD of three separate experiments (6 corneas/time point).

Fig 2. Mice receiving COX-2 inhibitors show reduced HSK severity

- A. Mean lesion HSK score at day 20 p. i. of mice infected with 5×10^5 PFU (Balb/c) HSV-1 RE. Each dot represents the HSK score from one eye. Horizontal bars and figures in the parentheses indicate the mean for each group.
- B. Bar diagram demonstrates the percentage severity of each group of Balb/c mice infected with 5×10^5 pfu at day 20 p. i. Figure in the parenthesis represents the percentage of eyes showing HSK score greater than or equal to 3.
- C. Mean lesion HSK score at day 20 p.i. of mice infected with 5×10^6 PFU (C57BL6) HSV-1 RE. Each dot represents the HSK score from one eye. Horizontal bars and figures in the parentheses indicate the mean for each group.
- D. Bar diagram demonstrates the percentage severity of each group of C57BL6 mice infected with 5×10^6 pfu at day 20 p. i. Figure in the parenthesis represents the percentage of eyes showing HSK score greater than or equal to 3.
- E. Mice (Balb/c) were infected with 5×10^5 pfu HSV-1 RE. Mice were terminated at day 20 p.i., and eyes were processed for paraffin embedding. H&E staining was carried out on 6μ sections. Original magnification, x200.

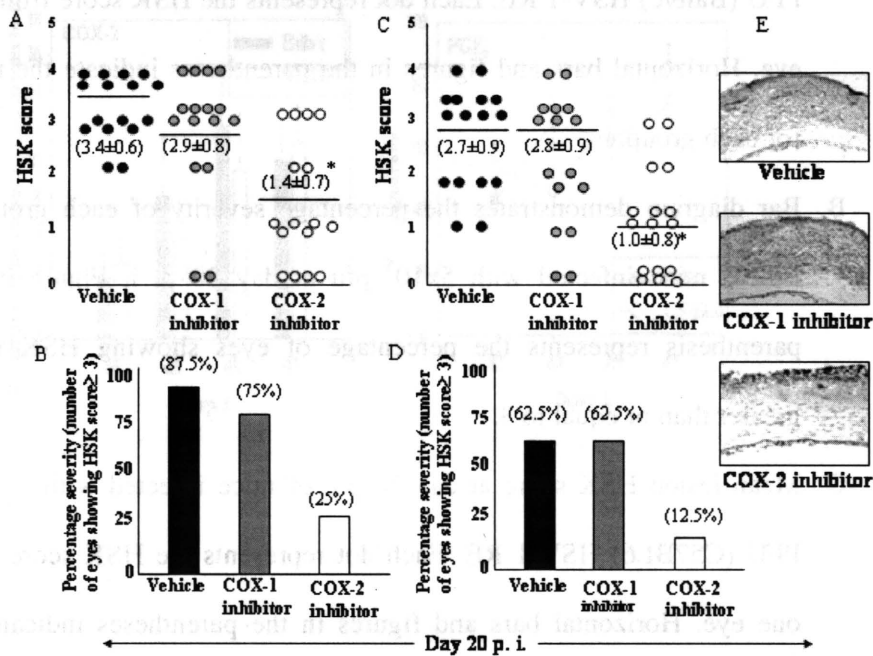


Fig 3. Mice receiving COX-2 inhibitor show diminished angiogenic response following HSV-1 infection at day 20 p. i.

- A. Angiogenesis scores for individual eyes of different groups of Balb/c mice infected with 5×10^5 PFU HSV-1 RE at day 20 p.i. Horizontal bars and figures show the mean for each group.
- B. At day 20 p.i., extensive growth of blood vessels can be seen in Balb/c mice receiving vehicle or COX-1 inhibitor and infected with 5×10^5 PFU HSV-1 RE. Mice receiving COX-2 inhibitor show minimum angiogenic sprouts near the limbal ring with the same dose.
- C. Angiogenesis scores for individual eyes of different groups of C57BL6 mice infected with 5×10^6 PFU HSV-1 RE at day 20 p.i. Horizontal bars and figures show the mean for each group.
- D. At day 20 p.i., extensive growth of blood vessels can be seen in C57BL6 mice receiving vehicle or COX-1 inhibitor and infected with 5×10^5 PFU HSV-1 RE. Mice receiving COX-2 inhibitor show minimum angiogenic sprouts near the limbal ring with the same dose.

Fig. 3. Mice receiving COX-2 inhibitor show diminished angiogenic response following HSV-1 infection at day 20 p.i.

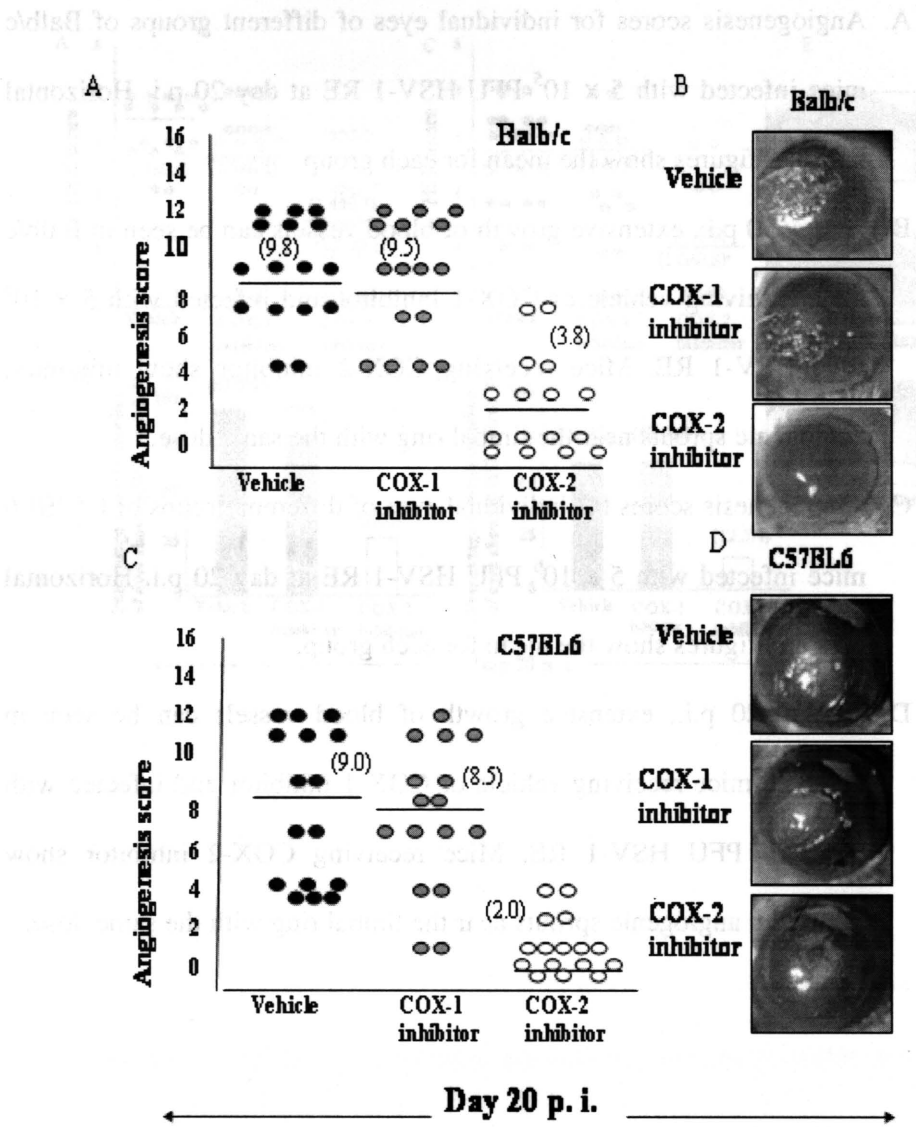


Fig 4. Uninfected stromal fibroblasts are the major producers of COX-2 following ocular HSV-1 infection.

- A. Mice (Balb/c) were infected with 5×10^5 PFU HSV-1-RE- pgC-GFP. At 24 hr p. i. corneas, GFP⁺ cells (infected) were sorted out from GFP⁻ cells (uninfected) and total RNA was extracted. Real-time PCR analysis was conducted to detect the COX-2 mRNA expression in corneas of mice infected HSV-1, as described in *Materials and Methods*. Results are shown as mean \pm SD of three separate experiments. *, Statistically significant differences ($p < 0.05$) in comparison to GFP⁺.
- B. Immunohistochemistry for COX-2 expression in corneas of Balb/c mice. (arrows) are detectable in corneal stroma of Balb/c mice infected with high, 5×10^5 PFU HSV-1 RE at day 1 p.i. Diaminobenzidine was used as substrate, and sections were counterstained with hematoxylin. Original magnification x200.

Fig 4. Uninfected stromal fibroblasts are the major producers of COX-2 following ocular HSV-1 infection.

A. Mice (Balb/c) were infected with 5×10^7 PFU HSV-1-RE-pGFP.

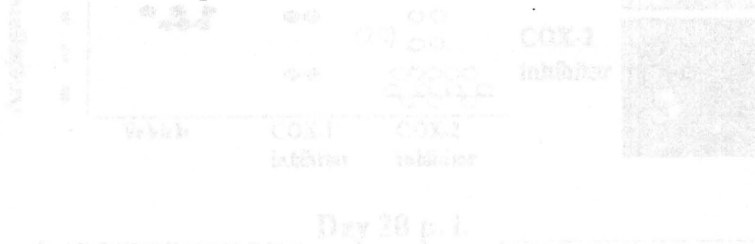
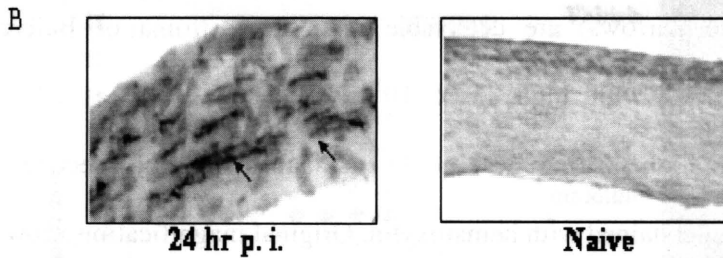
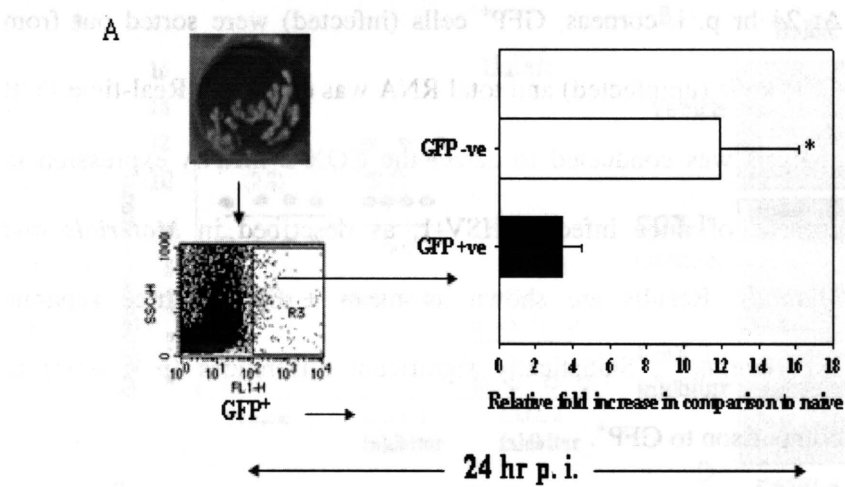


Fig 5. IL-1 β induced COX-2 expression in murine stromal fibroblast cell line.

- A. Murine stromal fibroblast cells were stimulated with different doses of murine rIL-1 β for 24 hr. After 24 hr post stimulation cells were collected and total RNA was extracted. Real-time PCR analysis was conducted to detect the COX-2 mRNA expression in corneas of mice infected with HSV-1, as described in *Materials and Methods*. Results are shown as mean \pm SD of three separate experiments. *, Statistically significant differences ($p < 0.05$) in comparison media control.
- B. Mice (Balb/c) were infected with 5×10^5 PFU HSV-1-RE. At different days p. i. 4 corneas/time point were taken and total RNA was extracted. Reverse transcriptase was conducted to detect the IL-1 β mRNA expression in corneas of mice infected with HSV-1, as described in *Materials and Methods*.
- C. Different concentrations of rIL-1 β (50, 200 ng) were administered in Balb/c corneas ($n = 8$) by corneal micropocket assay. Real-time PCR analysis was conducted at day 1 p. i. to detect the COX-2 mRNA expression in corneas of mice infected HSV-1, as described in *Materials and Methods*. Results expressed as mean \pm SD. *, Statistically significant differences ($p < 0.05$) in comparison to only pellet.
- D. Control C57BL6 mice and IL-1 ra Tg mice were infected with 5×10^6 pfu HSV-1 RE. At 1, 3, and 7 days postinfection, four corneas/group

were processed for the extraction of cellular mRNA. Real-time PCR analysis was conducted to detect the COX-2 mRNA expression in corneas of mice infected HSV-1, as described in *Materials and Methods*. Results are shown as mean \pm SD of three separate experiments. *, Statistically significant differences ($p < 0.05$) in comparison to control animals.

- E. Control C57BL6 mice and IL-1 ra Tg mice were infected with 5×10^6 pfu HSV-1 RE. At 1, 3, and 7 days p. i., levels of PGE₂ were estimated from corneas (6 corneas/ time point) of mice infected with HSV-1 RE by a competitive ELISA, as outlined in *Materials and Methods*. Results are expressed as mean \pm SD of three separate experiments (6 corneas/time point). *, Statistically significant differences ($p < 0.05$) in comparison to control animals.

Fig. 6. Reduced PMN influx in COX-2 inhibitor treated mice at 48 hr p.i.

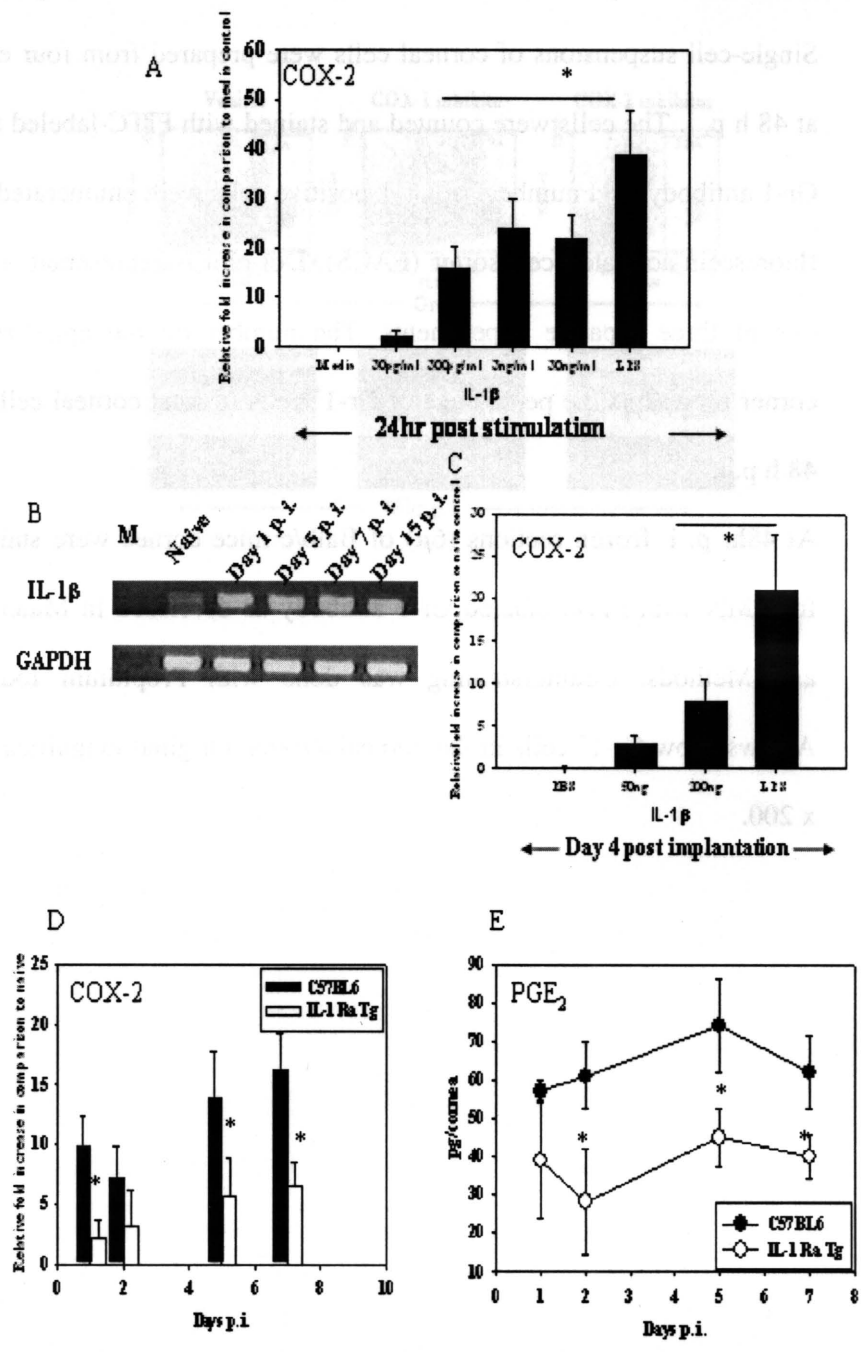


Fig 6. Reduced PMN influx in COX-2 inhibitor treated mice at 48 hr. p. i.

Single-cell suspensions of corneal cells were prepared from four eyes at 48 h p. i. The cells were counted and stained with FITC-labeled anti Gr-1 antibody, and numbers of Gr-1-positive cells were enumerated by fluorescein-activated cell sorter (FACS). Dot-plot is representative of one of three separate experiments. The number on the upper-right corner represents the percentage of Gr-1⁺ cells of total corneal cells at 48 h p. i.

At 48hr p. i. frozen sections (6 μ) of Balb/c mice cornea were stained for PMN with FITC labeled Gr-1 antibody as described in Materials and Methods. Counterstaining was done with Propidium Iodide. Arrows show Gr-1⁺ cells in the corneal stroma. Original magnification x 200.

Fig. 7. Reduced levels of Gr-1⁺ and F4/80⁺ in the course of COX-2

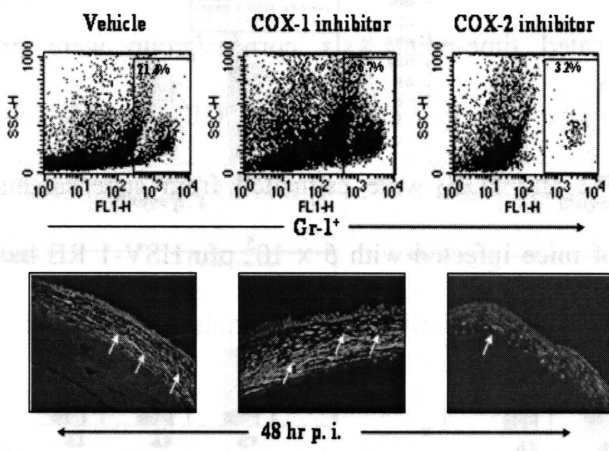
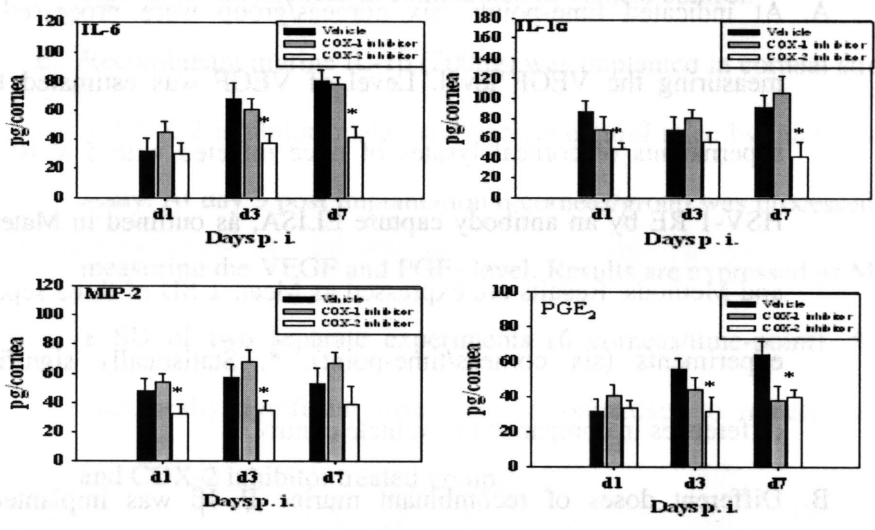


Fig 7. Reduced levels of Cytokines and Prostanoids in the cornea of COX-2 inhibitor treated mice

At indicated time-points, six corneas/group were processed for measuring the IL-6, IL-1 α , MIP-2 and PGE₂ levels. Levels of IL-6, IL-1 α , MIP-2 and PGE₂ were estimated from supernatants of corneal lysates of mice infected with 5×10^5 pfu HSV-1 RE by an antibody capture ELISA, as outlined in Materials and Methods. Results are expressed as Mean \pm SD of three separate experiments (six corneas/time-point). *, Statistically significant differences in comparison to vehicle control.

Fig 8. Compromised angiogenic responses in COX-2 inhibitor treated mice



corneal stroma by microprocket assay and extent of angiogenesis was measured at day 7 post-implantation as described in Materials and Methods. * Statistically significant differences in comparison to

control only.

C. Recombinant murine IL-1β (500ng) was implanted in corneal stroma by microprocket assay and at day 7 post-implantation frozen sections (5μ) of those implanted corneas were made. These sections were stained for COX-2 by immunohistochemistry as described in Materials and Methods. Diaminobenzidine was used as substrate. Original and sections were counterstained with hematoxylin. Original magnification X200.

D. Recombinant murine IL-1β (500ng) was implanted in corneal stroma of COX-2 inhibitor treated and vehicle control mice by microprocket assay. At day 7 post-implantation extent of angiogenesis was

Fig 8. Compromised angiogenic responses in COX-2 inhibitor treated mice

- A. At indicated time-points, six corneas/group were processed for measuring the VEGF level. Level of VEGF was estimated from supernatants of corneal lysates of mice infected with 5×10^5 pfu HSV-1 RE by an antibody capture ELISA, as outlined in Materials and Methods. Results are expressed as Mean \pm SD of three separate experiments (six corneas/time-point). *, Statistically significant differences in comparison to vehicle control.
- B. Different doses of recombinant murine IL-1 β was implanted in corneal stroma by micropocket assay and extent of angiogenesis was measured at day 3 post implantation as described in Materials and Methods. *, Statistically significant differences in comparison to pellet only.
- C. Recombinant murine IL-1 β (200ng) was implanted in corneal stroma by micropocket assay and at day 3 post implantation frozen sections (6 μ) of those implanted corneas were made. These sections were stained for COX-2 by immunohistochemistry as described in Materials and Methods. Diaminobenzidine was used as substrate, and sections were counterstained with hematoxylin. Original magnification x200.
- D. Recombinant murine IL-1 β (200ng) was implanted in corneal stroma of COX-2 inhibitor treated and vehicle control mice by micropocket assay. At day 3 post implantation extent of angiogenesis was

measured as described in Materials and Methods. *, Statistically significant differences in comparison to vehicle control.

- E. Recombinant murine IL-1 β (200ng) was implanted in corneal stroma of COX-2 inhibitor treated and vehicle control mice by micropocket assay. At day 3 post implantation 6 corneas/group was processed for measuring the VEGF and PGE₂ level. Results are expressed as Mean \pm SD of two separate experiments (6 corneas/time-point). * **, Statistically significant differences in comparison to vehicle control and COX-2 inhibitor treated group.

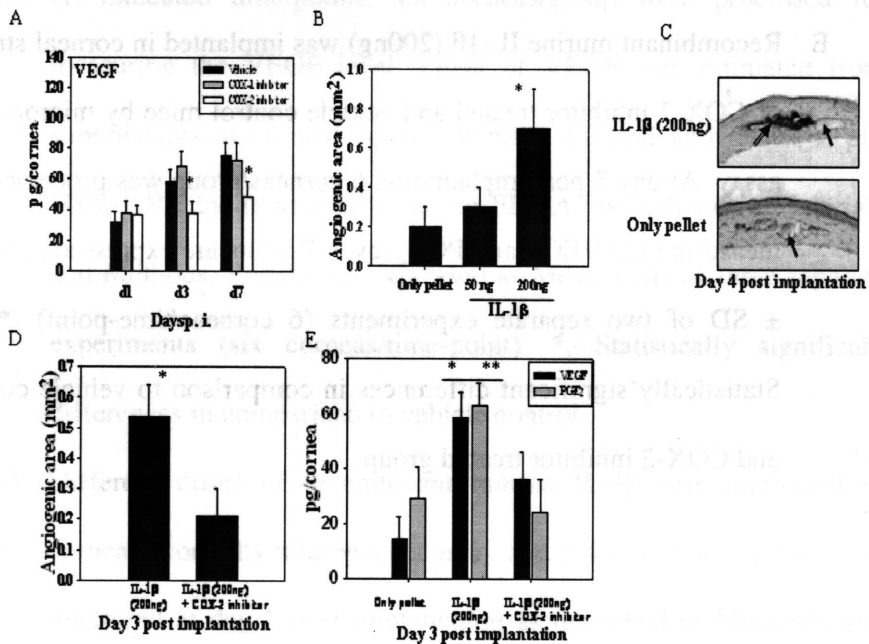


Figure 5. Effects of recombinant murine IL-1β on corneal angiogenesis. (A) Recombinant murine IL-1β (200ng) was implanted in corneal stroma by micro-pellet assay and at day 1, 3 and 7 post-implantation frozen sections (6a) of those implanted corneas were made. These sections were stained for VEGF by immunohistochemistry as described in Materials and Methods. (B) Recombinant murine IL-1β (200ng) was implanted in corneal stroma by micro-pellet assay and at day 4 post-implantation frozen sections (6b) of those implanted corneas were made. These sections were stained for COX-2 by immunohistochemistry as described in Materials and Methods. (C) Recombinant murine IL-1β (200ng) was implanted in corneal stroma by micro-pellet assay and at day 4 post-implantation frozen sections (6c) of those implanted corneas were made. These sections were stained for COX-2 by immunohistochemistry as described in Materials and Methods. (D) Recombinant murine IL-1β (200ng) was implanted in corneal stroma by micro-pellet assay and at day 3 post-implantation frozen sections (6d) of those implanted corneas were made. These sections were stained for COX-2 by immunohistochemistry as described in Materials and Methods. (E) Recombinant murine IL-1β (200ng) was implanted in corneal stroma by micro-pellet assay and at day 3 post-implantation frozen sections (6e) of those implanted corneas were made. These sections were stained for VEGF and FGF by immunohistochemistry as described in Materials and Methods. * Statistically significant differences in comparison to only pellet.

Recombinant murine IL-1β (200ng) was implanted in corneal stroma by micro-pellet assay and at day 4 post-implantation frozen sections (6a) of those implanted corneas were made. These sections were stained for COX-2 by immunohistochemistry as described in Materials and Methods. Diarranobenzidine was used as substrate and sections were counterstained with hematoxylin. Original magnification X200.

Recombinant murine IL-1β (200ng) was implanted in corneal stroma by micro-pellet assay and at day 4 post-implantation frozen sections (6b) of those implanted corneas were made. These sections were stained for COX-2 by immunohistochemistry as described in Materials and Methods. Diarranobenzidine was used as substrate and sections were counterstained with hematoxylin. Original magnification X200.

PART V

COUNTERACTING CORNEAL

IMMUNOINFLAMMATORY LESION WITH

INTERLEUKIN- 1 RECEPTOR ANTAGONIST

PROTEIN

Research described in this chapter is a slightly modified version of an article published in 2004 in *Journal of Leukocyte Biology* by Partha Sarathi Biswas, Kaustuv Banerjee, Mei Zheng and Barry T. Rouse.

Biswas, P. S., K. Banerjee, M. Zheng, and B. T. Rouse. 2004. Counteracting corneal immunoinflammatory lesion with interleukin-1 receptor antagonist protein. *J Leukoc Biol.* 76(4):868. Copyright 2004. The American Association of Immunologists, Inc.

In this chapter “we” and “our” refers to co-authors and me. My contributions in the paper include (1) selection of the topic (2) data analysis and interpretation (3) planning experiments (4) compiling and interpretation of the literature (5) understanding how results fit with the literature (7) compilation of contributions into one paper (8) providing structure to the paper (9) making graphs, figures and tables (10) writing and editing.

ABSTRACT

Herpetic Stromal Keratitis (HSK) is a T cell orchestrated immunoinflammatory lesion that results from corneal HSV infection. Previous reports indicate an essential role for proinflammatory cytokine IL-1 in HSK pathogenesis. The present study evaluates the efficacy of IL-1 receptor antagonist (IL-1 ra) protein in the management of HSK. Mice receiving IL-1 ra had diminished disease severity. The administration of IL-1 ra was shown to reduce the influx into the cornea of cells of both the innate and adaptive

immune response. In addition, the treatment also diminished corneal VEGF levels resulting reduced angiogenic response. Our results show the importance of targeting early proinflammatory molecules such as IL-1 to counteract HSK and advocate IL-1 ra as an effective agent to achieve this.

INTRODUCTION

In almost 20% of individuals with a Herpes simplex virus (HSV) infection a blinding immunoinflammatory lesion, called herpetic stromal keratitis (HSK), develops (1). Management of HSK usually requires indefinite corticosteroid therapy (2). In some cases corneal damage results in permanent loss of vision necessitating transplantation. Studies with the murine model have revealed a complicated pathogenesis, the critical event being the influx of CD4⁺ T cells (3, 4). Leading to the influx of these crucial cells are several events that include proinflammatory cytokine and chemokine production, influx of innate immune cells and angiogenesis (5-7). Both IL-1 and IL-6 are likely the mediators of corneal inflammation (8-10), and have been recently demonstrated as essential in the pathogenesis of corneal disease following HSV-1 infection (11).

To test our hypothesis that IL-1 represents one of the first mediators to initiate the inflammatory cascade, we blocked its activity using the IL-1 receptor antagonist protein (IL-1 ra). The IL-1 ra protein is a naturally occurring isoform of IL-1 and can bind to IL-1 receptors with high-affinity but fails to induce signal transduction (12). The protein is routinely used in treatment of human immunoinflammatory conditions such as rheumatoid

arthritis (13). Interleukin -1 receptor antagonist protein administered systemically down regulates cytokine production in humans and rats (14-16). In the ocular alkali burn murine model, IL-1 ra has been shown to have a therapeutic potential (16). We show using a combination of systemic and local IL-1 ra administration, that the severity of corneal angiogenesis and HSK is diminished following ocular HSV infection. This was a consequence of a down regulation of various inflammatory mediators, normally induced by IL-1 in HSV infected corneas. Thus blocking IL-1 activity using IL-1 ra protein could represent a valuable therapeutic approach in managing HSK.

MATERIALS AND METHODS

Mice

Wild type female 6 to 8 weeks old C57BL/6 mice were purchased from Harlan Sprague-Dawley (Indianapolis, Indiana). Animals were sex and age matched for all experiments. Mice transgenic for IL-1 receptor antagonist protein (T14 hemizygous line) were kindly provided by Dr. David Hirsh (Department of Biochemistry and Molecular Biophysics, College of Physician and Surgeons, Columbia University). All manipulations involving the immunocompromized mice were performed in a laminar flow hood. All experimental procedures were in complete agreement with the Association for Research in Vision and Ophthalmology (ARVO) resolution on the use of animals in research.

Virus

HSV-1 RE (obtained from Dr. Robert Hendricks Laboratory, University of Pittsburgh School of Medicine) was used in the present study. The virus was propagated and titrated on monolayer of Vero cells (ATCC, Cat No. CCL81) using standard protocols (17). Infected Vero cells were harvested, titrated and stored in aliquots at -80°C until used.

Corneal HSV-1 infection

Mice were ocularly infected with HSV-1 RE under deep anesthesia induced by intraperitoneal injection of Avertin (Sigma-Aldrich, St. Louis, MO). Mice were lightly scarified on their corneas with a 27-gauge needle and a 4 μl drop containing the required dose of virus was applied to the eye and gently massaged with the eyelids.

Clinical observations and Angiogenesis Scoring

The eyes were examined on different days post infection by a slit-lamp biomicroscope (Kowa Co. Nagoya, Japan), and the clinical severity of keratitis of individually scored mice was recorded as described before (11). Angiogenesis severity was measured as described previously (18). Briefly, a grade of 4 for a given quadrant of the circle represents a centripetal growth of 1.5mm toward the corneal center. The score of the 4 quadrants of the eye were then summed to derive the NV index (range 0-16) for each eye at a given point.

Subconjunctival inoculations

Subconjunctival inoculation of recombinant human IL-1 ra protein [0.5mg/cornea, 1mg/cornea] (supplied by Amgen Inc., Thousand Oaks, CA) was performed as described previously (8). Briefly, subconjunctival inoculations were done using a 2 cm 32 gauge needle and syringe (Hamilton, Reno, NV) to penetrate the perivascular region of conjunctiva and required dose of IL-1 ra protein was delivered into the subconjunctival space. Control mice received 0.2% sodium hyaluronate in PBS only. Mice received recombinant human IL-1 ra one day before corneal infection with HSV-1.

Alzet infusion pump implantation

Alzet osmotic pumps (Palo Alto, CA) were used to deliver IL-1 ra subcutaneously as described before (19). Briefly, the micro-osmotic pumps (Model 1007D) were implanted 24 hr before ocular infection. The pumps were loaded with IL-1 ra or vehicle as per the manufacturer's instructions under sterile condition. The mice were weighed, marked and anaesthetized using Isoflurane (Abbott Laboratories, North Chicago, IL). Mice were placed into dorsal recumbancy, clipped over the shoulder area and prepared for the surgery. A small 1 cm incision was made caudal to the shoulder area, the skin was undermined with a hemostat and then the pump was placed into the prepared pocket. Skin was then closed with 9 mm autoclips (Braintree Scientific Inc., Braintree, MA). The pump was taken out after 7 days and the skin was closed again with 9mm clips. With a mean pumping rate of 0.5 μ l/hr (mean fill volume of 100 μ l), calculated drug infusion rates were 5mg/kg

b.wt/hr for 7days, 2.5mg/kg b.wt/hr for 7days and 1mg/kg b.wt/hr for 7days. Control mice received osmotic pumps with vehicle only for the same period of time.

Histopathology

For histopathological analysis, eyes were extirpated at day 20 p. i. and fixed in 10% buffered neutral formalin. Staining was performed with Hematoxylin and Eosin (Richard Allen Scientific, Kalamazoo, MI).

Immunofluorescence staining

For immunofluorescence staining, at day 20 p. i. eyes were frozen in optimum cutting temperature (OCT) compound (Miles, Elkart, IN). Six micron thick sections were cut, air dried and fixed in acetone for 20 minutes at 4° C. The sections were blocked with 3% BSA (Sigma) containing unconjugated anti CD16/32 (1:200) antibody (BD Pharmingen, San Diego, CA) for 3 hours at 37° C. For detection of CD4⁺ T cells, the sections were incubated with FITC labeled anti mouse CD4⁺ antibody (Clone RM4-5, Pharmingen) in 1% BSA at 4° C overnight. Sections were repeatedly washed in PBS and mounted with Vectashield mounting medium for fluorescence with Propidium Iodide (Vector Laboratories Inc. Burlingame, CA) and visualized under a microscope (Leica, Wetzlar, Germany).

Flow Cytometry

Single-cell suspensions were prepared from 4 corneas at different days post infection as described elsewhere (20), with some modifications. Briefly, corneal buttons were incubated with collagenase D (Roche, Mannheim, Germany) for 60 min at 37°C in a humidified atmosphere at 5% CO₂. After incubation, eyes were disrupted by grinding with a syringe plunger and passing through a cell strainer. Cells were washed and suspended in RPMI 1640 with 10% FBS. Blocking was done with unconjugated anti-CD16/32 (Pharmingen) for 30 min. Samples were incubated with FITC labeled anti Gr-1 antibody (Clone RB6-8C5, Pharmingen), FITC labeled anti CD4 antibody (Clone RM4-5, Pharmingen) and isotype controls for 30 minutes. All samples were collected on a FACScan (BD Biosciences, San Diego, CA), and data were analyzed using CellQuest 3.1 software (BD Biosciences).

Cytokine ELISA of corneal lysate

For preparation of corneal lysates, 6 corneas per time point were pooled and minced. All procedures were done on an ice bath. Minced pieces were collected in 1ml DMEM without FCS and homogenized using a tissue homogenizer (PRO Scientific Inc., Monroe, CT) four times, 15 seconds each, with a gap of 1 minute between homogenization to allow the sample to cool. The lysate was then clarified by centrifugation at 14,000 rpm for 5 minute at 4°C. The supernatant was collected and used immediately or stored at -80°C until further use. Lysates were analyzed using a standard sandwich ELISA protocol. Anti IL-6 capture and biotinylated detection antibodies were from

Pharminggen (Clone MP5-20F3) and standard recombinant murine IL-6 was from R&D Systems Inc, Minneapolis. Anti MIP-2 and anti VEGF₁₆₄ capture and biotinylated detection antibodies and recombinant standards for murine MIP-2 and murine VEGF₁₆₄ were from R & D Systems. For detection of recombinant human IL-1 ra, anti human IL-1 ra capture and detection antibody and recombinant human IL-1 ra were obtained from R&D Systems Inc. Minneapolis. The color reaction was developed using ABTS (Sigma) and measured with an ELISA reader (Spectramax 340, Molecular Devices, Sunnyvale, CA) at 405nm. Quantification was performed with Spectramax ELISA reader software version 1.2.

Statistical analysis

Unless specified a standard student's t test has been utilized.

RESULTS

Subconjunctival administration of IL-1 ra protein has no effect on HSK severity and corneal angiogenesis

To evaluate whether local administration of IL-1 ra protein modulates HSK severity and corneal angiogenesis following ocular HSV infection, three groups of mice were subconjunctivally injected with 0.5mg/cornea, 1mg/cornea and vehicle only, 24 hour before corneal infection. At day 3, 5 and 7 days post injection corneal levels of recombinant IL-1 ra protein was determined by ELISA. As demonstrated in Fig 1, IL-1 ra protein was

detectable in both the treated groups at day 3 post injection only. However, levels of IL-1 ra protein were undetectable at 5 and 7 days post infection.

Mice receiving subconjunctival injection of 0.5mg/cornea, 1 mg/cornea of IL-1 ra protein and vehicle were assessed clinically for the development of HSK following HSV-1 RE (5×10^6 pfu) ocular infection over a 20 days test period. Mice transgenic for the IL-1 ra protein were used as a positive control. As shown in Fig 2A, there was no difference in the severity of HSK in both treated and vehicle control mice [mean scores 2.9 ± 1.0 (0.5mg/cornea), 2.8 ± 1.2 (1mg/cornea) and 2.9 ± 1.1 (vehicle)]. In sharp contrast, mice transgenic for IL-1 ra protein demonstrated markedly reduced HSK severity (mean score of 1.3 ± 0.9) (Fig. 2A). Further, whereas treated and control groups showed clinically evident lesions (HSK score of 3 or more) in 56.3% (0.5mg/cornea), 50% (1mg/cornea) and 62.5% (vehicle control) of eyes, only 18.9% of IL-1 ra Tg eyes developed lesions (Fig 2B). Histopathological analysis of representative eyes of both treated and control C57BL/6 mice revealed severe inflammatory changes and cellular infiltration in the corneal stroma at day 20 p. i. (Fig. 2C). However, in mice transgenic for IL-1 ra protein only mild inflammatory changes and cellular infiltrations were evident (Fig. 2C).

No significant difference ($p < 0.05$) was observed in the extent of angiogenesis between IL-1 ra treated and control mice (Fig. 3A and C). However, mice transgenic for IL-1 ra protein showed significantly ($p < 0.05$) reduced corneal neovascularization in comparison to treated and control groups (Fig. 3A and C). By day 20 p. i, an angiogenesis score of 10 or greater

was observed in 8 of 16 vehicle control eyes, and in eyes receiving 1mg/cornea and 0.5mg/cornea. Only 2 of 16 eyes of IL-1 ra Tg mice developed such a score (Fig 3B). Taken together, these results indicate that administering IL-1 ra protein locally has no effect in modulating either angiogenesis or keratitis.

A combination of systemic and subconjunctival IL-1 ra administration diminishes HSK severity and corneal angiogenesis

A reason for the inability of subconjunctival administration in modulating HSK severity may be attributed to the short persistence of IL-1 ra in the cornea. To achieve biologically active concentrations for a sustained period in the corneal microenvironment, different doses of IL-1 ra recombinant protein were administered systemically via subcutaneous osmotic pump implantation for 7 days. In addition, mice also received a subconjunctival injection (1mg/cornea) (the highest concentration that could be achieved by subconjunctival injection). With this approach the IL-1 ra protein was detectable in the cornea by ELISA till day 7 post injection (last time point analyzed) (Fig 4). In addition, serum levels of the protein in treated mice were significantly higher than vehicle treated animals (data not shown).

Four groups of mice were injected with 5mg/kg body wt. /hr for 7days S/c + 1mg/cornea local (Group 1), 2.5mg/ kg body wt. /hr for 7days S/c + 1mg/cornea local (Group 2), 1mg/ kg body wt. /hr for 7days S/c + 1mg/cornea local (Group 3) of IL-1 ra and vehicle control (Group 4) respectively. Twenty-four hours later mice were ocularly infected with 5×10^6 pfu HSV-1 RE. Mice

transgenic for IL-1 ra protein were used as positive control. These mice were evaluated clinically for the development of HSK following HSV-1 (5×10^6 pfu) corneal infection over a 20 days test period. As shown in Fig 5A, the severity of HSK in Groups 1 and 2 was significantly diminished (mean score of 1.3 ± 0.9 and 1.4 ± 1.0 respectively) in comparison to Group 4 (mean score 2.9 ± 1.1). The severity in former groups was almost similar to the IL-1 ra Tg mice (mean score 1.2 ± 1.1). However, the severity of HSK in Group 3 and Group 4 were similar (mean score 2.5 ± 1.1 and 2.9 ± 1.1 respectively) (Fig 5A). In addition, whereas the incidence of disease was 56.3% of Group 4, it was only 25% of Groups 1 and 2 and 20% of IL-1 Ra Tg mice (Fig 5B). Increasing the virus dose in the transgenic animals made no difference to HSK scores (data not shown). Histopathological analysis of representative eyes of Groups 1 and 2 and IL-1 ra Tg mice revealed mild inflammatory changes in the corneal stroma at day 20 p. i. In contrast, vehicle treated eyes developed more severe inflammatory changes (Fig. 5C).

The extent of angiogenesis was significantly ($p < 0.05$) lower in Group 1, Group 2 and IL-1 ra Tg mice compared to vehicle treated mice (Fig 6A and C). At day 20 p. i., while an angiogenesis score of 10 or greater was observed in 11 of 16 vehicle control eyes, only 3 of 16 eyes in Groups 1 and 2 developed similar angiogenesis (Fig 6B). In conclusion, these results indicate that the protein is effective only when its concentration is maintained for at least 6-7 days after HSV-1 infection.

Reduction in the immuno-inflammatory response post IL-1 ra treatment

Normally, after a corneal HSV-1 infection, PMN infiltrate the corneal stroma within 6hrs, with peak numbers at 24-48 hrs (5). However, in mice treated with IL-1 ra and eventually showing a reduction in HSK severity the influx of PMN was severely compromised (Fig. 7). Thus in eyes from Group 2, PMN numbers, as judged by Gr-1 staining and flow cytometry was significantly lower at day 2 p. i. than in vehicle control (Group 4) (3.1 ± 0.8 % compared to 21.5 ± 4.3 %) (based on previous observation we have used Group 2 for subsequent studies). In addition, at day 20 p. i. there were very few CD4⁺ T cells in the cornea of IL-1 ra treated mice (12.4 ± 2.3 % of total lymphocytes). In sharp contrast, at day 20 p. i. vehicle control mice had an abundance of CD4⁺ T cells (64 ± 7.5 % of total lymphocytes) as judged by FACS analysis and immunofluorescence staining (Fig 8A and B).

We reasoned that the scarce cellular influx in the treated group was a result of a block in the induction of downstream events, as a consequence of impaired IL-1 activity. The prime candidates include both IL-6 and MIP-2 (8, 9). Treatment with IL-1 ra (Group 2) led to a significant ($p < 0.05$) decrease in the corneal IL-6 protein levels at day 5 and 7 days p. i. and MIP-2 at day 2 and 5 days p. i. in comparison to vehicle control (Fig 9A and B). However, no significant difference was observed in the protein levels of IL-1 α or IL-1 β (data not shown).

As mentioned above, mice treated with 2.5mg/ kg body wt. /hr for 7days S/c + 1mg/cornea local IL-1 ra protein developed significantly diminished angiogenic response in comparison to vehicle control. Vascular

Endothelial Growth Factor (VEGF) is one of the key players of corneal neovascularization following ocular HSV infection (21). To determine VEGF levels in these treated mice, we measured corneal VEGF protein levels at different days post infection. As expected, VEGF protein levels were significantly ($p < 0.01$) reduced in IL-1 ra treated mice at day 5 and 7 days p. i in comparison to vehicle control (Fig 9C). Thus the reduction in the severity of HSK seen with IL-1 ra treatment was attributable to a suppression of the inflammatory environment, the reduction in influx of cells of the immune system and the reduction of VEGF, a consequence of which was diminished angiogenesis.

DISCUSSION

Using a mouse model, we have evaluated the potential of the IL-1 ra protein in ameliorating an HSV-1 induced immuno-inflammatory corneal lesion HSK. This study yields two important findings. First, that blocking individual inflammatory molecules during the early stages of corneal HSV infection represents an alternative and effective approach to managing HSK. Second, the IL-1 ra protein, routinely used for the treatment of other immuno-inflammatory human diseases (13), appears to be effective in ameliorating HSK lesions. Our results also confirm the importance of the cytokine IL-1 in the pathogenesis of HSK (11).

Both molecular and cellular events involved in HSK pathogenesis were down regulated as a result of the IL-1 ra treatment. Blocking the IL-1 activity resulted in a block to the induction of downstream events and thereby altered

the environment normally conducive for the migration of inflammatory cells. Interleukin 1, produced from HSV infected cells (22), helps in the induction of other key cytokines such as IL-6 (23), also shown to be critical in the pathogenesis following ocular HSV infection (23). Linked with this process is also the production of chemokines such as IL-8 and MIP-2 (9, 16, 24), thought to be involved in the margination and extravasation of neutrophils at the corneal limbus. These events occur promptly following infection of the corneal epithelium and facilitating neutrophil influx (5). In addition an autocrine IL-1 feedback loop is possibly involved in tissue remodeling in the cornea through the induction of IL-8 (16). Interfering with these loops therefore can alter the overall response following HSV-1 infection and prevent tissue injury.

In the HSV infected mouse cornea peak numbers of neutrophils are attained within 2 days after infection (5). Due to lack of chemotactic signals resulting from the disruption of the normal IL-1 signaling neutrophils failed to attain peak numbers. These results are consistent with previous findings (8, 9) including the most recent study conducted with IL-1 ra Tg mice (11). It is clearly evident that neutrophils are the critical early cellular mediators of HSK pathogenesis, being involved in viral clearance (5, 6) and possibly tissue damage through the release of factors such as nitric oxide (25) or remodeling factors such as matrix metalloproteinases (MMPs) (26). In addition, neutrophils have also been considered as a source of molecules facilitating angiogenesis or angiogenic factors themselves such as MMP-9 (26) and VEGF

(27) respectively, and thereby, contributes significantly to the neovascularization process.

Many other cell types can be a potential source of angiogenic factors in the cornea. These include the stromal fibroblast themselves; epithelial cells and inflammatory cells such as macrophages (21). Possibly, with disease progression, there is a shift in the source of angiogenic factors. In addition, apart from VEGF (21), other angiogenic factors such as bFGF (our unpublished results) or C-X-C chemokines such as MIP-2 (28) may be involved in HSV induced corneal angiogenesis. The possibilities are innumerable and presently unclear. Whatever the scenario, our results indicate the effectiveness of IL-1 ra in blocking the overall angiogenesis process. Similar results have been obtained in other murine models of corneal angiogenesis (29).

The chronic inflammatory environment is maintained by the angiogenic response, allowing further delivery of inflammatory cells. The development of HSK lesions is dependent on this response, as shown in studies that have targeted the corneal neovascular response early after virus infection (7). One cell type crucial to HSK pathogenesis and presumably delivered by newly formed (and therefore leaky) blood vessels is the CD4⁺ T cell (3). Thus mice lacking CD4⁺ T cells, but possessing other components normally required in pathogenesis, fail to develop HSK (3, 4). Consistent with these reports, the lack of blood vessel development in the cornea of IL-1 ra treated mice prevented the influx of CD4⁺ T cells. Thus part of the anti-inflammatory effects observed with IL-1 ra therapy also involved the

impairment in the CD4⁺ T cell response. Hence, IL-1 ra treatment targeted at the early preclinical events also influenced subsequent clinical episodes in HSK pathogenesis.

Finally and most importantly, results indicate that the activity of IL-1 needs to be kept under continuous check to achieve significant results. The levels of IL-1 in the cornea after an HSV infection remains elevated till around day 9 p. i. (10). Thus the protocol aimed at abrogating IL-1 activity for an extended period of time produced the best results. Thus our results imply that neutralizing the inflammatory milieu at an early time point may prove beneficial in reducing the severity of HSK. This could be achieved by blocking IL-1 using IL-1 receptor antagonist protein. Antagonizing the proinflammatory environment abrogates the cascade of events that culminate in HSK. Thus, targeting IL-1 ra protein proved to be a worthwhile therapeutic approach for successful management of HSK, a blinding immunoinflammatory lesion of humans.

LIST OF REFERENCES

LIST OF REFERENCES

1. Streilein, J. W., M. R. Dana, and B. R. Ksander. 1997. Immunity causing blindness: five different paths to herpes stromal keratitis. *Immunol Today* 18:443.
2. Tullo, A. 2003. Pathogenesis and management of herpes simplex virus keratitis. *Eye* 17:919.
3. Russell, R. G., M. P. Nasisse, H. S. Larsen, and B. T. Rouse. 1984. Role of T-lymphocytes in the pathogenesis of herpetic stromal keratitis. *Invest Ophthalmol Vis Sci* 25:938.
4. Niemiłowski, M. G., and B. T. Rouse. 1992. Phenotypic and functional studies on ocular T cells during herpetic infections of the eye. *J Immunol* 148:1864.
5. Thomas, J., S. Gangappa, S. Kanangat, and B. T. Rouse. 1997. On the essential involvement of neutrophils in the immunopathologic disease: herpetic stromal keratitis. *J Immunol* 158:1383.
6. Tumpey, T. M., S. H. Chen, J. E. Oakes, and R. N. Lausch. 1996. Neutrophil-mediated suppression of virus replication after herpes simplex virus type 1 infection of the murine cornea. *J Virol* 70:898.
7. Zheng, M., S. Deshpande, S. Lee, N. Ferrara, and B. T. Rouse. 2001. Contribution of vascular endothelial growth factor in the neovascularization process during the pathogenesis of herpetic stromal keratitis. *J Virol* 75:9828.

8. Fenton, R. R., S. Molesworth-Kenyon, J. E. Oakes, and R. N. Lausch. 2002. Linkage of IL-6 with neutrophil chemoattractant expression in virus-induced ocular inflammation. *Invest Ophthalmol Vis Sci* 43:737.
9. Banerjee, K., P. S. Biswas, B. Kim, S. Lee, and B. T. Rouse. 2004. CXCR2^{-/-} mice show enhanced susceptibility to herpetic stromal keratitis: a role for IL-6-induced neovascularization. *J Immunol* 172:1237.
10. Staats, H. F., and R. N. Lausch. 1993. Cytokine expression in vivo during murine herpetic stromal keratitis. Effect of protective antibody therapy. *J Immunol* 151:277.
11. Biswas, P. S., K. Banerjee, B. Kim, and B. T. Rouse. 2004. Mice transgenic for IL-1 receptor antagonist protein are resistant to herpetic stromal keratitis: possible role for IL-1 in herpetic stromal keratitis pathogenesis. *J Immunol* 172:3736.
12. Arend, W. P., M. Malyak, C. J. Guthridge, and C. Gabay. 1998. Interleukin-1 receptor antagonist: role in biology. *Annu Rev Immunol* 16:27.
13. Kary, S., and G. R. Burmester. 2003. Anakinra: the first interleukin-1 inhibitor in the treatment of rheumatoid arthritis. *Int J Clin Pract* 57:231.
14. Kent, S., R. M. Bluthé, R. Dantzer, A. J. Hardwick, K. W. Kelley, N. J. Rothwell, and J. L. Vannice. 1992. Different receptor mechanisms mediate the pyrogenic and behavioral effects of interleukin 1. *Proc Natl Acad Sci U S A* 89:9117.

15. Ohlsson, K., P. Bjork, M. Bergenfeldt, R. Hageman, and R. C. Thompson. 1990. Interleukin-1 receptor antagonist reduces mortality from endotoxin shock. *Nature* 348:550.
16. Yamada, J., M. R. Dana, C. Sotozono, and S. Kinoshita. 2003. Local suppression of IL-1 by receptor antagonist in the rat model of corneal alkali injury. *Exp Eye Res* 76:161.
17. Spear, P. G., and B. Roizman. 1972. Proteins specified by herpes simplex virus. V. Purification and structural proteins of the herpesvirion. *J Virol* 9:143.
18. Dana, M. R., S. N. Zhu, and J. Yamada. 1998. Topical modulation of interleukin-1 activity in corneal neovascularization. *Cornea* 17:403.
19. Babin, M. C., K. Ricketts, J. P. Skvorak, M. Gazaway, L. W. Mitcheltree, and R. P. Casillas. 2000. Systemic administration of candidate antivesicants to protect against topically applied sulfur mustard in the mouse ear vesicant model (MEVM). *J Appl Toxicol* 20 Suppl 1:S141.
20. Deshpande, S., M. Zheng, S. Lee, K. Banerjee, S. Gangappa, U. Kumaraguru, and B. T. Rouse. 2001. Bystander activation involving T lymphocytes in herpetic stromal keratitis. *J Immunol* 167:2902.
21. Zheng, M., M. A. Schwarz, S. Lee, U. Kumaraguru, and B. T. Rouse. 2001. Control of stromal keratitis by inhibition of neovascularization. *Am J Pathol* 159:1021.
22. Tran, M. T., D. A. Dean, R. N. Lausch, and J. E. Oakes. 1998. Membranes of herpes simplex virus type-1-infected human corneal

- epithelial cells are not permeabilized to macromolecules and therefore do not release IL-1alpha. *Virology* 244:74.
23. Garat, C., and W. P. Arend. 2003. Intracellular IL-1Ra type 1 inhibits IL-1-induced IL-6 and IL-8 production in Caco-2 intestinal epithelial cells through inhibition of p38 mitogen-activated protein kinase and NF-kappaB pathways. *Cytokine* 23:31.
 24. Yan, X. T., T. M. Tumpey, S. L. Kunkel, J. E. Oakes, and R. N. Lausch. 1998. Role of MIP-2 in neutrophil migration and tissue injury in the herpes simplex virus-1-infected cornea. *Invest Ophthalmol Vis Sci* 39:1854.
 25. Daheshia, M., S. Kanangat, and B. T. Rouse. 1998. Production of key molecules by ocular neutrophils early after herpetic infection of the cornea. *Exp Eye Res* 67:619.
 26. Lee, S., M. Zheng, B. Kim, and B. T. Rouse. 2002. Role of matrix metalloproteinase-9 in angiogenesis caused by ocular infection with herpes simplex virus. *J Clin Invest* 110:1105.
 27. Kasama, T., K. Kobayashi, N. Yajima, F. Shiozawa, Y. Yoda, H. T. Takeuchi, Y. Mori, M. Negishi, H. Ide, and M. Adachi. 2000. Expression of vascular endothelial growth factor by synovial fluid neutrophils in rheumatoid arthritis (RA). *Clin Exp Immunol* 121:533.
 28. Xue, M. L., A. Thakur, and M. Willcox. 2002. Macrophage inflammatory protein-2 and vascular endothelial growth factor regulate corneal neovascularization induced by infection with *Pseudomonas aeruginosa* in mice. *Immunol Cell Biol* 80:323.

29. Moore, J. E., T. C. McMullen, I. L. Campbell, R. Rohan, Y. Kaji, N. A. Afshari, T. Usui, D. B. Archer, and A. P. Adamis. 2002. The inflammatory milieu associated with conjunctivalized cornea and its alteration with IL-1 RA gene therapy. *Invest Ophthalmol Vis Sci* 43:2905.
30. Deshpande, S., K. Banerjee, P. S. Biswas, and B. T. Rouse. 2004. Herpetic eye disease: immunopathogenesis and therapeutic measures. *Expert Rev Mol Med* 2004:1.
31. Strohmeier, D., F. Frauscher, A. Klauser, W. Recheis, G. Eibl, W. Horninger, H. Steiner, H. Volgger, and G. Bartsch. 2001. Contrast-enhanced transrectal color doppler ultrasonography (TRCDUS) for assessment of angiogenesis in prostate cancer. *Anticancer Res* 21:2907.
32. Hoffman, R. 2002. Green fluorescent protein imaging of tumour growth, metastasis, and angiogenesis in mouse models. *Lancet Oncol* 3:546.
33. Hristov, M., W. Erl, and P. C: Weber. 2003. Endothelial progenitor cells: mobilization, differentiation, and homing. *Arterioscler Thromb Vasc Biol* 23:1185.
34. Pober, J. S. 1987. Effects of tumour necrosis factor and related cytokines on vascular endothelial cells. *Ciba Found Symp* 131:170.
35. Vorkauf, W., M. Vorkauf, B. Nolle, and G. Duncker. 1995. Adhesion molecules in normal and pathological corneas. An

immunohistochemical study using monoclonal antibodies. *Graefes Arch Clin Exp Ophthalmol* 233:209.

APPENDIX

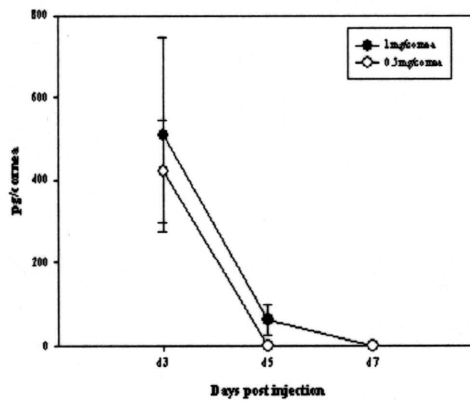


Fig 1. Following Subconjunctival injection, presence of IL-1 ra was detectable in cornea for short period of time.

At indicated time points, 6 corneas /group were processed for measuring the human recombinant IL-1 ra protein levels. Level of human recombinant IL-1 ra was estimated from supernatants of corneal lysates of mice infected with 5×10^6 pfu HSV-1 RE by an antibody capture ELISA as outlined in materials and methods. Results are expressed as Mean \pm SD of three separate experiments (6 corneas/time point).

Figure 2: No difference in HSK score between locally administered IL-1 ra treated mice and vehicle control mice.

A. Interleukin-1 receptor antagonist protein was administered subconjunctivally 24 hr before corneal infection. Mean lesion HSK score at day 20 p. i. of mice infected with 5×10^6 pfu HSV-1 RE. Each dot represents the HSK score from one eye. Horizontal bars and figures in the parenthesis indicate the Mean \pm SD for each group. Data is compiled from two separate experiments consisting of 8 eyes in each group. * Statistically significant differences in mean HSK score ($p < 0.05$) were observed between IL-1 Ra Tg mice to either vehicle control and IL-1 ra treated eyes.

B. Percentage severity of HSK score at day 20 p. i. of mice infected with 5×10^6 pfu HSV-1 RE. Each vertical bar represents number of eyes showing clinically evident lesions (HSK score ≥ 3). Data is compiled from two separate experiments consisting of 8 eyes in each group.

C. Mice were infected with 5×10^6 pfu HSV-1 RE. Mice were terminated at day 20 p. i. and eyes were processed for paraffin embedding. Hematoxylin and Eosin staining was carried out on 6μ sections. Magnification x 200.

Fig 3. Mice treated with IL-1 ra protein locally demonstrated similar angiogenic response like vehicle control.

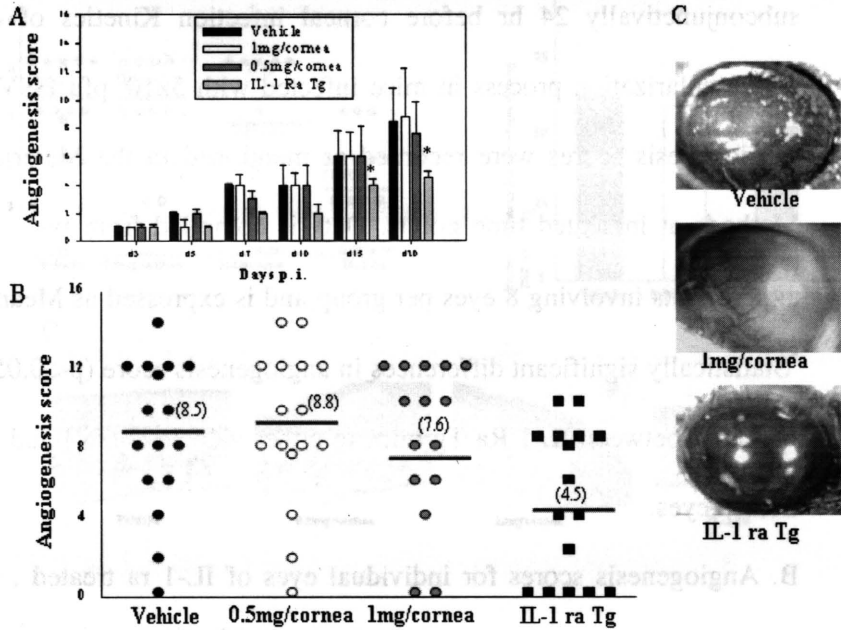
A. Interleukin-1 receptor antagonist protein was administered subconjunctivally 24 hr before corneal infection Kinetics of corneal neovascularization process in mice infected with 5×10^6 pfu HSV-1 RE. Angiogenesis scores were recorded as mentioned in the Materials and Methods at indicated time points. Data is compiled from two separate experiments involving 8 eyes per group and is expressed as Mean \pm SD.

*Statistically significant differences in angiogenesis score ($p < 0.05$) were observed between IL-1 Ra Tg mice to either vehicle control and IL-1 ra treated eyes.

B. Angiogenesis scores for individual eyes of IL-1 ra treated , vehicle control and IL-1 ra Tg mice infected with 5×10^6 pfu HSV-1 RE at day 20 p. i. Horizontal bars and figures show the mean for each group. Data are compiled from two separate experiments consisting of 8 eyes per group.

C. At day 20 p. i. extensive growth of blood vessels can be seen in IL-1 ra treated and vehicle control mice infected with 5×10^6 pfu HSV-1 RE. IL-1 Ra Tg mice show minimum angiogenic sprouts near the limbal ring with the same dose.

Fig. 3. Mice treated with IL-1 receptor antagonist protein were administered angiogenic response like vehicle control.



B. Angiogenesis score for individual eyes of IL-1 receptor antagonist protein treated, vehicle control and IL-1 receptor antagonist protein treated mice infected with 2×10^6 pfu HSV-1 RE at day 20 p.i. Horizontal bars and figures show the mean for each group. Data were compiled from two separate experiments consisting of 8 eyes per group.

C. At day 20 p.i. extensive growth of blood vessels can be seen in IL-1 receptor antagonist protein treated mice infected with 2×10^6 pfu HSV-1 RE. IL-1 receptor antagonist protein treated mice show minimum angiogenic sprouts near the limbal ring with the same dose.

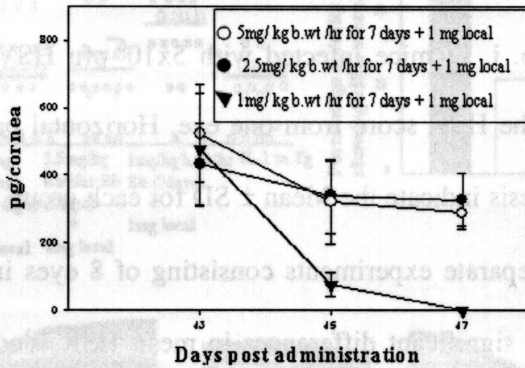


Fig 4. Human recombinant Interleukin-1 receptor antagonist protein was detected in mice receiving a combination of systemic and local administration till day 7 post injection.

At indicated time points, 6 corneas /group were processed for measuring the human recombinant IL-1 ra protein levels. Level of human recombinant IL-1 ra was estimated from supernatants of corneal lysates of mice infected with 5×10^6 pfu HSV-1 RE by an antibody capture ELISA as outlined in materials and methods. Results are expressed as Mean \pm SD of three separate experiments (6 corneas/time point).

Fig 5. Mice receiving IL-1 ra systemically in conjunction with local administration demonstrated reduced HSK severity.

A. Interleukin-1 receptor antagonist protein was administered systemically along with subconjunctival injection 24 hr before corneal infection as described in Materials and Methods. Mean lesion HSK score at day 20 p. i. of mice infected with 5×10^6 pfu HSV-1 RE. Each dot represents the HSK score from one eye. Horizontal bars and figures in the parenthesis indicate the Mean \pm SD for each group. Data is compiled from two separate experiments consisting of 8 eyes in each group. **,**

Statistically significant differences in mean HSK score ($p < 0.05$) were observed between mice treated with either 5mg/kg body wt. /hr for 7days S/c + 1mg/cornea local (Group 1) or 2.5mg/ kg body wt. /hr for 7days S/c + 1mg/cornea local IL-1 ra and vehicle control.

B. Percentage severity of HSK score at day 20 p. i. of mice infected with 5×10^6 pfu HSV-1 RE. Each vertical bar represents number of eyes showing clinically evident lesions (HSK score ≥ 3). Data is compiled from two separate experiments consisting of 8 eyes in each group.

C. Mice were infected with 5×10^6 pfu HSV-1 RE. Mice were terminated at day 20 p. i. and eyes were processed for paraffin embedding. Hematoxylin and Eosin staining was carried out on 6μ sections. Magnification x 200.

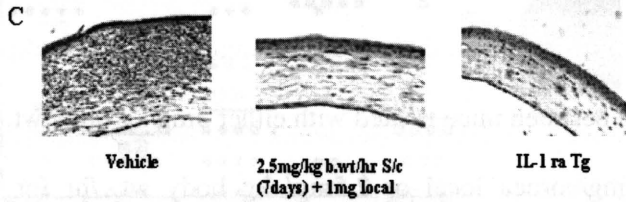
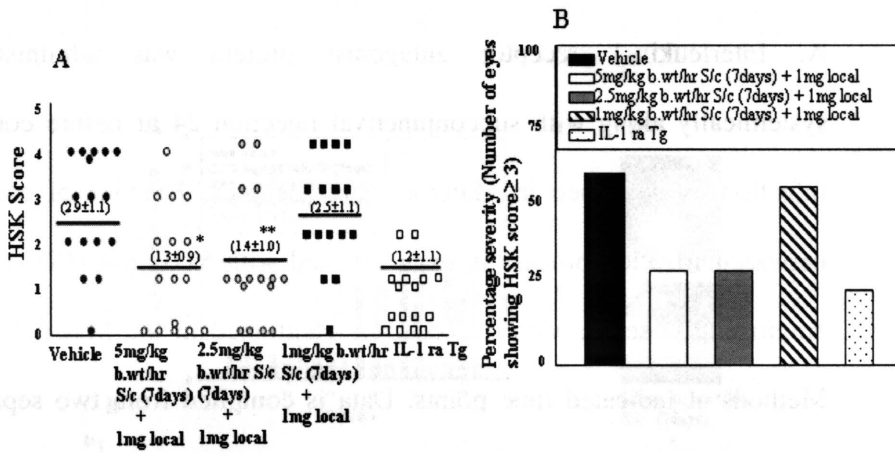


Fig 6. Mice receiving a combination of systemic and local administration of IL-1 ra protein showed diminished angiogenesis following ocular infection.

A. Interleukin-1 receptor antagonist protein was administered systemically along with subconjunctival injection 24 hr before corneal infection as described in Materials and Methods. Kinetics of corneal neovascularization process in mice infected with 5×10^6 pfu HSV-1 RE. Angiogenesis scores were recorded as mentioned in the Materials and Methods at indicated time points. Data is compiled from two separate experiments involving 8 eyes per group and is expressed as Mean \pm SD.* Statistically significant differences in angiogenesis score ($p < 0.05$) were observed between mice treated with either 5mg/kg body wt. /hr for 7days S/c + 1mg/cornea local or 2.5mg/ kg body wt. /hr for 7days S/c + 1mg/cornea local IL-1 ra and vehicle control.

B. Angiogenesis scores for individual eyes of IL-1 ra treated , vehicle control and IL-1 ra Tg mice infected with 5×10^6 pfu HSV-1 RE at day 20 p. i. Horizontal bars and figures show the mean for each group. Data are compiled from two separate experiments

C. At day 20 p. i. extensive growth of blood vessels can be seen in IL-1 ra treated and vehicle control mice infected with 5×10^6 pfu HSV-1 RE. IL-1 ra treated mice show minimum angiogenic sprouts near the limbal ring. In comparison, vehicle control eyes demonstrated extensive growth of blood vessels with the same dose.

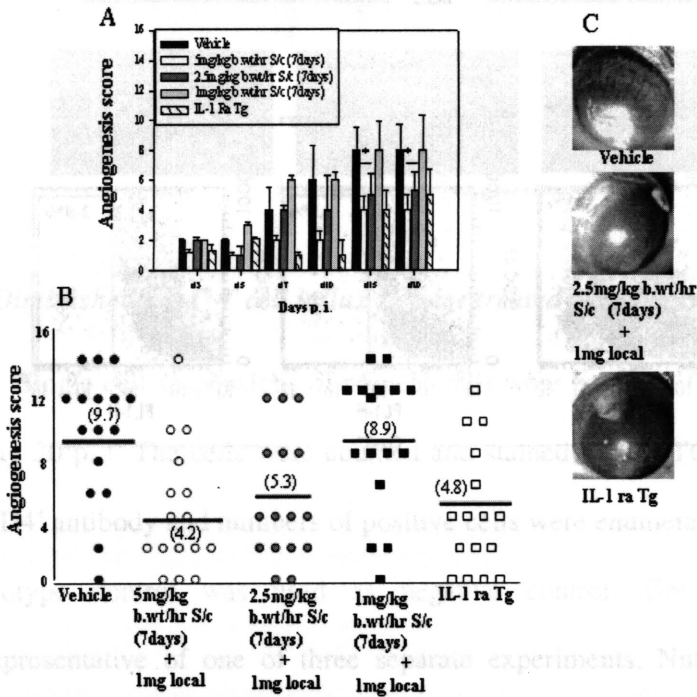


Fig 6. Mice receiving a combination of systemic and local administration of IL-1 ra protein showed diminished angiogenesis following ocular infection.

A Interleukin-1 receptor antagonist protein was administered systemically along with subconjunctival injection 24 hr before corneal

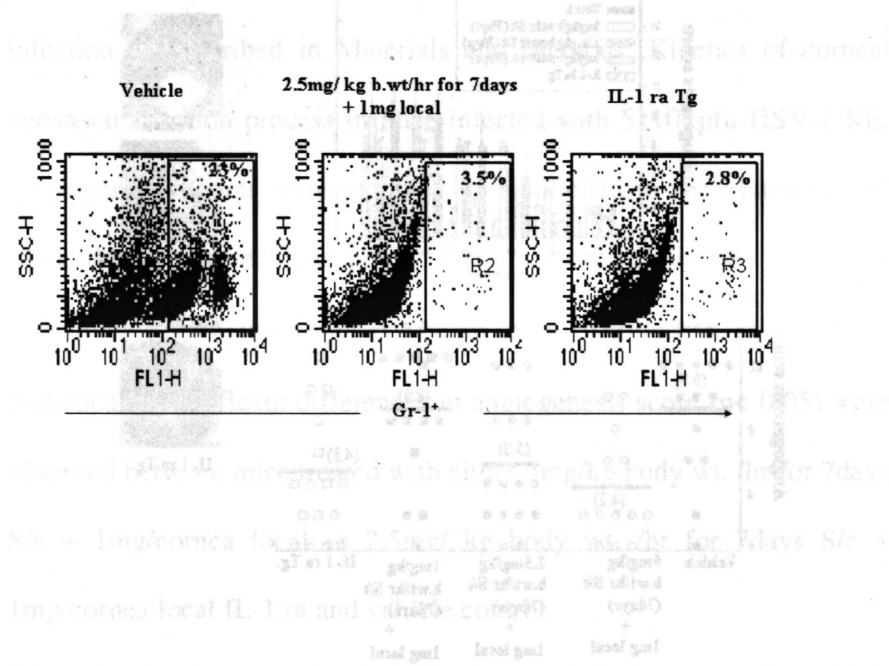


Fig 7. Presence of abundant Gr-1+ve cells in the cornea of vehicle control mice but not in IL-1 ra treated mice at 48 hr p. i.

Single cell suspensions of corneal cells were prepared from 4 eyes at 48 hr p. i. The cells were counted and stained with FITC labeled anti Gr-1 antibody and numbers of Gr-1 positive cells were enumerated by FACS. Dotplot is representative of one of three separate experiments. The number on the upper right corner represents the percentage of Gr-1+ cells of total corneal cells at 48 hr. p. i.

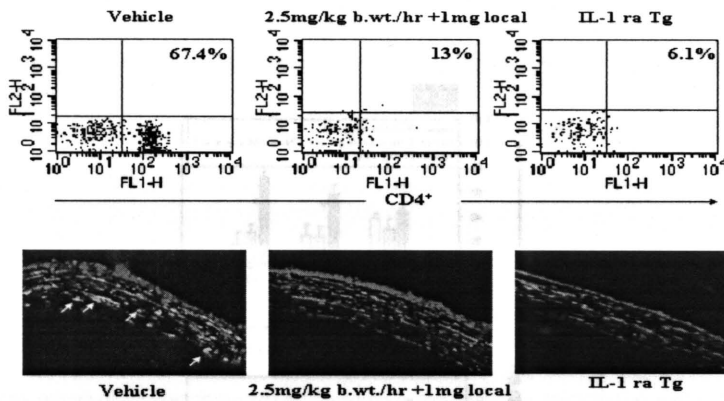


Fig 8. Diminished CD4⁺ T cell influx in mice treated with IL-1 ra protein.

A. Single cell suspensions of corneal cells were prepared from 4 eyes at day 20 p. i. The cells were counted and stained with FITC labeled anti CD4⁺ antibody and numbers of positive cells were enumerated by FACS.

Isotype control was used as negative control. Dot plot is the representative of one of three separate experiments. Numbers on the upper right corner represents the percentage of CD4⁺ T cells of total gated lymphocytes at day 20 p. i..

B. At day 20 p. i., representative eyes were taken and snap frozen in OCT compound and 6 μ sections were cut. The sections were stained for CD4⁺ T cells using an FITC labeled anti CD4⁺ antibody as described in Materials and Methods. Corneas were mounted with Vectashield mounting medium for fluorescence with Propidium Iodide and visualized under a microscope. The white arrows indicate the CD4⁺ T cells in the corneas.

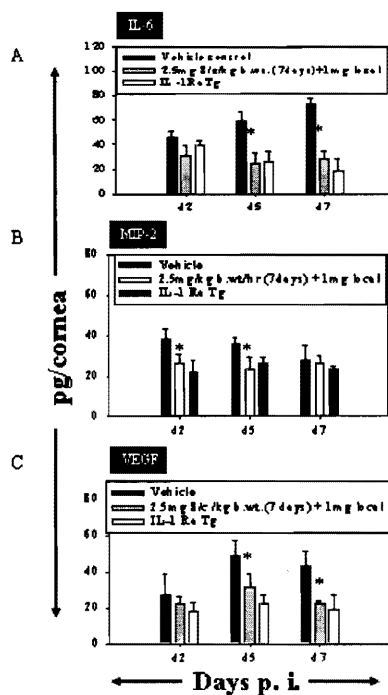


Fig 9. IL-1 ra treated mice demonstrated reduced protein levels of IL-6, MIP-2 and VEGF.

A, B & C. At indicated time points, 6 corneas /group were processed for measuring the IL-6, MIP-2 and VEGF protein levels. Levels of IL-6, MIP-2 and VEGF was estimated from supernatants of corneal lysates of mice infected with 5×10^6 pfu HSV-1 RE by an antibody capture ELISA as outlined in materials and methods. Results are expressed as Mean \pm SD of three separate experiments (6 corneas/time point). *Statistically significant differences in IL-6, MIP-2 and VEGF level ($p < 0.05$) were observed between IL-1 ra treated mice to vehicle control mice.

PART VI

A NOVEL FLOW CYTOMETRY BASED

ASSAY FOR QUANTIFICATION OF

CORNEAL ANGIOGENESIS IN THE MOUSE

MODEL OF HERPETIC STROMAL

KERATITIS

Research described in this chapter is a slightly modified version of an article published in 2005 in *Experimental Eye Research* by Partha Sarathi Biswas, Kaustuv Banerjee, Bumseok Kim, Jordan Smith and Barry T. Rouse.

Biswas, P. S., K. Banerjee, B. Kim, J. Smith, and and B. T. Rouse. 2005. A novel flow cytometry based assay for quantification of corneal angiogenesis in mouse model of herpetic stromal keratitis . *Exp. Eye Res.* 80(1):73. Copyright 2004. *The American Association of Immunologists, Inc.*

In this chapter “we” and “our” refers to co-authors and me. My contributions in the paper include (1) selection of the topic (2) data analysis and interpretation (3) planning experiments (4) compiling and interpretation of the literature (5) understanding how results fit with the literature (7) compilation of contributions into one paper (8) providing structure to the paper (9) making graphs, figures and tables (10) writing and editing.

ABSTRACT

In this study a novel flow cytometry based quantitative assay for measuring corneal angiogenesis is demonstrated. Corneas of Balb/c mice were lightly scarified and infected with 5×10^5 , 5×10^4 and 5×10^3 pfu HSV-1 RE virus. Development of corneal angiogenesis was studied on day 15 post infection by direct visualization of infected cornea with a slit-lamp biomicroscope. Endothelial cells constituting the newly developed blood vessels in cornea were stained with murine anti CD31 antibody on frozen corneal sections and

corneal whole mounts at day 15 p. i. Total number of endothelial cells was quantified at day 15 post infection by flow cytometry. Mice infected with different doses of HSV-1 RE developed severe to mild corneal angiogenesis at day 15 p. i. Endothelial cells constituting the newly formed blood vessels expressed CD31 at day 15 post infection. Flow cytometry revealed that, the number of CD31 positive cells isolated from diseased corneas increased with the increase in Neovascularization index. The flow cytometry analysis used in this present study is a useful, accurate and cost effective method for quantifying corneal angiogenesis.

INTRODUCTION

Herpetic stromal keratitis (HSK) is an immunoinflammatory lesion in the corneal stroma that ensues from ocular infection with Herpes simplex virus (HSV) (1). Studies in murine models have revealed a complex pathogenesis, involving multiple molecular and cellular events (2). One of these is neovascularization of the normally avascular cornea. New blood vessels sprout from vessels at the corneal limbus within 24 h of HSV infection (3), and eventually extend to the central cornea within the next 10–15 days (3). Such angiogenesis impairs vision and appears necessary for the ingress of T cells responsible for orchestrating HSK (2). Measuring corneal angiogenesis is normally accomplished by direct visualization with a slit-lamp biomicroscope and recording the area occupied by new vessels (4). This technique is tedious and subject to error especially when performed on living animals. In addition the approach fails to account for any difference in the vessel thickness. Other

techniques, including ultrasound micro-imaging and other microimaging technologies (5, 6) for angiogenesis quantification have been used but these require sophisticated instrumentation and trained personnel.

In this report, an alternative approach for the quantification of corneal angiogenesis using a flow cytometry based assay is presented. Our results indicate that, following HSV infection endothelial cells constituting the newly formed blood vessels in corneal stroma express CD31 (PECAM 1). By targeting this surface marker by a fluorescently labeled antibody, number of endothelial cells in inflamed murine cornea could be quantified. The numbers of CD31⁺ cells were proportional to the growth of blood vessels in the infected cornea, as measured by biomicroscopy. In addition, number of CD31⁺ cell/cornea correlated with the angiogenic score. The flow cytometry based assay efficiently discriminated the difference in angiogenic response between mice infected with different doses of virus. Thus, estimation of angiogenesis on the basis of number of endothelial cells proved to be a potential technique for the quantification of corneal neovascularization.

MATERIALS AND METHODS

Mice

Wild type female 6 to 8 weeks old Balb/c mice were purchased from Harlan Sprague-Dawley (Indianapolis, Indiana). Animals were sex and age matched for all experiments. To prevent bacterial superinfections, all mice received prophylactic treatment with Sulphatrim pediatric suspension (Barre-National

Baltimore, MD). All experimental procedures were in complete agreement with the Association for Research in Vision and Ophthalmology (ARVO) resolution on the use of animals in research.

Virus

HSV-1 RE (obtained from Dr. Robert Hendricks Laboratory, University of Pittsburgh School of Medicine) was used in the present study. The virus was propagated and titrated on monolayer of Vero cells (ATCC, Cat No. CCL81) using standard protocols (7). Infected Vero cells were harvested, titrated and stored in aliquots at -80°C until used.

Corneal HSV-1 infection

Corneal infections of all mice groups were conducted under deep anesthesia induced by intraperitoneal injection of Avertin (Sigma, St. Louis, MO). Mice were scarified on their corneas with a 27-gauge needle and a $4\mu\text{l}$ drop containing the required dose of virus (5×10^5 , 5×10^4 and 5×10^3 pfu) was applied to the eye and gently massaged with the eyelids.

Angiogenesis Scoring

The eyes were examined on day 15 post infection by a slit-lamp biomicroscope (Kowa Co. Nagoya, Japan) and angiogenesis severity was measured as described previously (4). Briefly, a grade of 4 for a given quadrant of the circle represents a centripetal growth of 1.5mm toward the

corneal center. The score of the 4 quadrants of the eye were then summed to derive the Neovascularization (NV) index (range 0-16) for each eye.

Confocal Microscopy

For immunohistochemistry, at day 15 p. i. eyes were frozen in optimum cutting temperature (OCT) compound (Miles, Elkart, IN). Six-micron-thick sections were cut, air dried, and fixed in cold acetone for 10 min at -20° C. The sections were blocked with 3% BSA (Sigma) containing unconjugated anti-CD16/32 (1:200) antibody (Pharmingen, San Diego, CA) for 2 hour at 37° C. For detection of endothelial cells in the stroma, the sections were incubated with FITC-coupled monoclonal anti-mouse CD31 antibody (anti mouse PECAM1) (Clone MEC13.3, Pharmingen) at a concentration of 1:500 in 1% BSA at 4°C overnight. Corneas were repeatedly washed in PBS and then mounted with Vectashield mounting medium for fluorescence with Propidium Iodide (Vector Laboratories Inc, Burlingame, CA) and visualized with a confocal microscope (Leica, Wetzlar, Germany).

Immunofluorescence staining of blood vessels on corneal whole mounts

Immunohistochemical staining for vascular endothelial cells was also performed on corneal flatmounts. At day 15 p. i. corneas from infected mice were dissected under stereo-microscope (Leica, Wetzlar, Germany). Then corneal wholemounts were rinsed in PBS for 30 minutes and flattened on a glass slide under stereo-microscope (Leica, Wetzlar, Germany). Corneal flatmounts were dried and fixed in 100% acetone (Sigma, St. Louis, MO) for

10 minutes at -20° C. Nonspecific binding was blocked with 5% BSA (Sigma) containing unconjugated anti-CD16/32 (1:200) antibody (Pharmingen) for 2 hour at 37° C. Incubation with FITC-coupled monoclonal anti-mouse CD31 antibody (anti mouse PECAM1) (Clone MEC13.3, Pharmingen) at a concentration of 1:250 in 1% BSA at 4° C overnight was followed by subsequent washes in PBS at room temperature. Corneas were mounted with Vectashield mounting medium for fluorescence with Propidium Iodide (Vector Laboratories Inc, Burlingame, CA) and visualized with a fluorescence microscope (Leica, Wetzlar, Germany).

Flow Cytometry

Mice were infected with different doses of HSV-1 RE. At day 15 p. i., Neovascularization index of individual eyes were determined by direct visualization of infected corneas with slit-lamp biomicroscope. Two corneas with similar NV index were pooled together and stained for number of CD31⁺ cells/cornea. This was repeated three times.

In another set of experiments, three groups of mice were infected with 5×10^5 , 5×10^4 and 5×10^3 pfu HSV-1 RE. At day 15 p. i., NV index of individual eyes were determined by direct visualization of infected corneas with slit-lamp biomicroscope. Two corneas with a NV index and closest to the Mean NV index of that group were pooled together and stained for number of CD31⁺ cells/cornea. This experiment was repeated thrice.

Staining procedure: Corneas were dissected carefully under a stereomicroscope (Leica, Wetzlar, Germany). All precautions were taken to avoid

the limbal blood vessels. Single-cell suspensions were prepared from 2 corneas at day 15 post infection as described elsewhere (8), with some modifications. Briefly, corneal buttons were incubated with collagenase D (Roche) for 60 min at 37°C in a humidified atmosphere at 5% CO₂. After incubation, corneas were disrupted by grinding with a syringe plunger and passing through a cell strainer. Cells were washed and suspended in RPMI 1640 with 10% FBS and counted by Trypan Blue staining. The F_c receptors on the cells were blocked with unconjugated anti-CD16/32 (Pharmingen) for 30 min. Samples were incubated with FITC labeled anti CD31 antibody (Clone MEC13.3, Pharmingen) and isotype controls for 30 minutes. All samples were collected on a FACScan (BD Biosciences, San Diego, CA), and data were analyzed using CellQuest 3.1 software (BD Biosciences, San Diego, CA).

Statistical Analysis

Data obtained were analyzed for statistical significance by Student's *t* test. Pearson's Product Moment Correlation Coefficient was used to determine correlation coefficient.

RESULTS

Endothelial cells constituting the newly developed blood vessels express CD31 (PECAM 1) following corneal HSV-1 infection.

Endothelial cells making up the newly formed blood vessels are characterized by the expression of adhesion molecules such as CD31 (PECAM 1), Vascular endothelial – cadherin (VE-cad) and von Willebrand factor (9). Expression of

these surface molecules on endothelial cells are regulated by inflammatory mediators (10, 11). To find out whether endothelial cells constituting the newly developed blood vessels express CD31, corneas of infected mice were stained for CD31. As demonstrated in Fig. 1A, endothelial cells making up the newly grown blood vessels in corneal stroma expressed CD31 (PECAM 1) at day 15 p. i. In addition, fluorescently labeled anti CD31 antibody stained the blood vessels on corneal whole mounts at the same time point (Fig. 1B). Thus, targeting CD31 with a fluorescently coupled antibody may prove to be a reliable and efficient tool to label and quantify the number of endothelial cells in corneal angiogenesis.

Increase in the number of CD31⁺ cells is associated with the increase in Neovascularization (NV) index

At day 15 p. i., the NV index of individual eyes was determined by slit-lamp biomicroscopy. Two corneas with similar NV index were pooled together and the number of CD31⁺ cells was counted by FACS analysis. As demonstrated in Fig 2A, 2B and 2C, corneas with higher NV index have more CD31⁺ cells/cornea. In contrast to naïve cornea, there was a gradual increase in the number of CD31⁺ cells/cornea with the increase in NV index. In addition, a strong correlation ($r = 0.965$, $p \leq 0.0002$) was observed between NV index and number of CD31⁺ cells/cornea. Isotype control showed no background staining. Greater than 65% of mouse brain endothelial cells (positive control) stained positive for CD31 (data not shown). Overall, this experiment revealed that, the cell based assay closely resemble the NV index obtained by direct

visualization of infected cornea at day 15 p. i.

Difference in the number of CD31⁺ cells/cornea in mice infected with different doses of virus

Three groups of mice were infected with 5×10^5 pfu, 5×10^4 pfu and 5×10^3 pfu HSV-1 RE respectively. At day 15 p. i., the NV index of individual eyes was scored by slit-lamp biomicroscopy. As shown in Fig. 3, groups of mice infected with 5×10^5 pfu, 5×10^4 pfu and 5×10^3 pfu HSV-1 RE had mean NV index of 10.7, 5.6 and 1.8 respectively. Mean NV index of mice infected with 5×10^5 pfu was significantly ($p < 0.05$) higher than mean NV index of mice infected with 5×10^4 and 5×10^3 pfu virus. Two eyes from each group with NV indexes close to the group mean were pooled together and number of CD31⁺ cells/cornea were quantified using flow cytometry. Once again there was a concordance between the two assays. Group infected with the highest dose (5×10^5 pfu) and showing higher mean NV index have significantly ($p < 0.05$) greater number of CD31⁺ cells/cornea ($18,365 \pm 3499$) in comparison to 5×10^4 pfu (925 ± 478) and 5×10^3 pfu (130 ± 61) (Fig. 4A, B and C). Thus in comparison with the average number of endothelial cells/cornea, mice infected with 5×10^5 pfu have approximately 20 fold (5×10^4 pfu) and 200 fold (5×10^3 pfu) more CD31⁺ cells/cornea.

DISCUSSION

In this study a novel flow cytometry based assay was used to quantify corneal angiogenesis following ocular HSV infection. Our results indicate that,

endothelial cells constituting the newly formed blood vessels in corneal stroma express CD31 (PECAM 1) at day 15 post infection. Thus, labeling the blood vessel endothelial cells by targeting this surface marker provided a unique opportunity to quantify the number of endothelial cells/cornea. The data revealed that, the number of CD31⁺ cells/cornea was proportional to the growth of blood vessels in infected cornea. In addition, this assay was able to pick up the difference in angiogenic response between mice infected with different doses of virus. Thus, estimation of angiogenesis on the basis of number of endothelial cells proved to be a useful approach to quantify corneal neovascularization.

Strongly woven endothelial cells on cellular matrix make up the wall for blood vessels. With the increase in length, thickness and number of vasculature, increase in the number of endothelial cells constituting the newly developed vessels were expected. Thus, quantifying the number of endothelial cells would directly reflect the amount of blood vessels present in the corneal tissue at a particular time point. By the virtue of this assay, we were able to consider the three-dimensional structure i.e. length, width and height of a blood vessel instead of relying on the visualization of surface vasculature during the process of quantification by conventional way.

As evident from our study, the cell-based assay was responsive enough to detect the gradual increase in the number of endothelial cells with the increase in NV index. To our knowledge, this is the first report where the growth of blood vessels has been successfully represented by a cell-based assay. In addition, this assay was able to differentiate the angiogenic response

observed following infection with various doses of virus. However, the flow cytometry based assay for quantification of corneal angiogenesis has some shortcomings. These include the fact that, this is a terminal assay and cannot be used for angiogenesis kinetics study. Besides this, in case of naïve mice, in spite of an absence of an angiogenic score, still approximately 0.1 % of cells were CD31⁺. We believe that this discordance was attributed to the underlined corneal endothelium layer. Adding up, was the possibility of overestimation due to possible contamination of limbal blood vessel endothelial cells. Currently we are in the process of overcoming these constraints to make it more accurate and reliable.

In this report, we demonstrated an alternative approach of quantification of corneal angiogenesis in mouse model of HSK. The cell based technique closely resembled the commonly used method to quantify corneal angiogenesis. It would be of particular interest to know whether this flow cytometry technique is useful in assessing angiogenesis in other corneal inflammatory models and tumor systems. Overall, estimation of angiogenesis on the basis of number of endothelial cells may be a potential technique for the quantification of corneal neovascularization.

LIST OF REFERENCES

LIST OF REFERENCES

1. Streilein, J. W., M. R. Dana, and B. R. Ksander. 1997. Immunity causing blindness: five different paths to herpes stromal keratitis. *Immunol Today* 18:443.
2. Deshpande, S., K. Banerjee, P. S. Biswas, and B. T. Rouse. 2004. Herpetic eye disease: immunopathogenesis and therapeutic measures. *Expert Rev Mol Med* 2004:1.
3. Zheng, M., M. A. Schwarz, S. Lee, U. Kumaraguru, and B. T. Rouse. 2001. Control of stromal keratitis by inhibition of neovascularization. *Am J Pathol* 159:1021.
4. Dana, M. R., S. N. Zhu, and J. Yamada. 1998. Topical modulation of interleukin-1 activity in corneal neovascularization. *Cornea* 17:403.
5. Strohmeyer, D., F. Frauscher, A. Klauser, W. Recheis, G. Eibl, W. Horninger, H. Steiner, H. Volgger, and G. Bartsch. 2001. Contrast-enhanced transrectal color doppler ultrasonography (TRCDUS) for assessment of angiogenesis in prostate cancer. *Anticancer Res* 21:2907.
6. Hoffman, R. 2002. Green fluorescent protein imaging of tumour growth, metastasis, and angiogenesis in mouse models. *Lancet Oncol* 3:546.
7. Spear, P. G., and B. Roizman. 1972. Proteins specified by herpes simplex virus. V. Purification and structural proteins of the herpesvirion. *J Virol* 9:143.

8. Deshpande, S., M. Zheng, S. Lee, K. Banerjee, S. Gangappa, U. Kumaraguru, and B. T. Rouse. 2001. Bystander activation involving T lymphocytes in herpetic stromal keratitis. *J Immunol* 167:2902.
9. Hristov, M., W. Erl, and P. C. Weber. 2003. Endothelial progenitor cells: mobilization, differentiation, and homing. *Arterioscler Thromb Vasc Biol* 23:1185.
10. Pober, J. S. 1987. Effects of tumour necrosis factor and related cytokines on vascular endothelial cells. *Ciba Found Symp* 131:170.
11. Vorkauf, W., M. Vorkauf, B. Nolle, and G. Duncker. 1995. Adhesion molecules in normal and pathological corneas. An immunohistochemical study using monoclonal antibodies. *Graefes Arch Clin Exp Ophthalmol* 233:209.

APPENDIX

Fig 1. Endothelial cells constituting the new blood vessels in corneal stroma express CD31 at day 15 post infection.

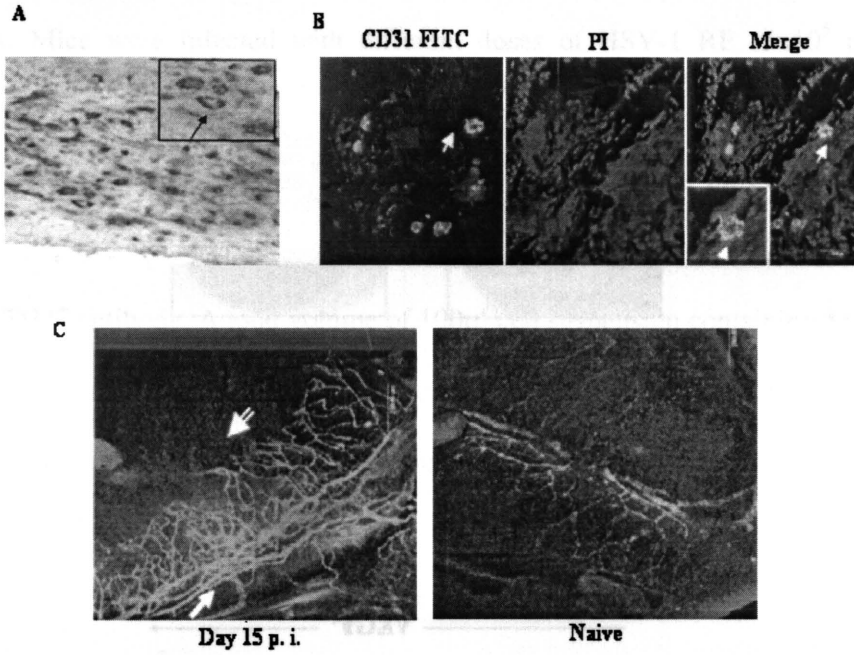
A. At day 15 p. i. eyes were frozen in OCT compound and six micron sections were made. The slides were stained with monoclonal anti mouse CD31 primary antibody and biotinylated anti rat IgG secondary antibody. Diaminobenzidine was used as substrate, and sections were counterstained with hematoxylin. Original magnification x200. The black arrow (inset) indicates the cross section of endothelial cells lining the lumen of a blood vessel in the corneal stroma.

B. At day 15 p. i. eyes were frozen in OCT compound and six micron sections were made. The slides were stained with FITC-coupled monoclonal anti mouse CD31 antibody. The slides were counterstained with Propidium Iodide and visualized under a Leica SP2 Laser scanning confocal microscope (Leica, Wetzlar, Germany). The white arrow (inset) indicates the cross section of endothelial cells lining the lumen of a blood vessel in the corneal stroma.

C. Immunohistochemical staining for vascular endothelial cells was performed on corneal flatmounts at day 15 post infections with FITC-coupled monoclonal anti-mouse CD31 antibody. Corneas were mounted with an antifading agent containing Propidium Iodide and visualized with a Leica SP2 Laser scanning confocal microscope (Leica, Wetzlar, Germany). Extensive neovascularization was observed from limbal blood vessels at day 15 post infection. Naïve mice showed little or no angiogenic sprouts near the limbal ring. The solid and double white

arrows indicate the limbal blood vessel and newly grown blood vessel in the cornea respectively.

Fig 3. Increase in the number of CD31⁺ cells is associated with the increase in NV index at day 15 p. i.



10⁷ pfu and 5x10⁷ pfu). Individual eyes were scored for angiogenesis (NV index) with the lamp bio microscope at day 15 p. i. Two controls of same strain (control 1 and control 2) were included with the infected eyes. The number of CD31⁺ cells in the vessel wall was determined by immunofluorescence. The eyes were fixed in Bouin's solution and embedded in paraffin. The sections were stained with hematoxylin and eosin (H&E) and mounted on slides. The sections were examined under a light microscope. The number of CD31⁺ cells was determined by immunofluorescence. The eyes were fixed in Bouin's solution and embedded in paraffin. The sections were stained with hematoxylin and eosin (H&E) and mounted on slides. The sections were examined under a light microscope. The number of CD31⁺ cells was determined by immunofluorescence. The eyes were fixed in Bouin's solution and embedded in paraffin. The sections were stained with hematoxylin and eosin (H&E) and mounted on slides. The sections were examined under a light microscope. The number of CD31⁺ cells was determined by immunofluorescence.

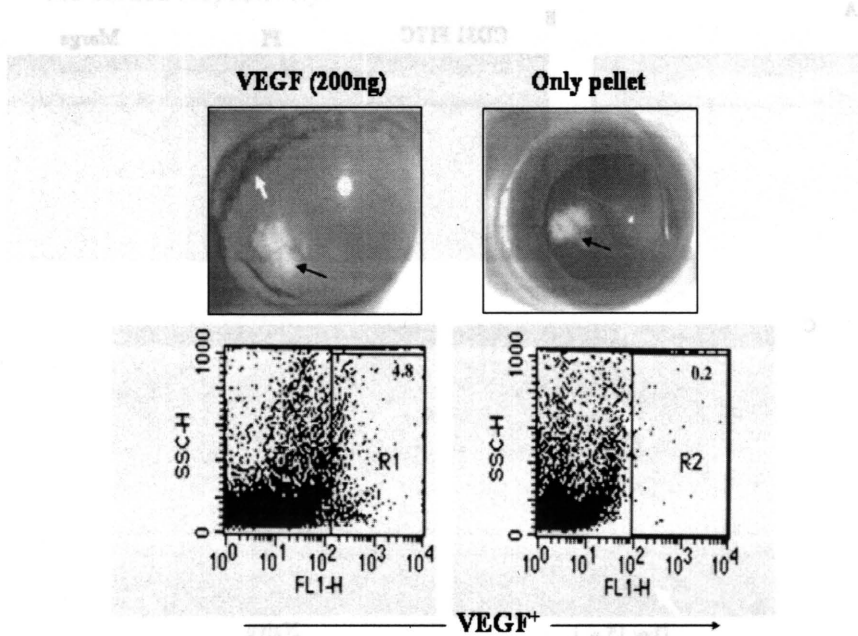


Fig 2. Increase in the number of CD31⁺ cells is associated with heightened angiogenic response following corneal micropocket assay.

Hydron pellets (black arrow) containing VEGF (200 ng) were implanted into the corneal pockets (n=6). Control mice received pellets only. At day 4 post implantation angiogenic response was assessed. Two corneas demonstrating similar angiogenic response were pooled together and number of CD31⁺ cells was enumerated by FACS analysis as described in Materials and Methods. The dot plot represents one of the three separate experiments. The number in the right hand corner represents percentage of CD31⁺ cells.

Fig 3. Increase in the number of CD31⁺ cells is associated with the increase in NV index at day 15 p. i.

A. Mice were infected with different doses of HSV-1 RE (5×10^5 pfu, 5×10^4 pfu and 5×10^3 pfu). Individual eyes were scored for angiogenesis (NV index) with slit lamp bio-microscope at day 15 p. i. Two corneas of same NV index were pooled together and stained with FITC labeled CD31⁺ antibody. A total volume of 100 μ l cell suspension containing 5×10^4 cells was spun down. The slides were counterstained with Propidium Iodide and visualized under a microscope (Leica, Wetzlar, Germany).

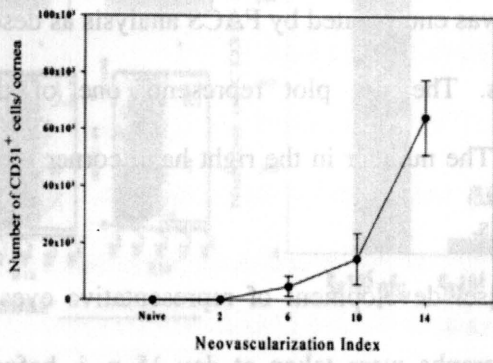
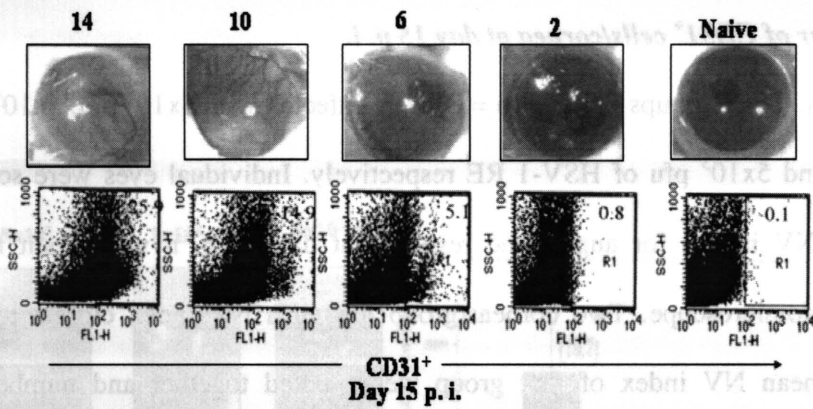
Original magnification x200

B. Mice were infected with different doses of HSV-1 RE (5×10^5 pfu, 5×10^4 pfu and 5×10^3 pfu). Individual eyes were scored for angiogenesis (NV index) with slit lamp bio-microscope at day 15 p. i. Two corneas of same NV index were pooled together and number of CD31⁺ cells was enumerated by FACS analysis as described in Materials and Methods. The dot plot represents one of the three separate experiments. The number in the right hand corner represents percentage of CD31⁺ cells.

C. Blood vessel development of representative eyes with various NV index. Photographs were taken at day 15 p. i. before FACS analysis. Representative eyes with NV index of 14 demonstrated extensive blood vessel development, whereas eyes with NV index of 2 show minimal blood vessel development.

D. The line diagram represents a steady increase in the number of CD31⁺ cells/cornea with the increase in NV index. The data is accumulated from three separate experiments and expressed as Mean \pm SD.

Fig. 4. Mice infected with higher dose of virus demonstrated increased



Representative eyes from different groups showing variable degree of angiogenic response at day 15 p. i.

C. The bar diagram represents the number of CD31⁺ cells/cornea at day 15 p. i. Figure in the parenthesis indicate the Mean NV index for each group. * Significant difference (p<0.05) in comparison to 2x10⁶ and 2x10⁷ pla.

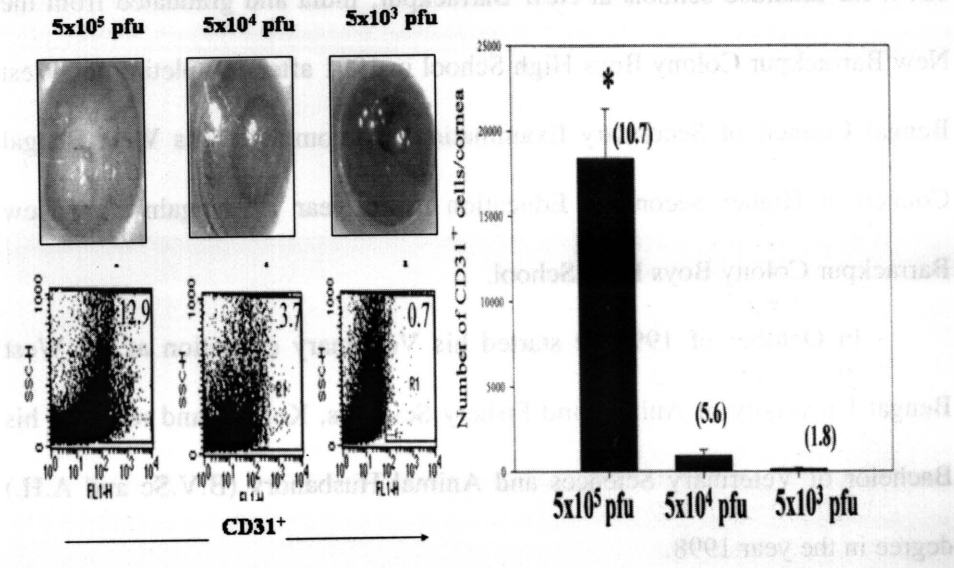
Fig 4. Mice infected with higher dose of virus demonstrated increased number of CD31⁺ cells/cornea at day 15 p. i.

A. Three groups of mice (n = 8) were infected with 5×10^5 pfu, 5×10^4 pfu and 5×10^3 pfu of HSV-1 RE respectively. Individual eyes were scored (NV index) for angiogenic response at day 15 p. i. with a slit lamp biomicroscope. Two corneas/group having a NV index closest to the mean NV index of that group were pooled together and number of CD31⁺ cells was enumerated by FACS analysis as described in Materials and Methods. The dot plot represents one of the three separate experiments. The number in the right hand corner represents percentage of CD31⁺ cells.

B. Blood vessel development of representative eyes with various NV index. Photographs were taken at day 15 p. i. before FACS analysis. Representative eyes from different groups showing variable degree of angiogenic response at day 15 p. i.

C. The bar diagram represents the number of CD31⁺ cells/ cornea at day 15 p. i. Figure in the parenthesis indicate the Mean NV index for each group. * Significant difference ($p < 0.05$) in comparison to 5×10^4 and 5×10^3 pfu.

Farhan Zahoori Bhanu was born in New Baniapur, India on September 14, 1974. He attended schools at New Baniapur, India and graduated from the



Farhan joined the Chaudhary Charan Singh Haryana Agricultural University, Haryana in October of 1998 and obtained his Master of Veterinary Sciences (M.V.Sc) degree from the department of Veterinary Microbiology in the year 2000. He joined The University of Tennessee, Knoxville in August 2000 and received the Doctor of Philosophy degree from the Department of Comparative and Experimental Medicine, College of Veterinary Medicine in May 2002. He plans to further pursue post doctoral training.

Vita

Partha Sarathi Biswas was born in New Barrackpur, India on September 14th, 1974. He attended schools at New Barrackpur, India and graduated from the New Barrackpur Colony Boys High School in 1991 after completing his West Bengal Council of Secondary Examination. He completed his West Bengal Council of Higher Secondary Education in the year 1993 again from New Barrackpur Colony Boys High School.

In October of 1993 he started his Veterinary education at the West Bengal University of Animal and Fishery Sciences, Kolkata and received his Bachelor of Veterinary Sciences and Animal Husbandry (B.V.Sc and A.H.) degree in the year 1998.

Partha joined the Chaudhury Charan Singh Haryana Agricultural University, Hisar, Haryana in October of 1998 and obtained his Master of Veterinary Sciences (M.V.Sc) degree from the department of Veterinary Microbiology in the year 2000. He joined The University of Tennessee, Knoxville in August 2000 and received the Doctor of Philosophy degree from the Department of Comparative and Experimental Medicine, College of Veterinary Medicine in May 2005. He plans to further pursue post doctoral training.